AD-A065 469 COLORADO STATE UNIV FORT COLLINS DEPT OF ATMOSPHERI--ETC F/G 4/2
A DIAGNOSTIC CASE STUDY OF THE 9-11 AUGUST PERIOD DURING GATE.(U)
1978 J J BUTCHKO NSF-ATM76-09370
UNCLASSIFIED AFIT-CI-79-114T NL

1 OF 2
AD
A 065469

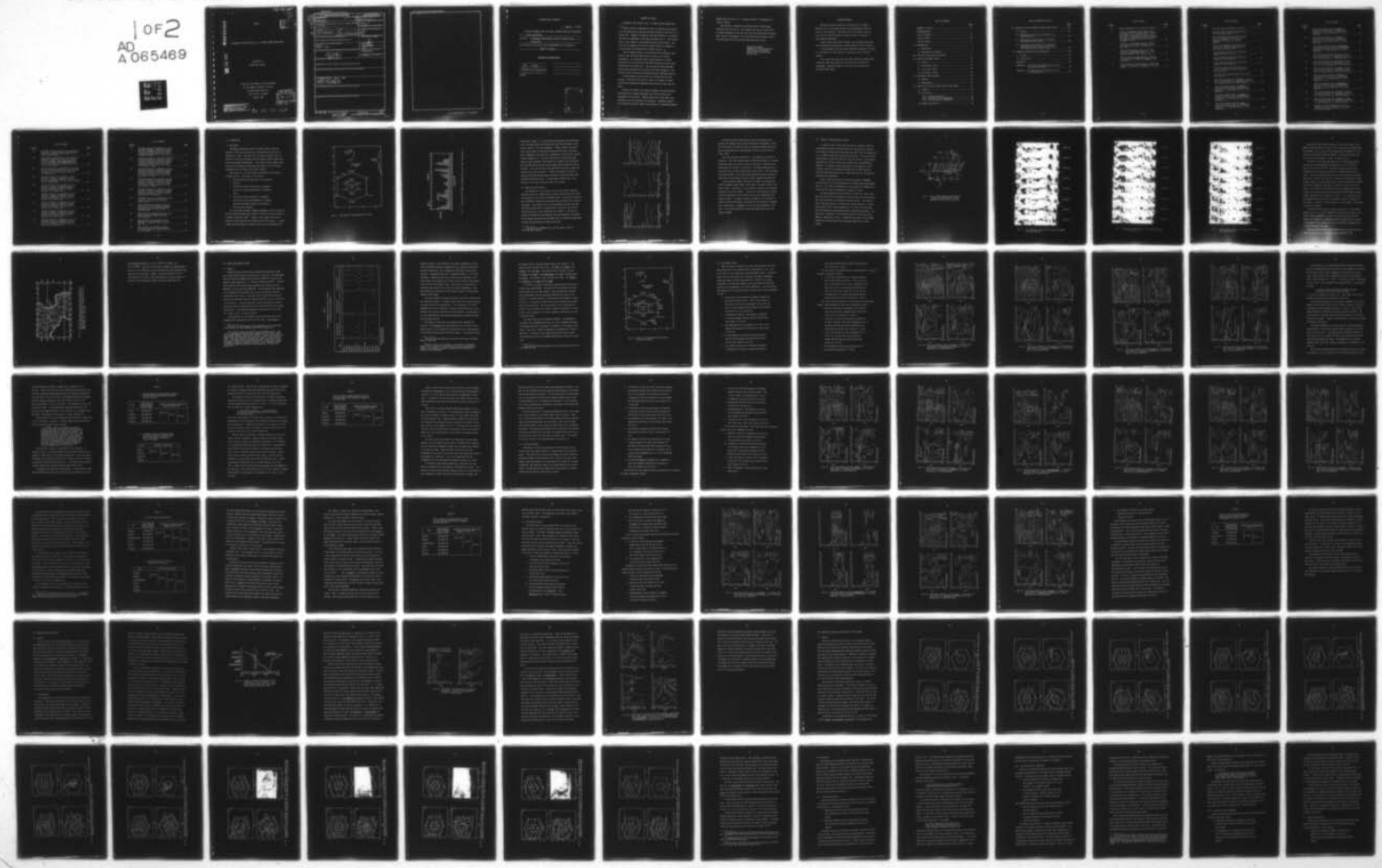

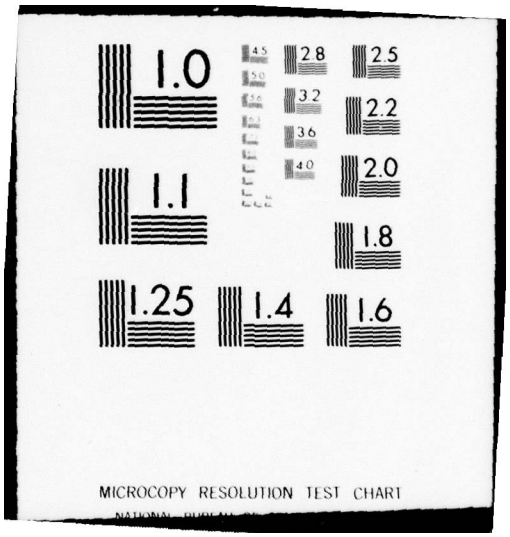
1.0
1.1
1.25
1.4
1.6
1.8
2.0
2.2
2.5
2.8
3.2
3.6
4.0
4.5
5.0
5.6
MICROCOPY RESOLUTION TEST CHART

CI 79-114T

AD A065469

DDC FILE COPY

THESIS

LEVEL II

# A DIAGNOSTIC CASE STUDY OF THE 9 - 11 AUGUST PERIOD DURING GATE

Submitted by

Joseph John Butchko

In partial fulfillment of the requirements

for the Degree of Master of Science

Colorado State University

Fort Collins, Colorado

Spring, 1978

DDC RECEIVED MAR 8 1979 E

DISTRIBUTION STATEMENT A
Approved for public release;
Distribution Unlimited

79 02 26 239

UNCLASSIFIED

SECURITY CLASSIFICATION OF THIS PAGE (When Data Entered)

(18) (19) **REPORT DOCUMENTATION PAGE**

READ INSTRUCTIONS BEFORE COMPLETING FORM

| | |
|---|---|
| 1. REPORT NUMBER: CI-79-114T | 2. GOVT ACCESSION NO. |
| 3. RECIPIENT'S CATALOG NUMBER | (9) Master's |
| 4. TITLE (and Subtitle): A Diagnostic Case Study of the 9-11 August Period During Gate, (6) | 5. TYPE OF REPORT & PERIOD COVERED: Thesis, |
| | 6. PERFORMING ORG. REPORT NUMBER |
| 7. AUTHOR(s): (10) Joseph John Butchko | 8. CONTRACT OR GRANT NUMBER(s): (15) NSF-ATM76-09370 |
| 9. PERFORMING ORGANIZATION NAME AND ADDRESS: AFIT Student at Colorado State University | 10. PROGRAM ELEMENT, PROJECT, TASK AREA & WORK UNIT NUMBERS (11) |
| 11. CONTROLLING OFFICE NAME AND ADDRESS: AFIT/CI WPAFB OH 45433 | 12. REPORT DATE: Spring 1978 |
| | 13. NUMBER OF PAGES: 102 |
| 14. MONITORING AGENCY NAME & ADDRESS (if different from Controlling Office): (12) 116p. | 15. SECURITY CLASS. (of this report): UNCLASSIFIED |
| | 15a. DECLASSIFICATION/DOWNGRADING SCHEDULE |

16. DISTRIBUTION STATEMENT (of this Report)

Approved for Public Release, Distribution Unlimited

17. DISTRIBUTION STATEMENT (of the abstract entered in Block 20, if different from Report)

18. SUPPLEMENTARY NOTES

FEB 8 1979

JOSEPH P. HIPPS, Major, USAF
Director of Information, AFIT

19. KEY WORDS (Continue on reverse side if necessary and identify by block number)

20. ABSTRACT (Continue on reverse side if necessary and identify by block number)

DD FORM 1 JAN 73 1473 EDITION OF 1 NOV 65 IS OBSOLETE

088310

UNCLASSIFIED

SECURITY CLASSIFICATION OF THIS PAGE (When Data Entered)

COLORADO STATE UNIVERSITY

Spring 1978

WE HEREBY RECOMMEND THAT THE THESIS PREPARED UNDER OUR SUPERVISION

BY Joseph John Butchko

ENTITLED A Diagnostic Case Study of the 9 - 11 August Period During GATE

BE ACCEPTED AS FULFILLING IN PART REQUIREMENTS FOR THE DEGREE OF

Master of Science

Committee on Graduate Work

Adviser

ACCESSION for
NTIS White Section X
DDC Buff Section
UNANNOUNCED
JUSTIFICATION
BY
DISTRIBUTION/AVAILABILITY CODES
Dist. Avail. and/or SPECIAL
A

ABSTRACT OF THESIS

A DIAGNOSTIC CASE STUDY OF THE 9 - 11 AUGUST PERIOD DURING GATE

Several analysis techniques are used to determine the structure of a disturbance which traversed the GATE A/B ship array from 9 to 11 August 1974. Emphasis is placed on the identification of an easterly wave and the tropospheric structure associated with it. The disturbance is also viewed as a pre-tropical cyclone cloud cluster. The vorticity, divergence and vertical motions fields are compared to fields derived from western Pacific cloud clusters.

The disturbance proves to be associated with an easterly wave which is best defined at 600 mb and is cold core in the mid-troposphere. The convection within the disturbance is closely associated with the position of the 600 mb trough axis and is also aligned with the surface flow. Two low level vortices developed within the disturbance but in regions of minimum convection. The northern vortex persisted and strong convection developed around it.

A mid-tropospheric jet (∿20 m/s) is evident after the wave passage. Associated with the jet is warm, dry Saharan air which significantly changes the temperature and moisture fields over the array.

Vertical wind shears are evident throughout the period and are associated with an upper-tropospheric jet (∿40 m/s) and a mid-tropospheric jet (∿20 m/s). Despite the vertical wind shear, the horizontal wind field appears very organized. Streamline analysis for the 600 mb and 150 mb levels show evidence of compensating motion

between the two levels (i.e. a trough at 600 mb is compensated by a ridge at 150 mb).

The vorticity, divergence and vertical motion fields appear different across the array. The intensity and shape of the profile are highly dependent on the area over which the computations are made. Qualitatively there appears to be little difference between profiles from the Western Pacific and the GATE A/B-scale ship array.

Joseph John Butchko
Atmospheric Science Department
Colorado State University
Fort Collins, Colorado 80523
Spring, 1978

ACKNOWLEDGEMENTS

The author wishes to express his gratitude to Dr. Wayne H. Schubert for his invaluable guidance and encouragement during the course of this research. The advice of Drs. Alan Betts, William Gray, William Frank and Howard Frisinger and Ms. Polly Martin is also greatly appreciated.

I would like to give special thanks to Ms. Dorothy Chapman who did the manuscript typing and Ms. Janella Owen who did the drafting.

I also benefited from discussions with many colleagues including: Ms. Jean Dewart, Ms. Pam Grube, Mr. James Hack, and Mr. Charles Solomon.

This research was done while the author attended Colorado State University under the sponsorship of the Air Force Institute of Technology. Technical support for this work was obtained from NSF Grant ATM 76-09370.

TABLE OF CONTENTS


| | | Page |
|---|---|---|
| | ABSTRACT OF THESIS | iii |
| | ACKNOWLEDGEMENTS | v |
| | TABLE OF CONTENTS | vi |
| | LIST OF TABLES | viii |
| | LIST OF FIGURES | ix |
| 1.0 | INTRODUCTION | 1 |
| | 1.1 Background | 1 |
| | 1.2 Objectives and Analyses | 4 |
| 2.0 | SATELLITE TIME-LONGITUDE SECTIONS | 7 |
| 3.0 | HEIGHT-TIME CROSS SECTIONS | 15 |
| | 3.1 General | 15 |
| | 3.2 The Northern Sector | 20 |
| | 3.3 The Central Sector | 32 |
| | 3.4 The Southern Sector | 46 |
| 4.0 | MERIDIONAL CROSS SECTIONS | 55 |
| | 4.1 General | 55 |
| | 4.2 Observations | 55 |
| 5.0 | ANALYSIS OF SELECTED LEVELS OVER THE GATE ARRAY | 63 |
| | 5.1 General | 63 |
| | 5.2 Discussion | 77 |
| | 5.2.1 Surface Streamlines | 77 |
| | 5.2.2 The 600 mb Level Streamlines | 79 |
| | 5.2.3 The 150 mb Level Streamlines | 81 |
| | 5.3 General Observation | 82 |

TABLE OF CONTENTS Continued


| | | Page |
|---|---|---|
| 6.0 | ANALYSIS OF THE PRE-TROPICAL STORM CLOUD CLUSTER | 84 |
| | 6.1 General | 84 |
| | 6.2 Computation of Vorticity, Divergence, and Vertical Motion | 84 |
| | 6.3 Comparisons of the Vorticity, Divergence, and Vertical Motion Fields | 86 |
| | 6.4 Comparisons of the Vorticity, Divergence, and Vertical Motion Profiles with Profiles from Western Pacific Cloud Clusters | 92 |
| 7.0 | SUMMARY OF OBSERVATIONS AND CONCLUSIONS | 94 |
| | 7.1 Summary | 94 |
| | 7.2 Conclusions | 95 |
| | REFERENCES | 96 |
| | APPENDIX A - The Criteria and Method Used to Select the Case Study Period | 99 |
| | APPENDIX B - The Method Used to Determine the Tilt of the Trough Axis | 103 |

LIST OF TABLES


| Table | | Page |
|---|---|---|
| 1 | Missing soundings during period of interest..... | 16 |
| 2 | Actual and estimated trough travel time. a) Actual value of trough passage at 600 mb and elapsed time between the Poryv and the next ship. b) Estimated elapsed time between the Poryv and the next ship and a speed of movement of 11 m/s..... | 28 |
| 3 | Actual values of trough passage at 150 mb and elapse time between the Poryv and the next ship..... | 30 |
| 4 | Actual and estimated trough travel time. a) Actual trough passage value. b) Estimated trough-tilt--34°, speed 11 m/s..... | 42 |
| 5 | Actual values of trough passage at 150 mb and elapsed time between the Quadra and the next ship..... | 45 |
| 6 | Actual values of trough passage at 150 mb and elapsed time between the Krenkel and the next ship..... | 53 |

LIST OF FIGURES


| Figure | | Page |
|---|---|---|
| 1 | Ship positions during Phase II of GATE..... | 2 |
| 2 | B-scale rainfall amounts determined from ship radar during Phase II..... | 3 |
| 3 | Mean meridional cross-sections for Phase II; a) u-component of the wind, b) v-component of the wind, c) relative humidity..... | 5 |
| 4 | Plot of the centers of the areas of convection from 0000 GMT on Julian 220 to 2100 GMT on Julian day 224..... | 8 |
| 5 | Time longitude sections of IR satellite imagery for Julian day 221..... | 9 |
| 6 | Time longitude sections of IR satellite imagery for Julian day 222..... | 10 |
| 7 | Time longitude sections of IR satellite imagery for Julian day 223..... | 11 |
| 8 | Plot of the centers of the areas of convection and the sea surface temperature for Julian 221..... | 13 |
| 9 | Division of the A/B and B-scale ship arrays into sectors..... | 19 |
| 10 | Time cross-sections over the Poryv; a) moisture and wind fields, b) temperature deviation, c) u-wind deviation, d) v-wind deviation..... | 22 |
| 11 | Time cross-sections over the Korolov; a) moisture and wind fields, b) temperature deviation, c) u-wind deviation, d) v-wind deviation..... | 23 |
| 12 | Time cross-sections over the Vanguard; a) moisture and wind fields, b) temperature deviation, c) u-wind deviation, d) v-wind deviation..... | 24 |
| 13 | Time cross-sections over the Priboy; a) moisture and wind fields, b) temperature deviation, c) u-wind deviation, d) v-wind deviation..... | 25 |

LIST OF FIGURES


| Figure | | Page |
|---|---|---|
| 14 | Time cross-sections over the Quadra, a) moisture and wind fields, b) temperature deviation, c) u-wind deviation, d) v-wind deviation | 35 |
| 15 | Time cross-sections over the Meteor; a) moisture and wind fields, b) temperature deviation, c) u-wind deviation, d) v-wind deviation | 36 |
| 16 | Time cross-sections over the Oceanographer; a) moisture and wind fields, b) temperature deviation, c) u-wind deviation, d) v-wind deviation | 37 |
| 17 | Time cross-sections over the Vize; a) moisture and wind fields, b) temperature deviation, c) u-wind deviation, d) v-wind deviation | 38 |
| 18 | Time cross-sections over the Gillis; a) moisture and wind fields, b) temperature deviation, c) u-wind deviation, d) v-wind deviation | 39 |
| 19 | Time cross-sections over the Dallas; a) moisture and wind fields, b) temperature deviation, c) u-wind deviation, d) v-wind deviation | 40 |
| 20 | Time cross sections over the Krenkel; a) moisture and wind fields, b) temperature deviation, c) u-wind deviation, d) v-wind deviation | 48 |
| 21 | Time cross-sections over the Researcher; a) moisture and wind fields, b) temperature deviation, c) u-wind deviation, d) v-wind deviation | 49 |
| 22 | Time cross-sections over the Zubov; a) moisture and wind fields, b) temperature deviation, c) u-wind deviation, d) v-wind deviation | 50 |
| 23 | Time cross-sections over the Okean; a) moisture and wind fields, b) temperature deviation, c) u-wind deviation, d) v-wind deviation | 51 |
| 24 | Location of the intersection of the zero change line of the u-component of the wind and the sea surface | 57 |

LIST OF FIGURES


| Figure | | Page |
|---|---|---|
| 25 | Meridional cross-sections of the temperature deviation a) before trough passage and b) after trough passage | 59 |
| 26 | Meridional cross-sections of the atmosphere immediately before the trough axis passed over the Vanguard, Vize, Oceanographer a) u-wind, b) v-wind, c) temperature deviation d) relative humidity | 61 |
| 27 | Selected analyses for 1200 GMT on Julian day 221, a) surface streamline b) 600 mb (60 kPa) streamline c) 150 mb (15 kPa) streamline d) radar mosaic | 64 |
| 28 | Selected analyses for 1500 GMT on Julian day 221 a) surface streamline b) 600 mb (60 kPa) streamline c) 150 mb (15 kPa) streamline d) radar mosaic | 65 |
| 29 | Selected analyses for 1800 GMT on Julian day 221 a) surface streamline b)600 mb (60kPa) streamline c) 150 mb (15 kPa) streamline d) radar mosaic | 66 |
| 30 | Selected analyses for 2100 GMT on Julian day 221 a) surface streamline b) 600 mb (60 kPa) streamline c) 150 mb (15 kPa) streamline d) radar mosaic | 67 |
| 31 | Selected analyses for 0000 GMT on Julian day 222 a) surface streamline b) 600 mb (60 kPa) streamline c) 150 mb (15 kPa) streamline d) radar mosaic | 68 |
| 32 | Selected analyses for 0300 GMT on Julian day 222 a) surface streamline b) 600 mb 60 kPa) streamline c) 150 mb (15 kPa) streamline d) radar mosaic | 69 |
| 33 | Selected analyses for 0600 GMT on Julian day 222 a) surface streamline b) 600 mb (60 kPa) streamline c) 150 mb (15 kPa) streamline d) radar mosaic | 70 |

LIST OF FIGURES


| Figure | | Page |
|---|---|---|
| 34 | Selected analyses for 0900 GMT on Julian day 222 a) surface streamline b) 600 mb (60 kPa) streamline c) 150 mb (15 kPa) streamline d) radar mosaic over-layed on a satellite image | 71 |
| 35 | Selected analyses for 1200 GMT on Julian day 222 a) surface streamline b) 600 mb (60 kPa) streamline c) 150 mb (15 kPa) streamline d) radar mosaic over-layed on a satellite image | 72 |
| 36 | Selected analyses for 1500 GMT on Julian day 222 a) surface streamline b) 600 mb (60 kPa) streamline c) 150 mb (15 kPa) streamline d) radar mosaic over-layed on a satellite image | 73 |
| 37 | Selected analyses for 1800 GMT on Julian day 222 a) surface streamline b) 600 mb (60 kPa) streamline c) 150 mb (15 kPa) streamline d) radar mosaic over-layed on a satellite image | 74 |
| 38 | Selected analyses for 2100 GMT on Julian day 222 a) surface streamline b) 600 mb (60 kPa) streamline c) 150 mb (15 kPa) streamline d) radar mosaic | 75 |
| 39 | Sub-areas used in the computation of the vorticity, divergence and vertical motion fields | 85 |
| 40 | Mean profiles of divergence, vorticity and vertical motion ($\omega$) for the entire A/B-scale array for 0900-2100 GMT on Julian Day 222 | 87 |
| 41 | Mean profiles of relative vorticity for each sub-area for 0900-2100 GMT on Julian Day 222 | 89 |
| 42 | Mean profiles of divergence for each sub-area for 0900-2100 GMT on Julian Day 222 | 90 |
| 43 | Mean profiles of vertical P-velocity for each sub-area for 0900-2100 GMT on Julian Day 222 | 91 |

# 1.0 INTRODUCTION

## 1.1 Background

The Global Atmospheric Research Program Atlantic Tropical Experiment (GATE) was carried out in three phases from June 15 to September 23, 1974. The entire area of study included an area of tropical land and sea extending from the eastern Pacific Ocean eastward to the western Indian Ocean. The project's basic objective was to collect data needed to understand the behavior of the tropical atmosphere and its effect on the global weather.

During Phase II, the GATE region was subdivided into several different scales. The scales are as follows:

1. The A-scale which covered most of the tropical Atlantic.
2. The A/B scale which consisted of a hexagonal array of six ships approximately 4° longitude apart.
3. The B-scale which consisted of a hexagonal array of six ships approximately 2° longitude apart and two ships located at the center of the array (see Figure 1).

This case study analyzes different parameters during a three-day period (Julian days 221-223) of Phase II (28 July (Julian day 209) to 17 August (Julian day 229)). Figures 2 and 3 depict some of the conditions that prevailed over the A/B-scale during Phase II. Figure 2 shows the total amount of rainfall over the area determined from

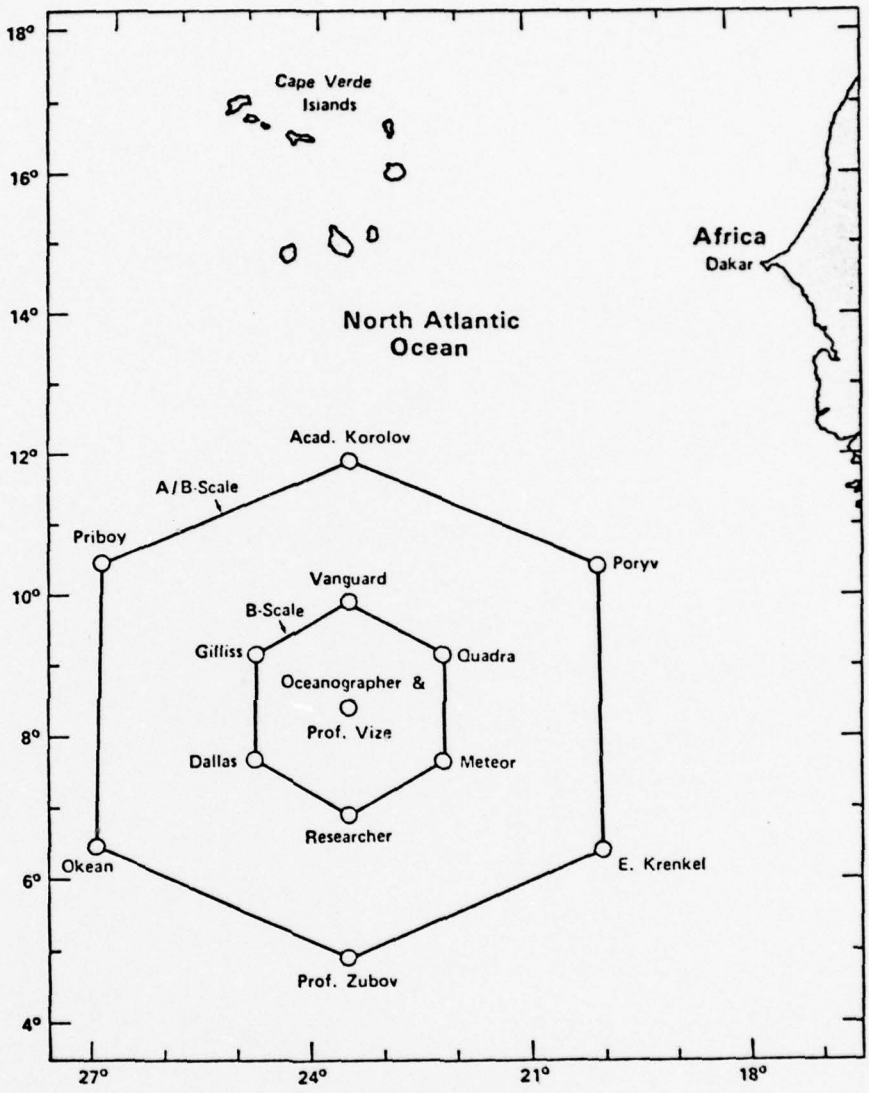


Fig. 1. Ship positions during Phase II of GATE.

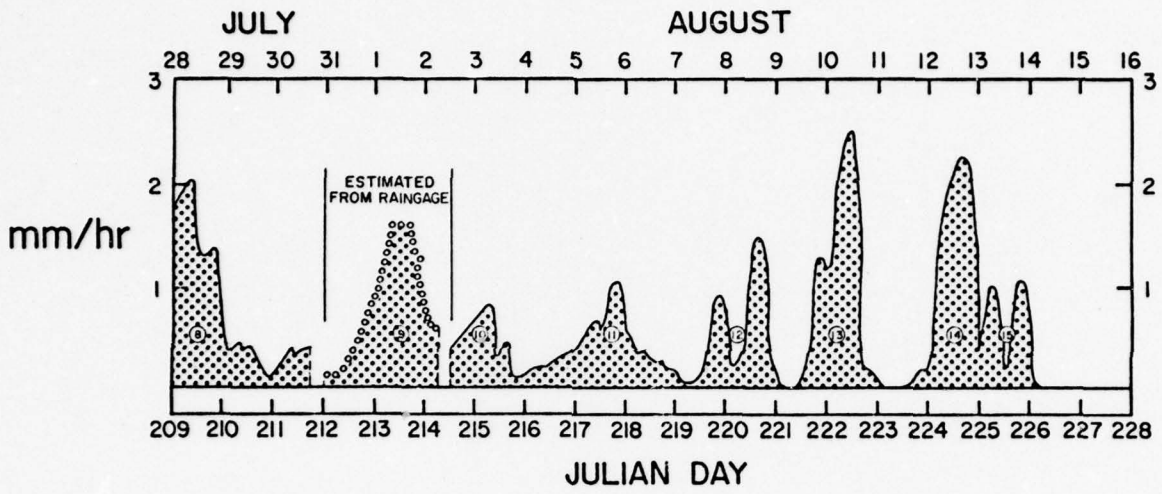


Fig. 2. B-scale rainfall amounts determined from ship radar during Phase II.

B-scale ship radars.[1] It can be seen from the chart that there were only a few days without any precipitation and that the peaks in the rainfall came in 2 to 4 day intervals. Figure 3 depicts the meridional cross section of the A/B and B-scale ship array of the phase mean v-component of the wind (a), u-component of the wind (b), and the relative humidity (c). The cross section of the zonal wind shows easterly shear dominant in the region with a middle level maximum of the wind near 600 mb (60 kPa) and an upper level maximum near 100 mb (10 kPa). The cross section of the meridional wind shows a mean confluence zone in the low levels. Figure 3(c) depicts the relative humidity cross-section and shows a maximum of moisture between 1000 and 850 mb (100 and 85 kPa). It also shows a slight peak in the moisture at all levels over the center of the array.

## 1.2 Objectives and Analysis

The objectives of the project as well as the type of analyses changed as more was learned about the period (Julian days 221 to 223) (see Appendix A for criteria and method used). The original objective was to perform a subjective, semi-quantitative analysis of an area of convection. The analysis was to be accomplished using the data set from GATE, and the area of study would be confined to the A/B and B-scale ship array of the experiment (see Figure 1). The area of study and the data set used remained the same throughout the project, but the type of analyses and the objectives of the project became more refined with two discoveries about the period.

---

[1]The author is indebted to Drs. W. Gray and W. Frank for providing this diagram.

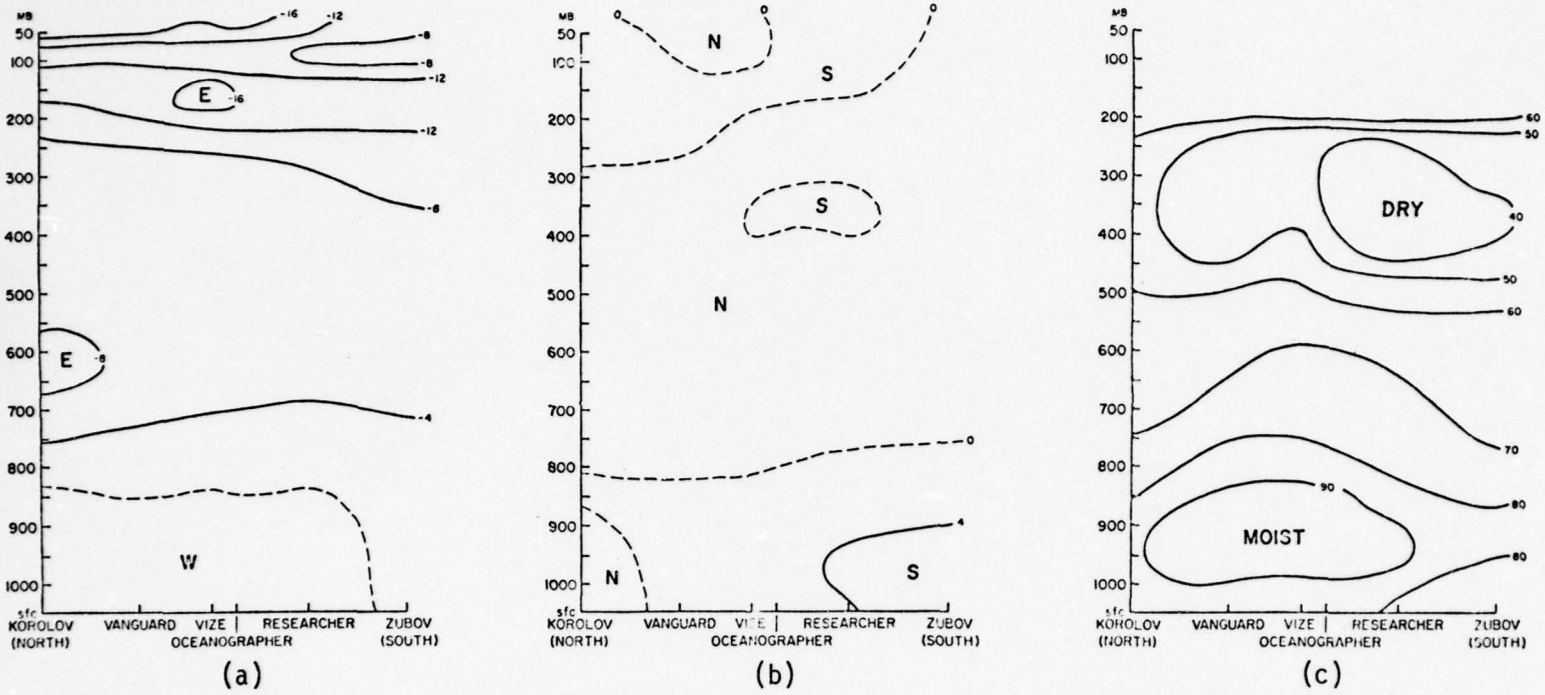


Fig. 3. Mean meridional cross-sections for Phase II: a) u-component of the wind, b) v-component of the wind, c) relative humidity.

The two discoveries were that the area of convection being studied later became Tropical Storm Alma (Betts and Rodenhuis, 1975; and Frank, 1975), and that the area of convection formed over Africa and was associated with a wave passage at Dakar on Julian day 220 (Frank, 1975).

With the additional information, it was decided to refine our objectives. The first objective was to identify the wave as it passed through the GATE array, and to study its structure, intensity, and relationship to the area of convection. The second objective was to study the area as a pre-tropical storm cloud cluster. With the objectives more refined, it was decided to design the analysis program so comparisons could be made with work already completed and published.

Three particular papers were used as a guide in designing the analysis program, Chang (1970), Yanai (1961), and Reed, Norquist and Recker (1977). From Chang, it was decided to produce time longitude sections of satellite imagery. From Yanai it was decided to produce vertical-time-height cross-sections for the wind, temperature and moisture fields. From Reed, Norquist and Recker it was decided to analyze vertical-time-height cross-sections of deviations of temperature, mixing ratio, v-component of the wind and u-component of the wind. The initial processing of data was accomplished using this analysis scheme.

## 2.0 SATELLITE TIME-LONGITUDE SECTIONS

In order to view as much satellite data as possible, satellite time-longitude sections were constructed for the period of interest. The original sections were constructed using SMS-1 data (IR images with 4 n.m. (7408 m) resolution) copied from microfilm. The sections were constructed for Julian days 220, 221, 222, 223 and 224. Each section consisted of 8 strips, one for each synoptic hour from 0000 GMT to 2100 GMT. The sections covered the area from the equator to 20°N latitude, and from the Greenwich meridian west to 60°W longitude. Using the time-longitude sections a speed and track for the center of convection was determined.

Figure 4 shows the trach of the Area of Convection (AROCON). Using the track, it was determined that the AROCON moved approximately 900 n.m. ($1.7 \times 10^6$m) from 0900 GMT on Julian day 221 to 0000 GMT on Julian day 223, which corresponds to a speed of $\sim$11 m/s.

The time-longitude sections depicted in Figures 5, 6 and 7 were made from high quality photographic prints obtained from the Satellite Data Services Branch of the National Climatic Center. The sections differ from the original in period cover (3 days compared to 5 days), area covered (10°E to 110°W compared to 0° to 70°W), and that they have been reduced by approximately 50% for publication purposes. The GATE array is depicted as the 6-sided figure and the center of the AROCON is depicted by a cross. Determining the center of the AROCON became very difficult when the area changed shape and size very rapidly.

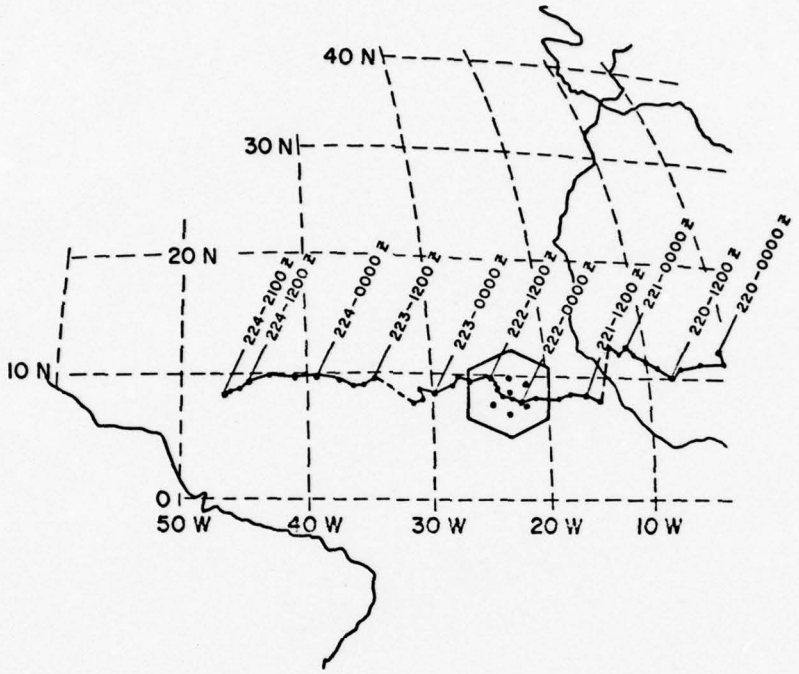


Fig. 4. Plot of the centers of the areas of convection from 0000 GMT on Julian day 220 to 2100 on Julian day 224.

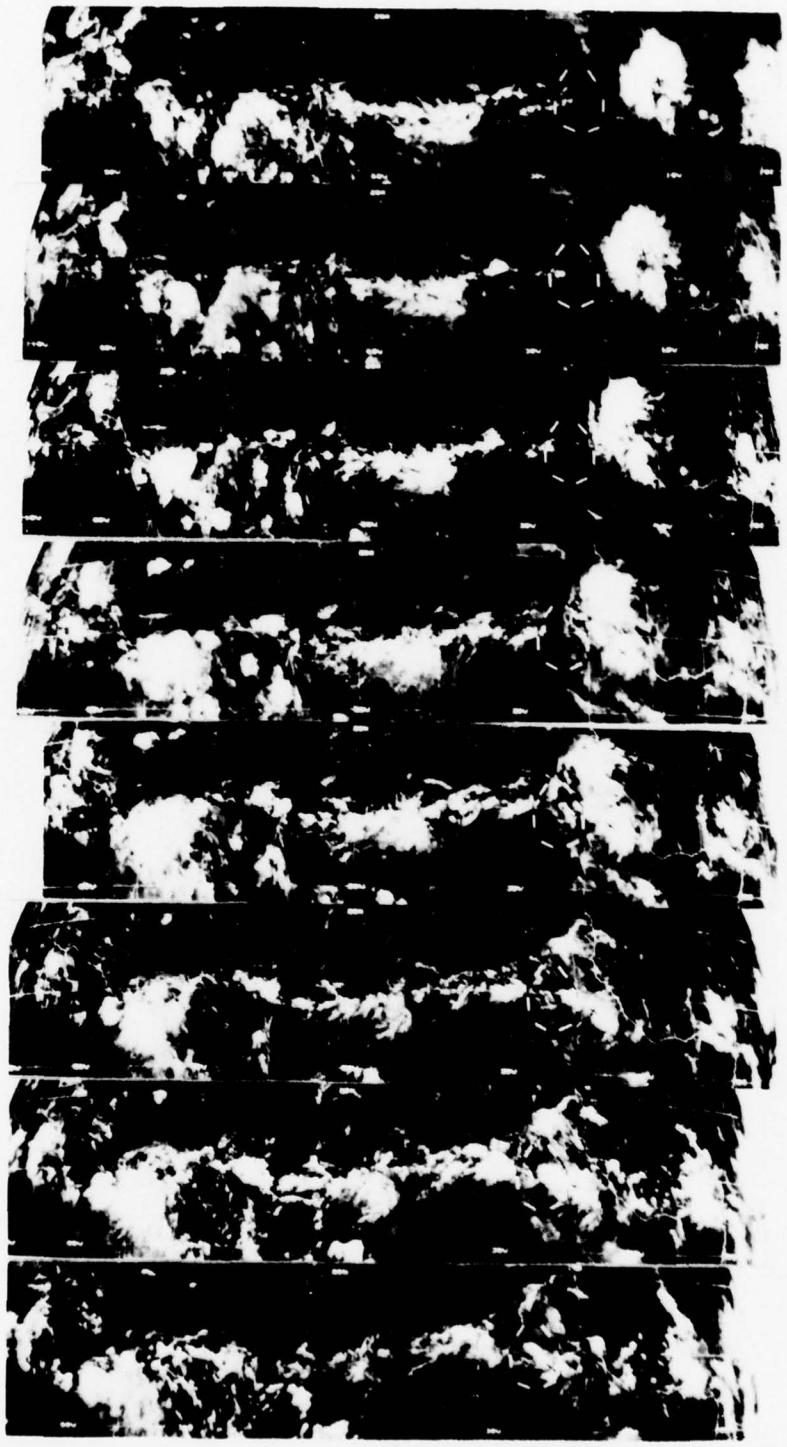


Fig. 5. Time longitude sections of IR satellite imagery for Julian day 221.

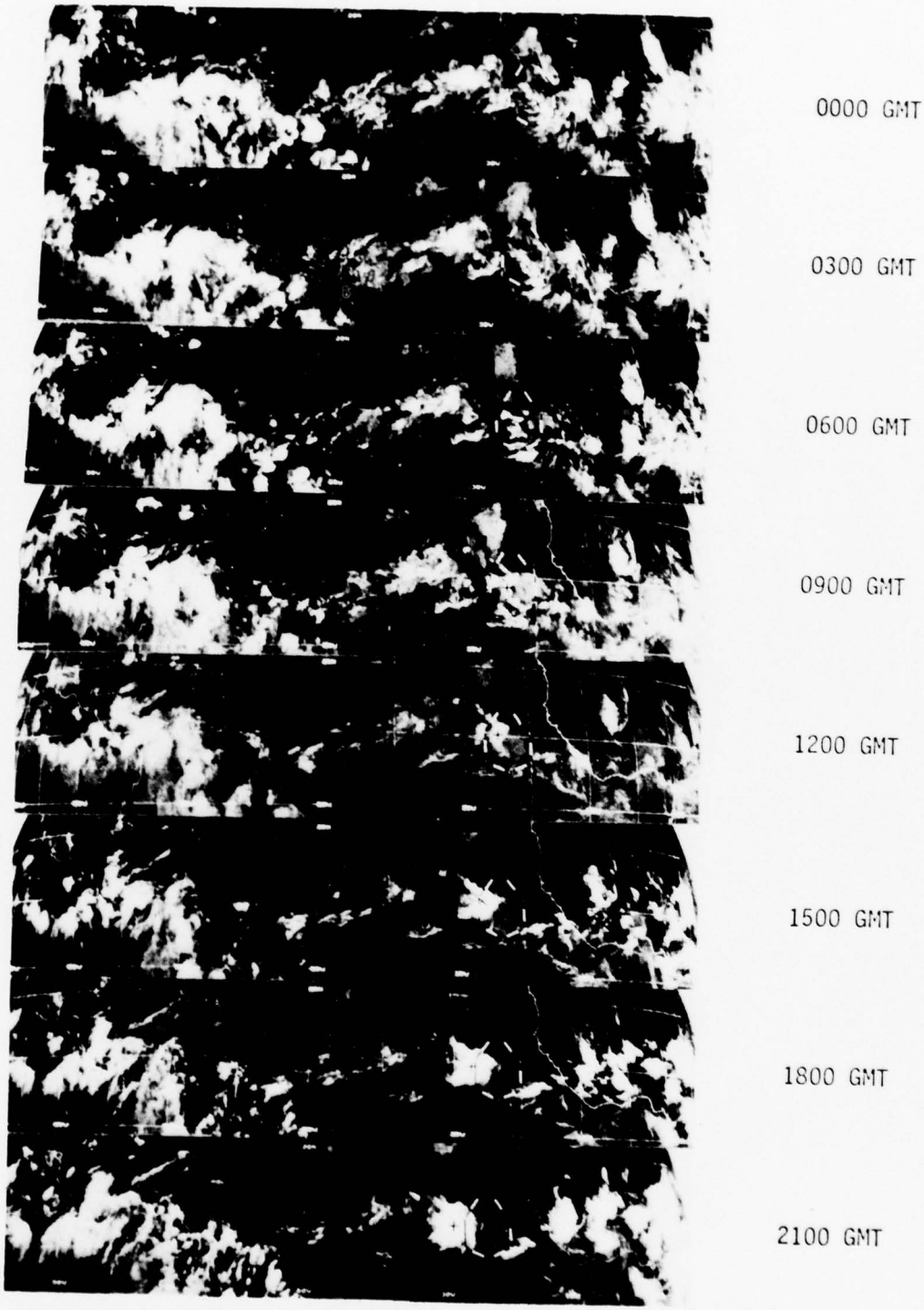


Fig. 6. Time longitude sections of IR satellite imagery for Julian day 222.

Fig. 7. Time longitude sections of IR satellite imagery for Julian day 223.

There were three distinct changes of the size and shape of the AROCON during the period of study: (1) on Julian day 221 between 0600 and 1500 GMT, (2) on Julian day 222 between 0000 and 0900 GMT, (3) on Julian day 223 between 0600 and 1500 GMT. Of the three changes the first was the most dramatic in terms of change in size.

During the first change the total area of cloudiness decreased over one-half from approximately 800,000 sq mi ($2.0 \times 10^{12}$ m$^2$) to 300,000 sq mi ($8.0 \times 10^{11}$ m$^2$). The greatest change came when the northern half of the area dissipated as it reached the east African coast. The rapid dissipation may be due to the colder water along the coast north of Dakar (see Figure 8). Although one case cannot be considered conclusive, the significance of a possible relationship between sea surface temperature and areas of convection should not be overlooked. The importance of threshold sea surface temperature for the formation of tropical storms has been noted by Palmen (1948) and Yanai (1964) (temperature must exceed 26° to 27°C). It is conceivable that the threshold theory could also be extended to area of convection in the tropics. Although I did not pursue this idea further, I do believe it should be studied.

The second change seems to be very complicated. The convection appears very disorganized at 0000 GMT on Julian 222 but within 9 hours a very distinct backward "S" pattern can be seen on the satellite imagery (see Figure 6). A detailed study of the day (Julian day 222) is the subject of my research and will be discussed in greater detail in other sections of the paper.

During the third change (0600 to 1500 GMT on Julian day 223) the total area of convection is reduced by more than 90%, from

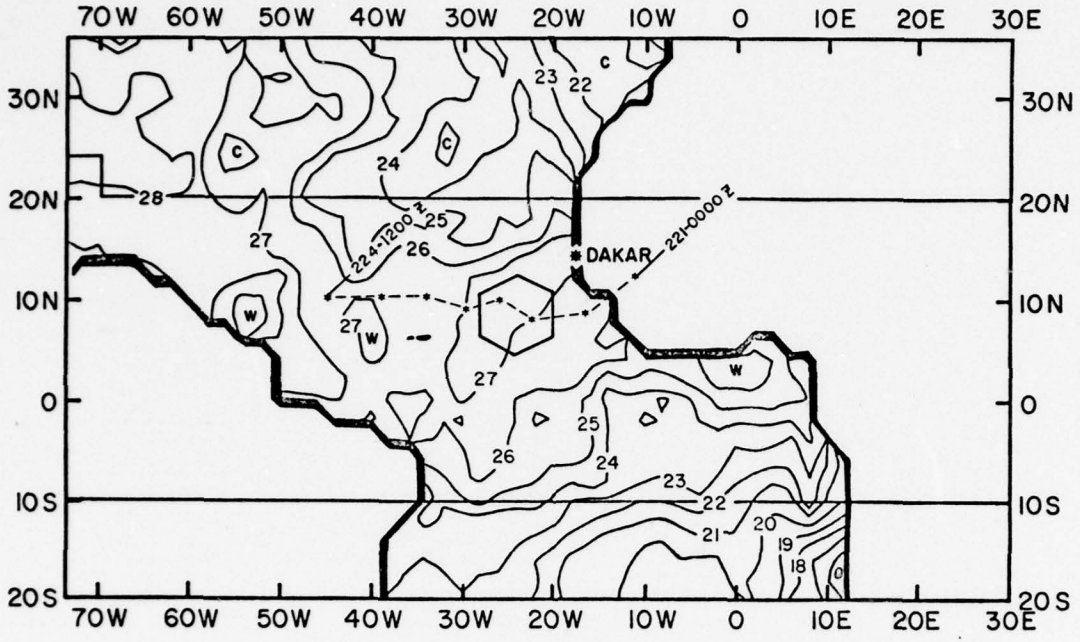


Fig. 8. Plot of the centers of the areas of convection and the sea surface temperature for Julian day 221. (Map copied from "Sea Surface Temperature for GATE, Report 76-3," Nov. 76, FSU.)

approximately 400,000 sq mi ($1.0 \times 10^{12} m^2$) to 28,500 sq mi ($7.0 \times 10^{10} m^2$). The area, at the time of change, was approximately 600 n.m. ($1.0 \times 10^{6} m$) west of the A/B-scale array and beyond the area constraints of the study. However, since the reduction in size occurred within 24 hours of the area becoming a tropical storm, it would be a very good case to study using the A-scale data set.

## 3.0 HEIGHT-TIME CROSS SECTIONS

### 3.1 General

Height-time cross sections were plotted[2] and analyzed for each ship in the A/B and B scale ship arrays (see Figure 1). The rawinsonde data were stored on magnetic tape and were a modified version of the magnetic tapes supplied by U. S. National Processing Center.[3] The time period used for the cross-sections extended from Julian day 221 at 0000 GMT to Julian day 224 at 0000 GMT. The rawinsondes were scheduled to be launched at each synoptic hour so the time interval for the cross-section was 3 hours. The levels used included the surface and then every 50 millibars from the 1000 mb (100 kPa) surface to the 50 mb (k kPa) surface. Although there were missing rawinsonde data during the period, 94% of the possible data for Julian day 222 were available (see Table 1). Ten different parameters were plotted for each ship for a total of 140 time-cross sections.

Cross-sections for ten parameters were plotted but four of the parameters were considered to be of little value. The parameters

---

[2]The CSU, CDC 6400 computer was programmed to plot height-time cross-sections for the parameters specified for each ship.

[3]The original tapes were modified by programmers at CSU. The u and v components of the wind were averaged to 25 millibars levels. The averaging process involved five levels: the two levels above the center level, the two levels below the center level, and the center level. The actual values of temperature, height, and mixing ratio were used at each level and were not altered. In addition, the data "flagged" by CEDDA as suspect was deleted. More information about the original tapes can be found in GATE Report No. 13 (Part II), section 10.

Table 1

Missing Soundings During Period of Interest
(x indicates missing sounding)

| Ship | Julian day 221 | | | | | | | | Julian day 222 | | | | | | | | Julian day 223 | | | | | | | | |
|---|---|---|---|---|---|---|---|---|---|---|---|---|---|---|---|---|---|---|---|---|---|---|---|---|---|
| | 00 | 03 | 06 | 09 | 12 | 15 | 18 | 21 | 00 | 03 | 06 | 09 | 12 | 15 | 18 | 21 | 00 | 03 | 06 | 09 | 12 | 15 | 18 | 21 | 24 |
| Poryr | | | | | | | | | | | | | | | | | | | | x | | x | | x | |
| Krenkel | | | | | | | | | | | | | | | | | | | | x | | x | | x | |
| Quadra | | | | | | | | | | | | | | | | | | | | x | | x | | x | x |
| Meteor | | | x | | | | | x | | | | | | | | | | | | | | x | | | |
| Korolov | | | | | | | | | | | | | | | | | | | | x | | x | | x | |
| Vanguard | | x | | x | | | | | | | | | | | | | | | | x | | x | | x | |
| Oceano | x | | x | | x | | x | | | | | | | | | | x | | x | | x | | x | | x |
| Vize | | | | | | | | | | | | | | | | | | | | x | | x | | x | |
| Researcher | x | x | x | x | x | x | x | x | x | x | x | x | | | | | | | | | | | | | |
| Zubor | | | | | | | | | | | | | | | | | | | | x | | x | | x | |
| Gillis | x | | | | | | | | | | | | | | | | | | | x | | x | | x | |
| Dallas | | | | | | x | | | | x | | | | | | x | | | | x | | x | x | x | x |
| Priboy | | | | | | | | | | | | | | | x | | | | | | | | | | |
| Okean | | | | | | | | | | | | | | | | | | | | x | | x | | x | |

(Total possible 350
# mission 67 (19%))

plotted included: wind direction, wind speed, temperature, mixing ratio, equivalent potential temperature ($\theta_e$), saturation equivalent potential temperature ($\theta_e^*$), temperature deviation[4], mixing ratio deviation, u-component deviation, v-component deviation. Of the ten parameters, temperature and mixing ratio are not presented in this paper because the changed in the fields were too small to be detected with a 50 mb (5 kPa) height scale. The $\theta_e$ and $\theta_e^*$ fields are not presented; they simply did not yield any useful information. Each cross-section was analyzed with the primary purpose of identifying a synoptic scale[5] event.

Since the synoptic scale was being used, short term variations in the field were ignored. A "mental" time filter of six hours was used to smooth the data for presentation. If a fluctuation in a field appeared on only one rawinsonde, it was not considered to be on the synoptic scale and was smoothed out of the analysis. The analysis of all the cross-sections shows strong evidence that an easterly trough moved through the area.

The analysis of the wave also showed the wave changed with latitude. The dependence upon latitude as well as an effort to present the data in the clearest manner possible leads to the separation of the A/B and B-scale ships into three sectors: the northern sector,

---

[4]The deviation was defined as the actual value minus the phase mean for each ship.

[5]Synoptic scale, for this paper, is defined as a phenomena observed in the network of stations making up the A/B and B-scale arrays. For example, an easterly trough would be considered a synoptic scale phenomenon.

the central sector, and the southern sector (see Figure 9). The northern sector includes four ships: the Poryv, the Korolov, the Vanguard, and the Priboy. The central sector includes six ships: the Quadra, the Meteor, the Oceanographer, the Vize, the Gillis and the Dallas. The southern sector includes four ships: the Krenkel, the Researcher, the Zubov and the Okean.

In an effort to show as much data as possible some of the cross-sections were consolidated. The wind field and moisture field were consolidated into one cross-section. The wind speed and direction were consolidated using the standard meteorological plotting convention.[6] An isotach analysis is depicted for wind speeds of 15 m/s and 20 m/s. The moisture field (mixing ratio deviation) was traced onto the cross-section. The zero deviation line is depicted as a dashed line, an increase of at least 1 gm/kgm is depicted as an area of dots, and a decrease of at least 1 gm/kgm is depicted as an area of parallel lines.

The other cross-sections presented include: the temperature deviation, the u-component deviation, and the v-component deviation. The temperature field is depicted in increments of one degree centigrade. The u and v fields are depicted in increments of 4 units of deviation. In addition, the trough positions were drawn on each cross-section as well as a histogram depicting the rain fall at each ship.

---

[6]The wind direction was plotted using a protractor and each full wind barb is 5 m/s.

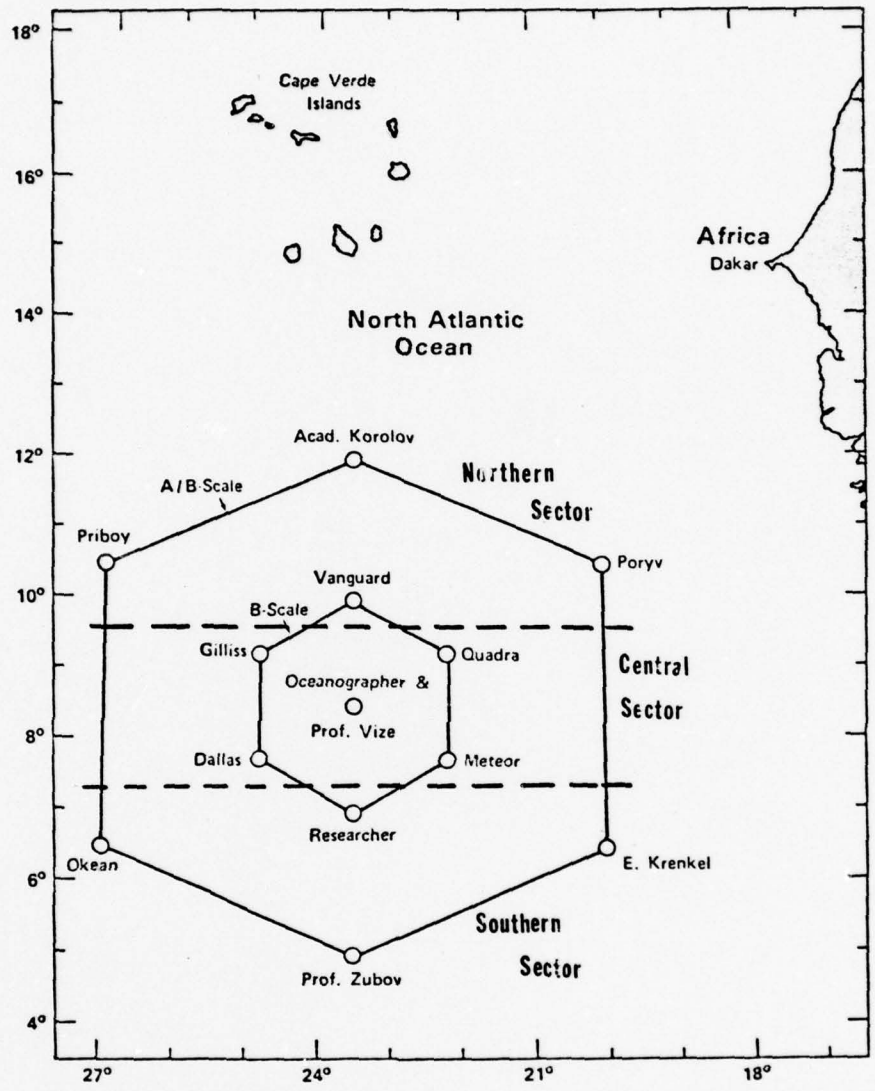


Fig. 9. Division of the A/B and B-scale ship arrays into sectors.

3.2 The Northern Sector

There are several similarities in the cross-section of the four ships which make up the northern sector (see Figures 10 - 13). The similarities can be categorized into three general areas: those that appear directly associated with a trough in the lower troposphere, those that appear directly associated with a trough in the upper troposphere, and those that appear to be associated with some other synoptic scale phenomenon in the lower troposphere. The similarities that appear directly associated with a trough in the lower troposphere include:

1. A wind shift from northeast to southwest between 700 and 500 mb (70 and 50 kPa). This is also evident in the abrupt shift in the v-component of the wind from north to south between 700 and 500 mb (70 and 50 kPa) (see Figures 10 - 13 (a) and (d)).
2. A pronounced increase in the easterly u-component of the wind between 700 and 500 mb (70 and 50 kPa) (see Figures 10 - 13 (c)).
3. The appearance of a wind maximum of at least 15 m/s between 700 and 500 mb (70 and 50 kPa) (see Figures 10 - 13 (a)).
4. A large amount of precipitation associated with the wind shifts between 700 and 500 mb (70 and 50 kPa) (see Figures 10 - 13 (a)).
5. An increase in mixing ratio deviation (increase in moisture) of at least 1 gm/kgm preceding the

wind shifts between 700 and 500 mb (70 and 50 kPa) (see Figures 10 - 13 (a)).

The similarities that appear directly associated with a trough in the upper troposphere include:

1. A wind shift from northeast to southeast between 200 and 100 mb (20 and 10 kPa). This is also evident in the abrupt shift in the v-component of the wind from north to south between 200 and 100 mb (20 and 10 kPa) (see Figures 10 - 13 (a) and (d)).
2. The appearance of a wind maximum between 200 and 100 mb (20 and 10 kPa) (see Figures 10 - 13 (a)).

The similarities that appear to be associated with some other synoptic scale phenomenon in the lower troposphere include:

1. Warming in the lower troposphere ∿12 to 18 hours after the wind shifts between 500 and 700 mb (50 and 70 kPa) (see Figures 10 - 13 (b)).
2. A decrease in mixing ratio deviation (drying) of at least 1 gm/kgm in the lower troposphere ∿15 to 18 hours after the wind shifts between 500 and 700 mb (50 and 70 kPa) (see Figures 10 - 13 (a)).
3. A shift to the north of the v-component of the wind ∿15 to 18 hours after the wind shifts between 500 and 700 mb (50 and 70 kPa) (see Figures 10 - 13 (d)).
4. Mid-tropospheric cooling during most of the 3 day period (see Figures 10 - 13 (b)).

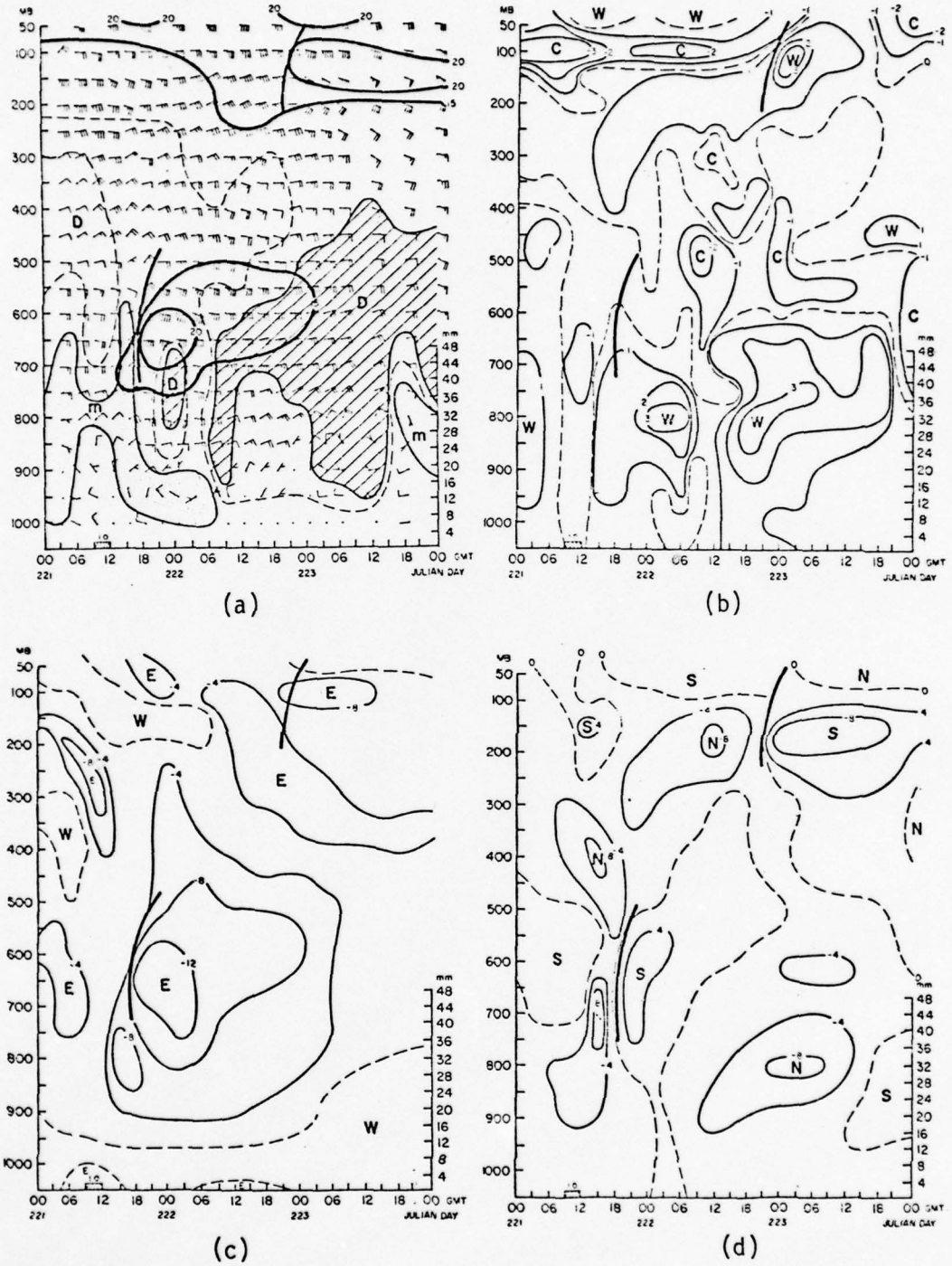


Fig. 10. Time cross-sections over the Poryv: a) moisture and wind fields, b) temperature deviation, c) u-wind deviation, d) v-wind deviation.

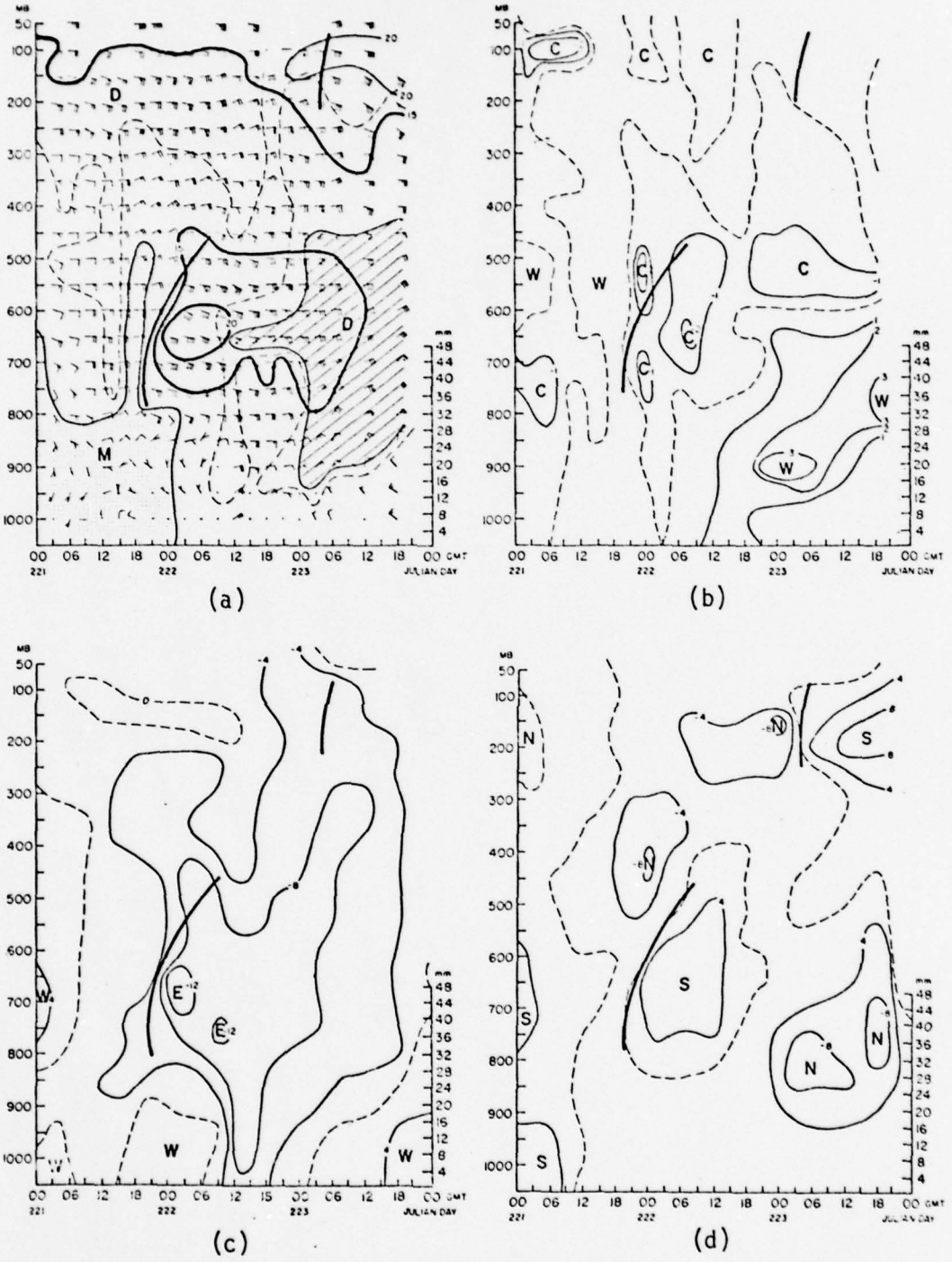


Fig. 11. Time cross-sections over the Korolov: a) moisture and wind fields, b) temperature deviation, c) u-wind deviation, d) v-wind deviation.

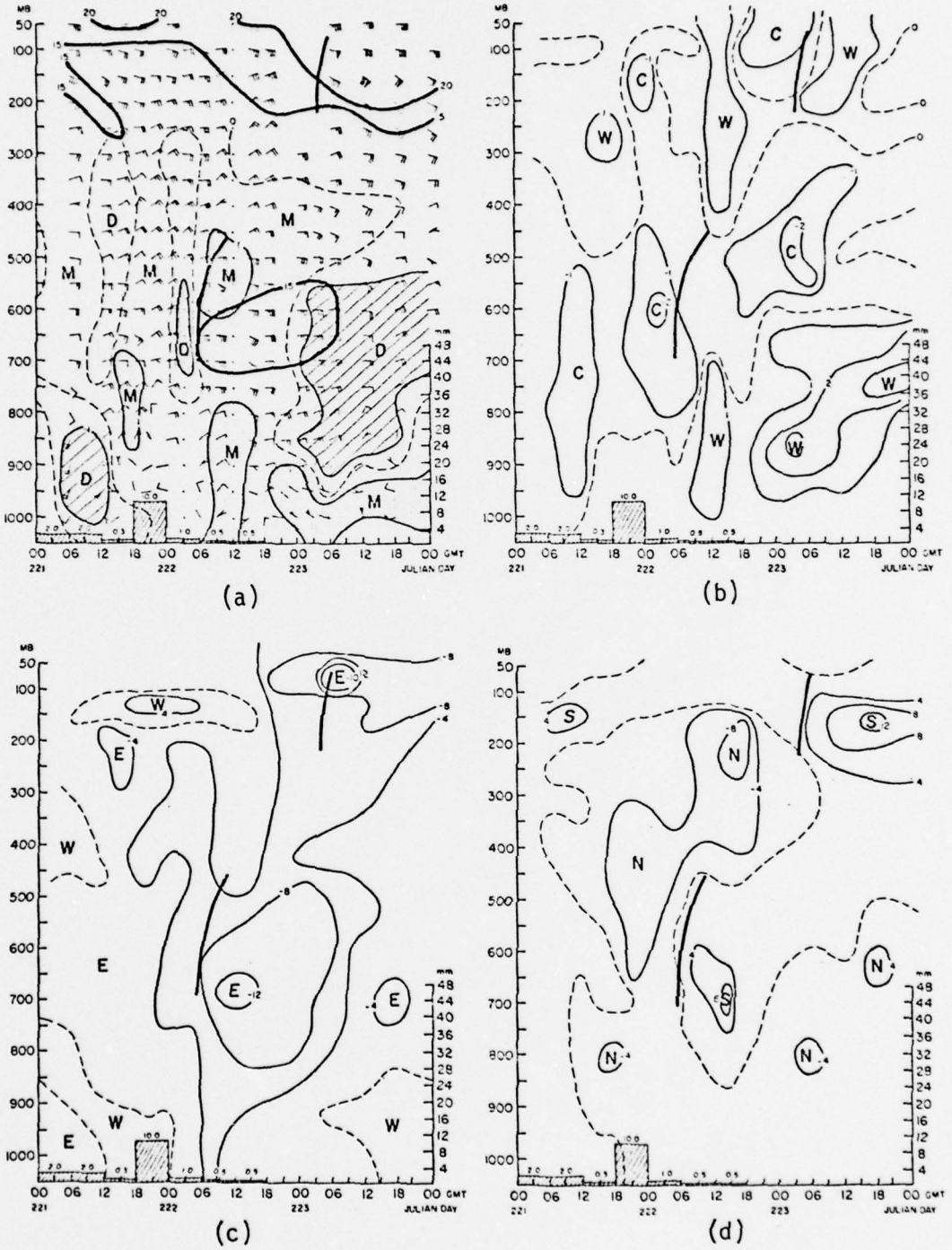


Fig. 12. Time cross-sections over the Vanguard: a) moisture and wind fields, b) temperature deviation, c) u-wind deviation, d) v-wind deviation.

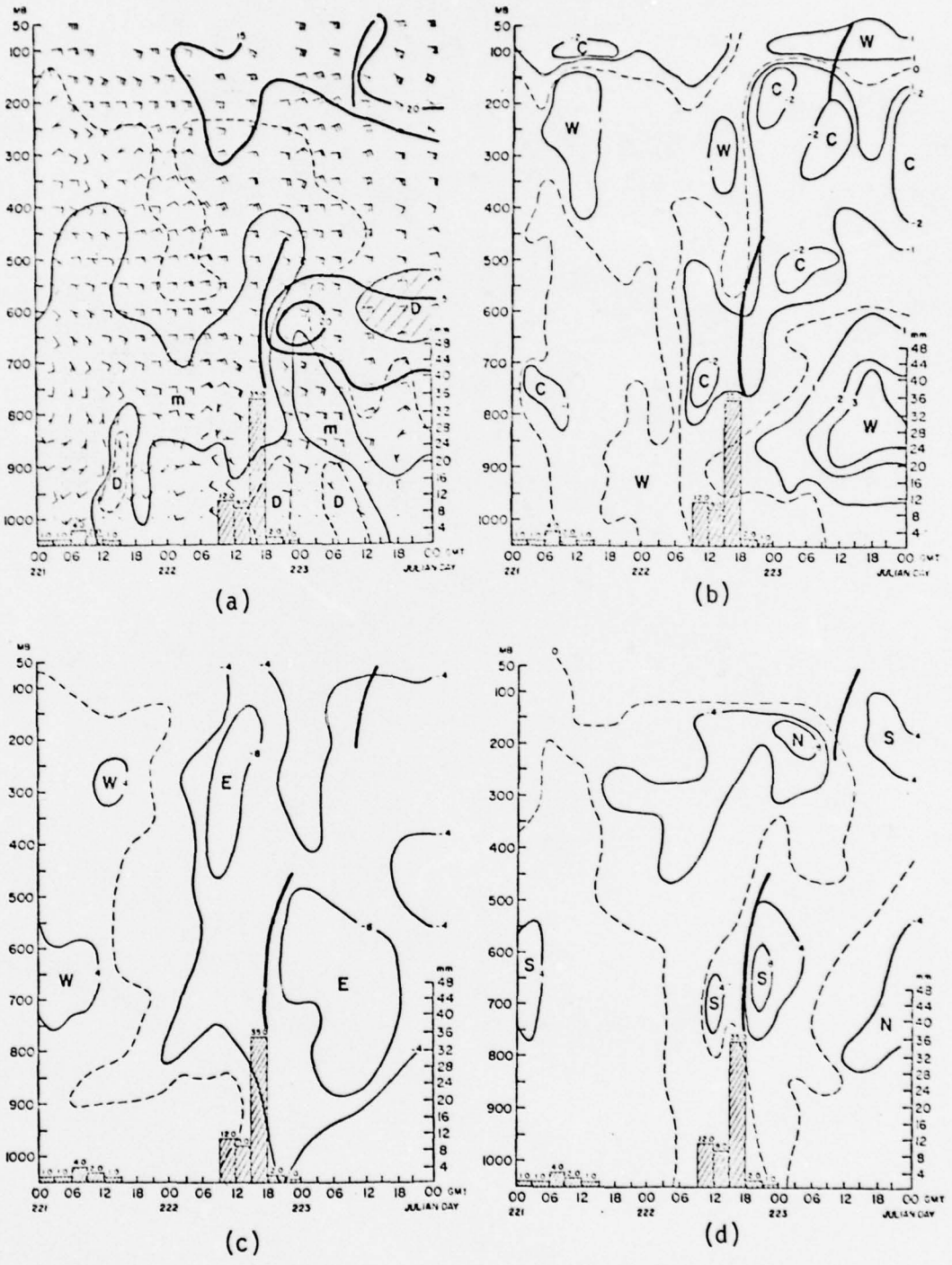


Fig. 13. Time cross-sections over the Priboy: a) moisture and wind fields, b) temperature deviation, c) u-wind deviation, d) v-wind deviation.

The existence of a trough between 700 mb and 500 mb (70 kPa and 50 kPa) is substantiated by the wind shift from northeast to southeast and the abrupt shift in the v-component of the wind from north to south. These factors are in agreement with the results of Burpee (1974, 1975) and Reed et al. (1977). In addition, rainfall associated with the wave is also in agreement with Burpee (1974). In that paper he noted,

> "...South of 12.5°N the rainfall maxima occur near the trough and the minima near the ridge...."

It is also in agreement with Reed et al. (1977) whose results show a maximum of precipitation preceding the trough axis.

The pronounced increase in the easterly u-component of the wind between 700 and 500 mb (70 and 50 kPa) differs from the structure of the composite wave developed by Reed et al. (1977). Their results showed easterlies preceding the trough and westerlies behind. The cross section in the study shows easterly dominating the flow before and after the trough. I believe the difference is caused by the shape of the wave in question.

The trough examined in this study had very strong southeasterly winds behind it, which would indicate either a westward tilt to the wave or no tilt at all. The composite wave developed by Reed et al. (1977) had a ∿30° tilt towards the east, thus explaining the southwesterly winds behind the trough. An examination of the trough passage times at each ship supports the concept of a westward tilt to the wave.

By using the trough passage times at 600 mb (60 kPa) and the speed of movement of area of convection (∿11 m/s) from the previous section,

it was estimated the trough in question has a westward tilt of ∿46°±18°. Table 2 (a) gives the time of 600 mb trough passage at each ship and the elapsed time between passage at the Poryv to passage at the other ships. Table 2 (b) gives the estimated elapsed time between passage at Poryv to passage at the other ships, using a tilt of 46°±18° and speed of ∿11 m/s (∿21 knots). Two assumptions used in the calculations were: the trough moved at constant speed across the array, and the trough retained a tilt of 46°±18° as it traveled across the array. (The method of calculation is shown in Appendix B.)

The appearance of the mid-tropospheric wind maximum is significant as far as position is concerned. Carlson (1969) explained the existence of a mid-tropospheric jet as follows:

> "...At middle levels the temperature gradient reverses from that at low levels, and the thermal wind reversal leads to a very narrow easterly jet centered between 600 and 700 mb at 15°-17°N. The strength of the jet is variable in time and space and is often as high as 30 or 40 knots (a shear of 40 or 50 kts from 2000 ft). Outside the region of the African bulge the meridional temperature contrast is less pronounced, and the strong middle level easterlies are therefore confined to the area between long. 15°E and 20°W...."

The position of the jet is significant in two respects: it extends at least 5° latitude further south than Carlson noted, and it extends at least 400 n.m. (741,000 m) further west. Since the maximum wind speeds are consistent with Carlson, I believe the core of the jet is within the GATE A/B-scale ship array. I also believe this supplies further evidence for a trough passage through the GATE area.

It appears that after the trough passage, a strong easterly ridge began dominating the region and forced the band of easterlies south of

Table 2.

a. Actual values of trough passage at 600 mb and the elapsed time between the Poryv and the next ship.

| Ship | Julian day and time of 600 mb trough passage | Elapsed time between passage at Poryv and next ship |
|---|---|---|
| Poryv | 221-1800 GMT | 6±2 hrs; 12±2 hrs; 24±2 hrs |
| Korolov | 222-0000 GMT | |
| Vanguard | 222-0600 GMT | |
| Priboy | 222-1800 GMT | |

b. Estimated elapsed time between Poryv and next ship with a trough tilt of 46°±18° and speed of movement of 11 m/s (21 knots).

| Ship | Estimate Elapsed Time |
|---|---|
| Poryv | 7±2 hrs; 13±2 hrs; 20±2 hrs |
| Korolov | |
| Vanguard | |
| Priboy | |

its normal position. The idea of a strong easterly ridge is supported, to a degree, by Burpee (1975) who showed that the upper level clouds shifted from ∿10°N on Julian day 222 to ∿5°N on Julian day 223.

The increase in mixing ratio deviation or increase in moisture preceding the trough is not in agreement with the composite developed by either Burpee (1974) or Reed et al. (1977). It is also inconsistent with Reed et al. (1977) comment that,

> "...The relative humidity..., is highest where the winds are southerly and lowest in the region of northerly winds...."

These facts have lead me to believe that the increase in moisture was probably due to the instruments going through the convection out ahead of the trough axis. Although the Korolov did not report rain during the period, infrared satellite imagery indicates clouds were in the vicinity of the ship at the time of observation.

Although there is substantial evidence supporting a trough passage in the mid troposphere, evidence supporting the upper tropospheric trough is sparse and sometimes inconsistent. The existence of a trough between 200 and 100 mb (20 and 10 kPa) is substantiated by the wind shift from the northeast to southeast and the abrupt shift in the v-component of the wind from north to south. However the increase in wind speed behind the trough is not well defined. Sometimes it occurs before the trough and sometimes after. Another inconsistency involves the time of trough passage at each ship. Table 3 shows that the trough passed over Korolov and the Vanguard at the same time. This would indicate the tilt of the trough has changed with height or the two waves are independent of each other in the vertical.

Table 3.

Actual values of trough passage at 150 mb and the elapsed time between the Poryv and the next ship.

| Ship | Julian day and time of 150 mb trough passage | Elapsed time between passage at Poryv and next ship |
|---|---|---|
| Poryv | 222-2100 GMT | 7±2 hrs; 7±2 hrs; 15±2 hrs |
| Korolov | 223-0400 GMT | |
| Vanguard | 223-0400 GMT | |
| Priboy | 223-1200 GMT | |

Since it took only 15±2 hours for the trough to travel between the Poryv and the Priboy or ∿15 m/s faster than the mid-tropospheric trough, it is likely that the two troughs are independent of each other. In addition, the strong vertical wind shears present in the upper-troposphere would tend to break down any vertical structure in the wave.

The failure of the wind speed to change more abruptly in the upper-troposphere is puzzling. It indicates that either the easterly jet covered a greater latitudinal area or it was farther south than the mid-troposphere jet. Palmen and Newton (1969) favor the latter view and depict the tropical easterly jet stream (at 20 kPa) off the east coast of Africa centered at ∿8°N. If the idea that the easterly ridge has forced the entire band of easterlies south is true then we should find even stronger winds in the central and southern sectors of the array.

The similarities that appear to be associated with some other synoptic scale phenomenon and the factors discovered after studying the mid- and upper-troposphere troughs tend to support the existence of an easterly ridge. Clearly the shift to the north of the v-component of the wind 15 to 18 hours after the trough would support the passage of a ridge axis. It is also consistent with the v-component field of the composite developed by Reed et al. (1977).

In addition to the factors supporting a ridge over the area, there is evidence of hot dry Saharan air dominating the sector. The decrease in mixing ratio deviation (drying), the shift to the north of the v-component of wind, and the low level warming all support the

idea that hot dry air from the Sahara was dominating the region. This idea is also supported by the way the drying decreases as the distance from the African coast increases. The fact that the low levels become moist as the distance from the coast increases suggests that the air is being modified as it is advected over the ocean. If this hypothesis is true, we should see a decrease in the drying in the central and southern sectors of the array.

The one unaccounted for similarity between the ships is the large-scale cooling present in the middle levels (60 kPa - 20 kPa). Reed et. al (1977) do show middle level cooling associated with an easterly ridge and warming associated with the trough. The lack of warming after trough passage in this case may be attributed to the strength of the trough. The warming associated with the trough could not overcome the cooling associated with the ridge that passed through the area, or the trough has a cold core structure to a higher level. This aspect of the case study will be discussed further in section 4.2.

### 3.3 The Central Sector

Similarities in the cross-sections of the ships making up the central sector are almost identical to those noted for the northern sector. The similarities again can be grouped into three categories: those that appear to be associated with a trough in the lower troposphere, those that appear to be associated with a trough in the upper troposphere, and those that appear to be associated with an easterly ridge. The similarities that appear to be associated with a trough between 700 and 500 mb (70 and 50 kPa) include:

1. A wind shift in the total wind field from northeast to southeast between 700 and 500 mb (70 and 50 kPa). This is also evident in the abrupt shift of the v-component of the wind from north to south between 700 and 500 mb (70 and 50 kPa) (see Figures 14-19 (a) and (d)).
2. A pronounced increase in the easterly u-component of the wind following the wind shift between 700 and 500 mb (70 and 50 kPa) (see Figures 14-19 (c)).
3. The appearance of a wind maximum of at least 15 m/s between 700 and 500 mb (70 and 50 kPa) (see Figures 14-19 (a)).
4. Precipitation preceding the wind shifts between 700 and 500 mb (70 and 50 kPa) (see Figures 14-19 (a)).
5. An increase in mixing ratio deviation of at least 1 gm/kgm preceding the wind shifts between 700 and 500 mb (70 and 50 kPa) (see Figures 14-19 (a)). (It was noted earlier that this is probably due to cumulus scale phenomenon but it is still associated with the trough.)
6. At the ships Meteor and Dallas the u-component of wind field showed an abrupt shift from west to east (see Figures 14 and 19 (c)).

The similarities that appear directly associated with a trough in the upper troposphere include:

1. A wind shift from the northeast to southeast between 200 and 100 mb (20 and 10 kPa). This is also evident in the abrupt shift in the v-component of the wind from north to south between 200 and 100 mb (20 and 10 kPa) (see Figures 14-19 (a) and (d)).
2. The appearance of a wind maximum of at least 20 m/s between 200 and 100 mb (20 and 10 kPa) (see Figures 14-19 (a)).
3. An abrupt shift in the u-component of the wind field from west to east (see Figures 14-19 (d)).

The similarities that appear to be associated with an easterly ridge in the lower troposphere include:

1. Warming in the lower troposphere 9 to 15 hours after the wind shifts between 700 and 500 mb (70 and 50 kPa) (see Figures 14-19 (b)).
2. A decrease of mixing ratio deviation (drying) in the middle and lower troposphere 12 to 27 hours after the wind shifts between 700 and 500 mb (70 and 50 kPa) (see Figures 14-19 (a)).
3. A shift from south to north in the v-component of the wind 15 to 27 hours after the wind shift (see Figures 14-19 (d)).
4. Middle tropospheric cooling during most of the 3-day period.

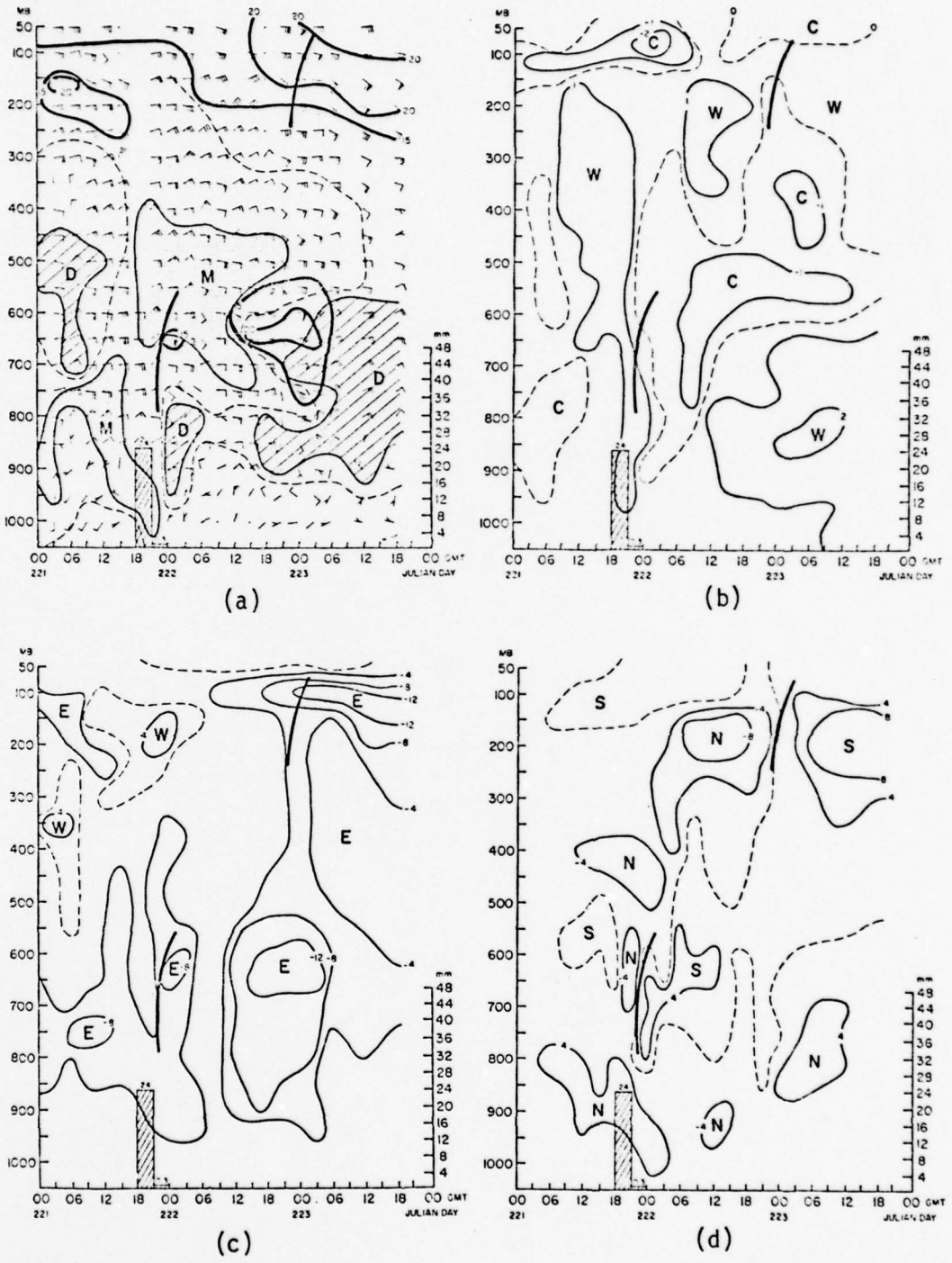


Fig. 14. Time cross-section over the Quadra: a) moisture and wind fields, b) temperature deviation, c) u-wind deviation, d) v-wind deviation.

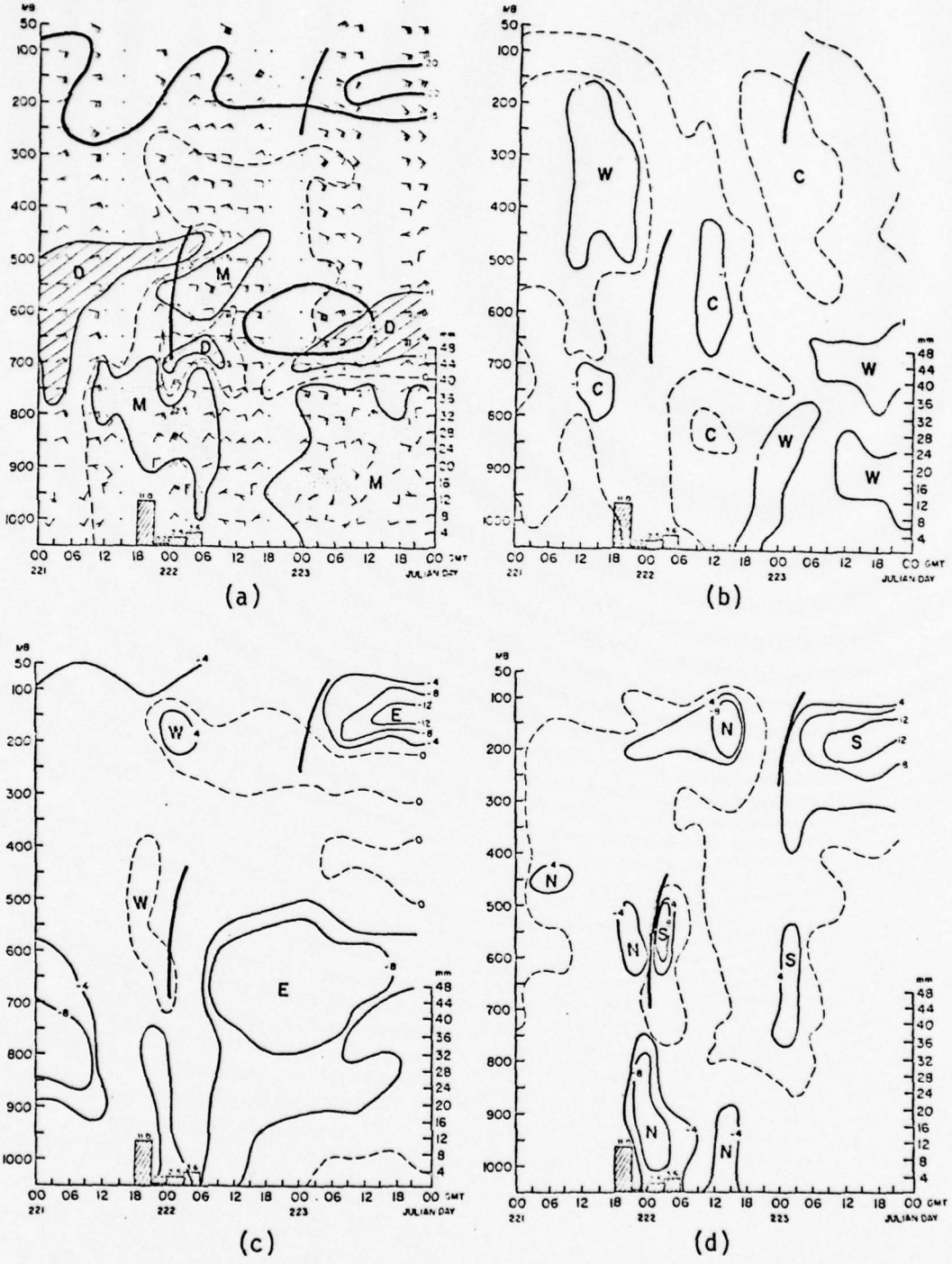


Fig. 15. Time cross-sections over the Meteor: a) moisture and wind fields, b) temperature deviation, c) u-wind deviation, d) v-wind deviation.

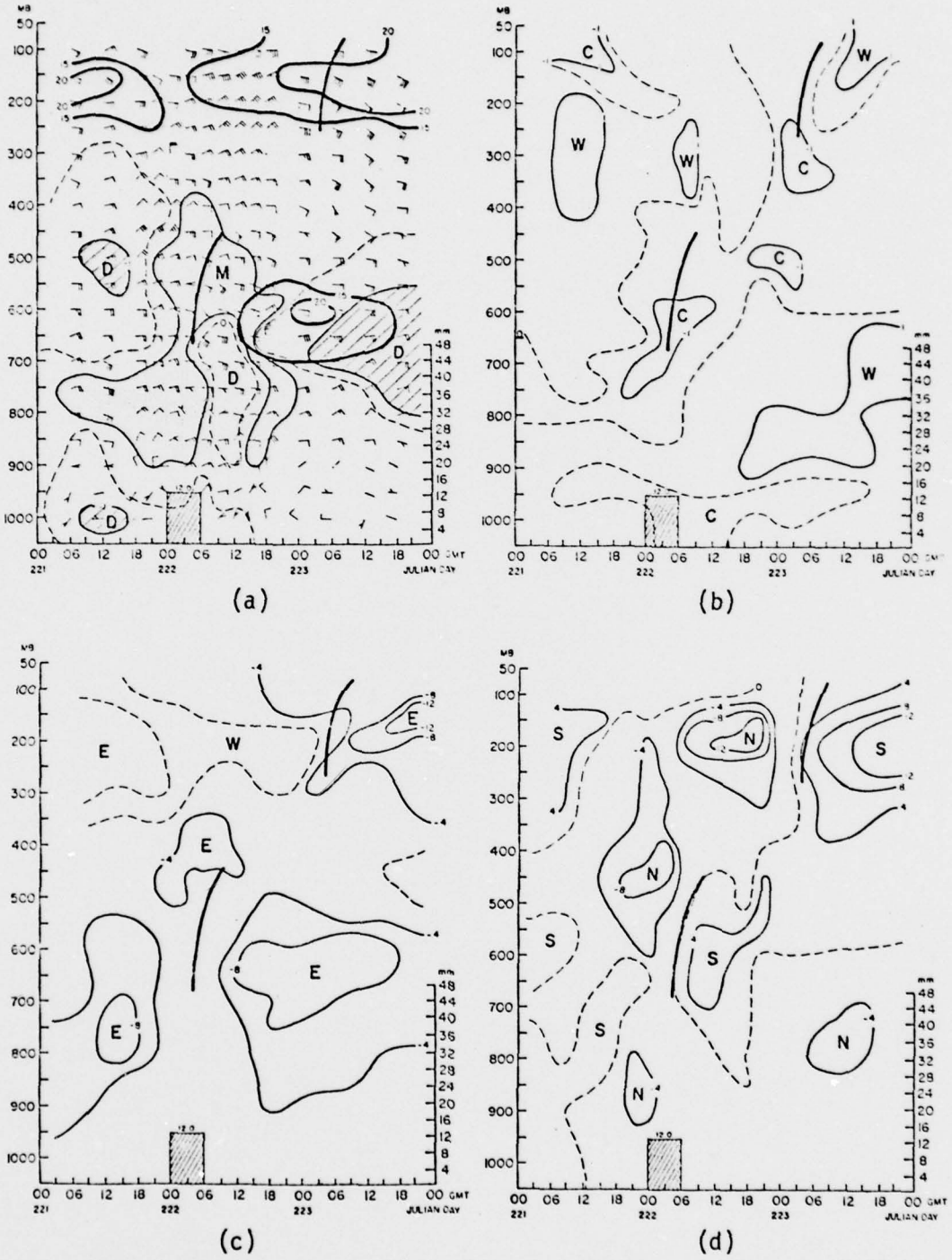


Fig. 16 Time cross-sections over the Oceanographer: a) moisture and wind fields, b) temperature deviation, c) u-wind deviation, d) v-wind deviation.

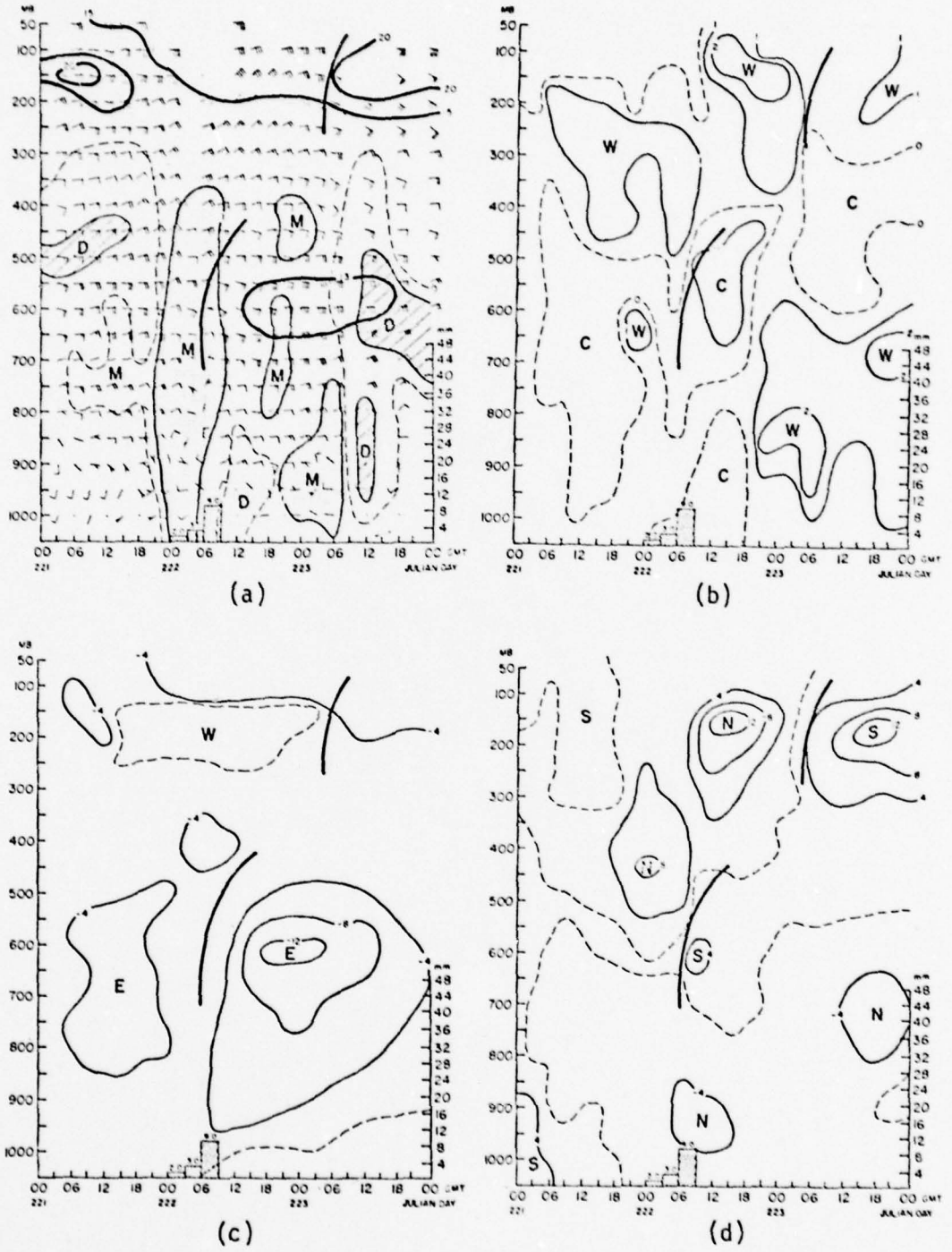


Fig. 17. Time cross-sections over the Vize: a) moisture and wind fields, b) temperature deviation, c) u-wind deviation, d) v-wind deviation.

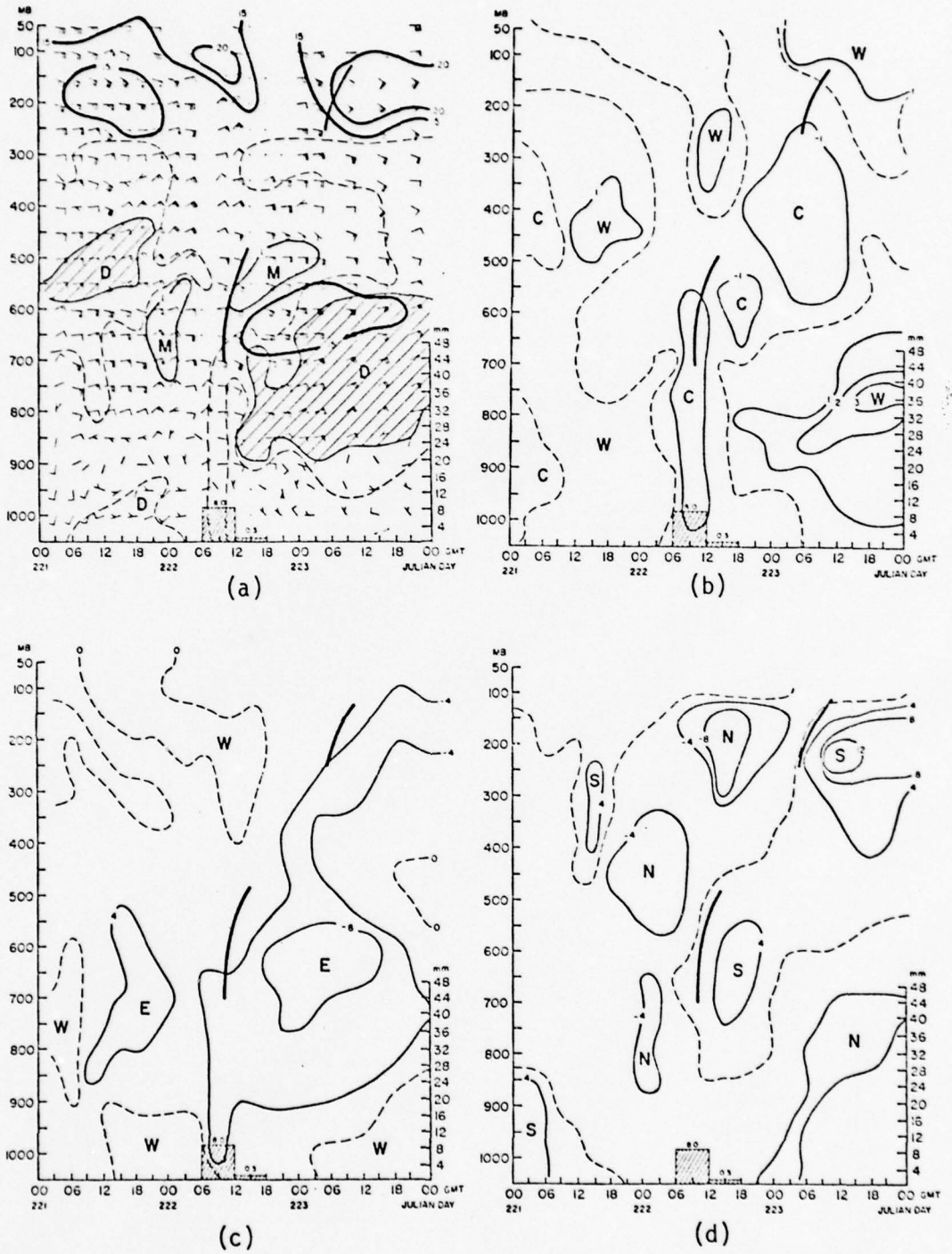


Fig. 18. Time cross-sections over the Gillis: a) moisture and wind fields, b) temperature deviation, c) u-wind deviation, d) v-wind deviation.

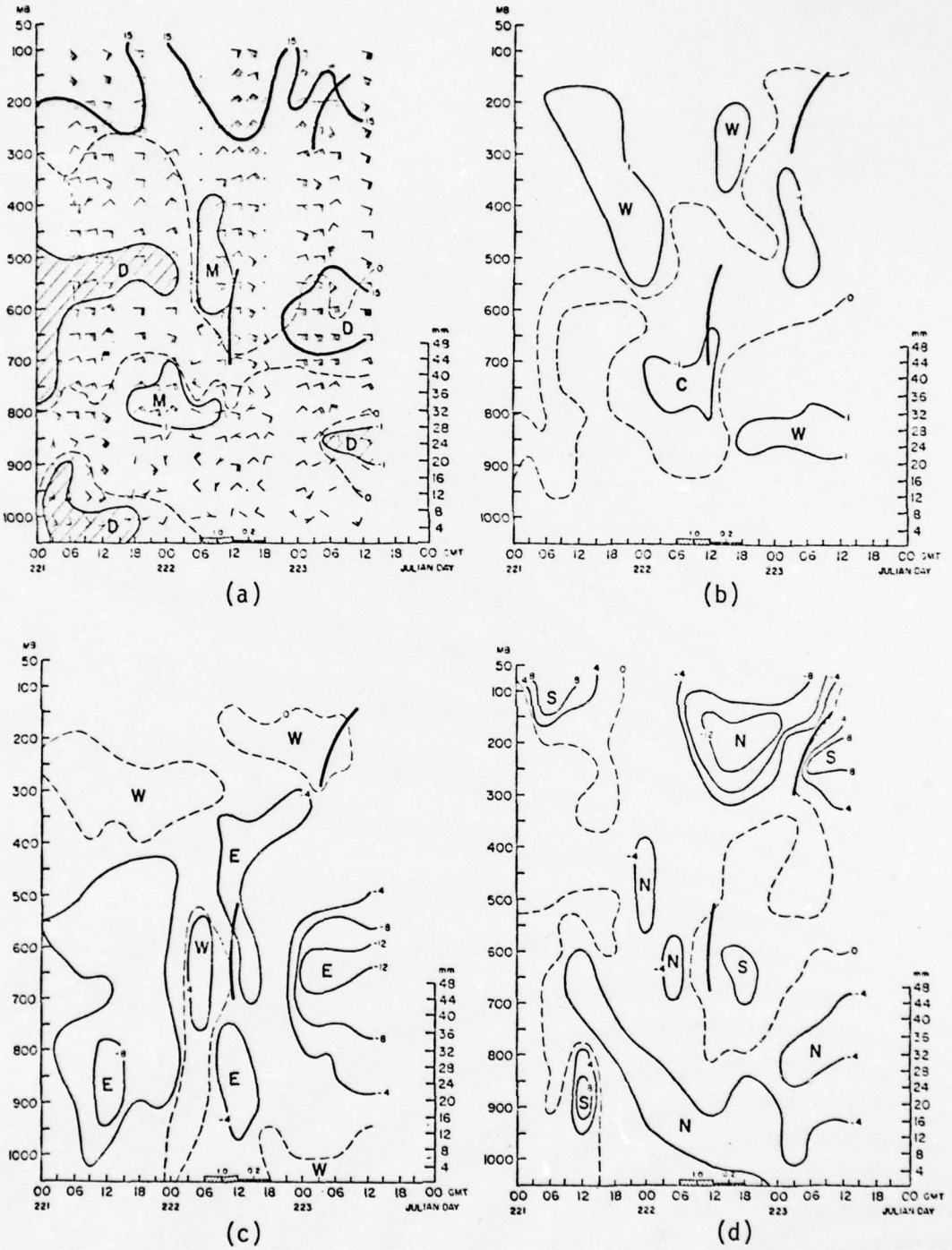


Fig. 19. Time cross-sections over the Dallas: a) moisture and wind fields, b) temperature deviation, c) u-wind deviation, d) v-wind deviation.

The existence of a trough between 700 and 500 mb (70 and 50 kPa) is substantiated by the wind shift from the northeast to the southeast and the abrupt shift of the v-component of the wind from north to south. Several factors which support a trough passage such as the appearance of a wind maximum after the wind shift, the rainfall preceding the trough, and the increase in mixing ratio deviation preceding the wind shift, were discussed in detail in the previous section. In an effort to avoid being repetitive, I have simply mentioned these factors here and refer the reader back to previous sections for a detailed discussion about them. The remainder of this section will be devoted to the differences between the northern and central sectors.

The two features which appear to be significantly different in the central sector are: the tilt of the trough in the horizontal (600 mb surface), and the u-component wind field at the ships Meteor and Dallas. Table 4 (a) gives the times of the 600 mb (60 kPa) trough passage at each ship, and the elapsed time from passage at the Quadra to the next ship. Table 4 (b) gives the estimated elapsed time between the trough passage at the Quadra and the next ship if the trough had a tilt toward the west of 34°±15°[7] and moved at the speed of 11 m/s (≈21 knots) (see Appendix B).

The assumptions made in the estimation were that the trough retains a constant tilt and moves at a constant speed and direction.

---

[7]The 34°±15° was arrived at by trial and error. The objective was to estimate an angle that together with the speed of 21 knots would yield times that were close to the actual times.

Table 4.

a. Actual trough passage values.

| Ship | Julian day and time of 600 mb trough passage | Elapsed time between passage at Quadra and next ship |
|---|---|---|
| Quadra | 222-0000 GMT | 3±2 hrs; 6±2 hrs; 9±2 hrs; 12±2 hrs |
| Meteor | 222-0300 GMT | |
| Oceanographer | 222-0600 GMT | |
| Vize | 222-0600 GMT | |
| Gillis | 222-0900 GMT | |
| Dallas | 222-1200 GMT | |

b. Estimated trough-tilt 34°±15°, speed 11 m/s (~21 knots).

| Ship | Estimate Elapsed Time |
|---|---|
| Quadra | 3±2 hrs; 5±2 hrs; 8±2 hrs; 11±2 hrs |
| Meteor | |
| Oceanographer | |
| Vize | |
| Gillis | |
| Dallas | |

The twelve degree difference in tilt between the northern and central sectors indicates that the trough changes shape from north to south. A factor which indicates a change in structure as well as shape is the u-component wind field at the Meteor and Dallas. Both ships are located near eight degrees north latitude, and both show an abrupt shift from west to east in the u-component wind field. The abrupt change in both the v- and u-component fields indicates that there is a strong cyclonic shear in that portion of the trough. Although this data is not conclusive, it appears likely that a vortex could be located near eight degrees north latitude. The possibility of a vortex is discussed in section 5.2.2 of the paper.

Another factor which is significant is the existence of the mid-troposphere jet. The jet appears at all six ships which is further evidence of the extreme southern shift of the easterlies after the trough passage.

Although the structure of the mid-tropospheric trough does vary slightly between the two sectors, the similarities associated with upper tropospheric trough vary considerably between the two sectors. The similarities associated with the upper tropospheric trough indicate that the trough is better developed in the central sector. In addition to the wind shift from northeast to southeast, the abrupt shift in the v-component wind field from north to south and the appearance of a stronger wind maximum, there is also an abrupt change from west to east in the u-wind field at 5 of the 6 ships. This together with a closer association between the trough and the 20 m/s isotach support a well developed trough in the upper troposphere.

The increase in winds also supports the premise made in the previous sector that the upper tropospheric jet should appear stronger because the climatic position is farther south.

The strong wind shears are also present in the central sector which provides further evidence that the upper level and the middle level troughs are not closely related in the vertical. Table 5 gives the trough passage at each ship and the elapsed time from the Quadra to the Meteor. Since the trough appeared over both the Gillis and the Dallas at the same time, it would indicate that the trough in the upper-troposphere has a different shape in the horizontal than the mid-tropospheric trough.

The similarities that appear to be associated with an easterly ridge support the findings noted in the previous section. The shift in the v-component of the wind from south to north and the drying clearly support an easterly ridge. In addition the extent and magnitude of the drying at each ship also support the hypothesis that warm dry Saharan air was dominating the region. Once again the drying was the strongest at the northernmost ship and decreased rapidly from north to south. In fact the Meteor's cross-section showed the drying confined to a region between 700 and 600 mb (70 and 60 kPa) with an increase in moisture below. The Dallas cross-section shows a very slight and weak warming with a slight increase in moisture dominating most of the lower-troposphere.

The cooling in the mid-troposphere continued to dominate the region. Again, it appears that the cooling associated with the easterly ridge passing through the area is simply dominating any

Table 5.

Actual values of trough passage at 150 mb and the elapsed time between the Quadra and the next ship.

| Ship | Julian day and time of 600 mb trough passage | Elapsed time between passage at Quadra and next ship |
|---|---|---|
| Quadra | 223-0000 GMT | 3±2 hrs; 6±2 hrs; 9±2 hrs |
| Meteor | 223-0300 GMT | 6±2 hrs; 9±2 hrs |
| Oceanographic | 223-0600 GMT | 9±2 hrs |
| Vize | 223-0600 GMT | 9±2 hrs |
| Gillis | 223-0900 GMT | 9±2 hrs |
| Dallas | 223-0900 GMT | 9±2 hrs |

warming associated with the trough, or the trough in this case is cold core to higher levels. The temperature structure of the trough is discussed in detail in section 4.2.

3.4 The Southern Sector

The similarities in the cross-sections of the ships in the southern sector are slightly different than those of the northern and central sectors. The lower troposphere appears dominated by zonal flow and there is very little evidence of a trough over the sector. There are two kinds of similarities that can be grouped in the same categories that were used in the previous sections: those that appear associated with a trough in the upper-troposphere, and those that appear associated with an easterly ridge. The factors that support zonal flow are almost the opposite of those that support a trough:

1. No easily identifiable wind shift from northeast to southeast (see Figures 20-23 (a)).
2. A uniform field of the u-component of the wind (see Figures 20-23 (d)).
3. A uniform field of mixing ratio deviation (see Figures 20-23 (a)).
4. A weak wind maximum appears at only two of the four ships (see Figures 20-23 (a)).
5. The precipitation that would be associated with the trough previously identified was only reported at the Researcher. (The Researcher data is hard to evaluate because

the ship was off station for the first half of the period.) (See Figures 20-23 (a).)

6. The v-component of the wind does show a weak shift from north to south at the Zubov and the Okean, but without other supporting data the position or strength of a wave cannot be determined (see Figures 20-23 (d)).

The similarities that appear directly associated with an upper troposphere trough include:

1. A wind shift from northeast to southeast between 200 and 100 mb (20 and 10 kPa). This is also evident in the abrupt shift in the v-component of the wind from north to south (see Figures 20-23 (a) and (d)).
2. The appearance of a wind maximum of at least 20 m/s (see Figures 20-23 (a)).

Although the similarities that support the existence of an easterly ridge are not as conclusive as those in the northern and central sectors, they are present and include:

1. Cooling in the middle levels throughout the period (see Figures 20-23 (b)).
2. Warming in the lower levels at all ships in the later part of the period (see Figures 20-23 (b)).
3. Weak dominance of the northerly v-component of the wind during the second half of the period (see Figures 20-23 (d)).

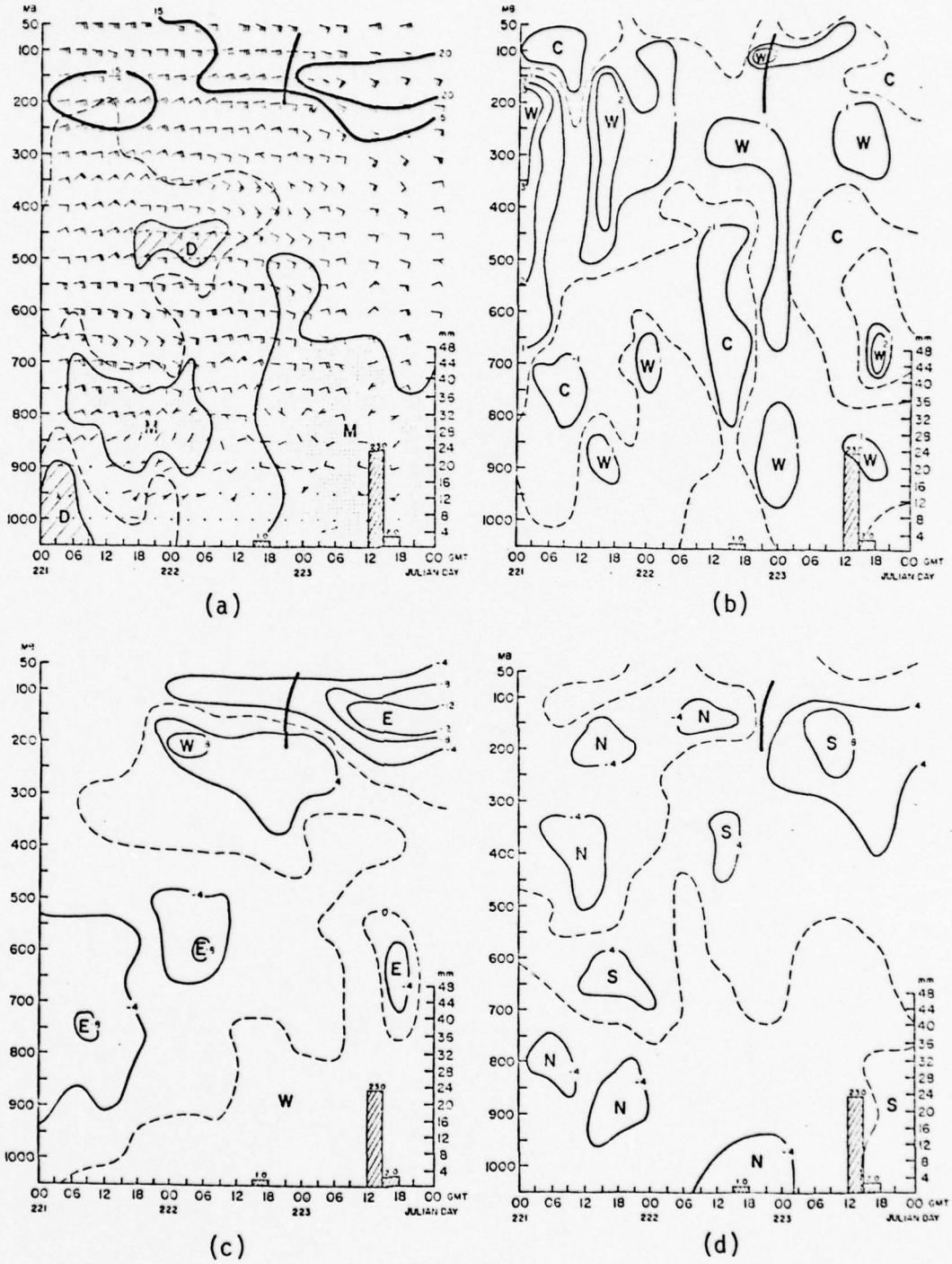


Fig. 20. Time cross-sections over the Krenkel: a) moisture and wind fields, b) temperature deviation, c) u-wind deviation, d) v-wind deviation.

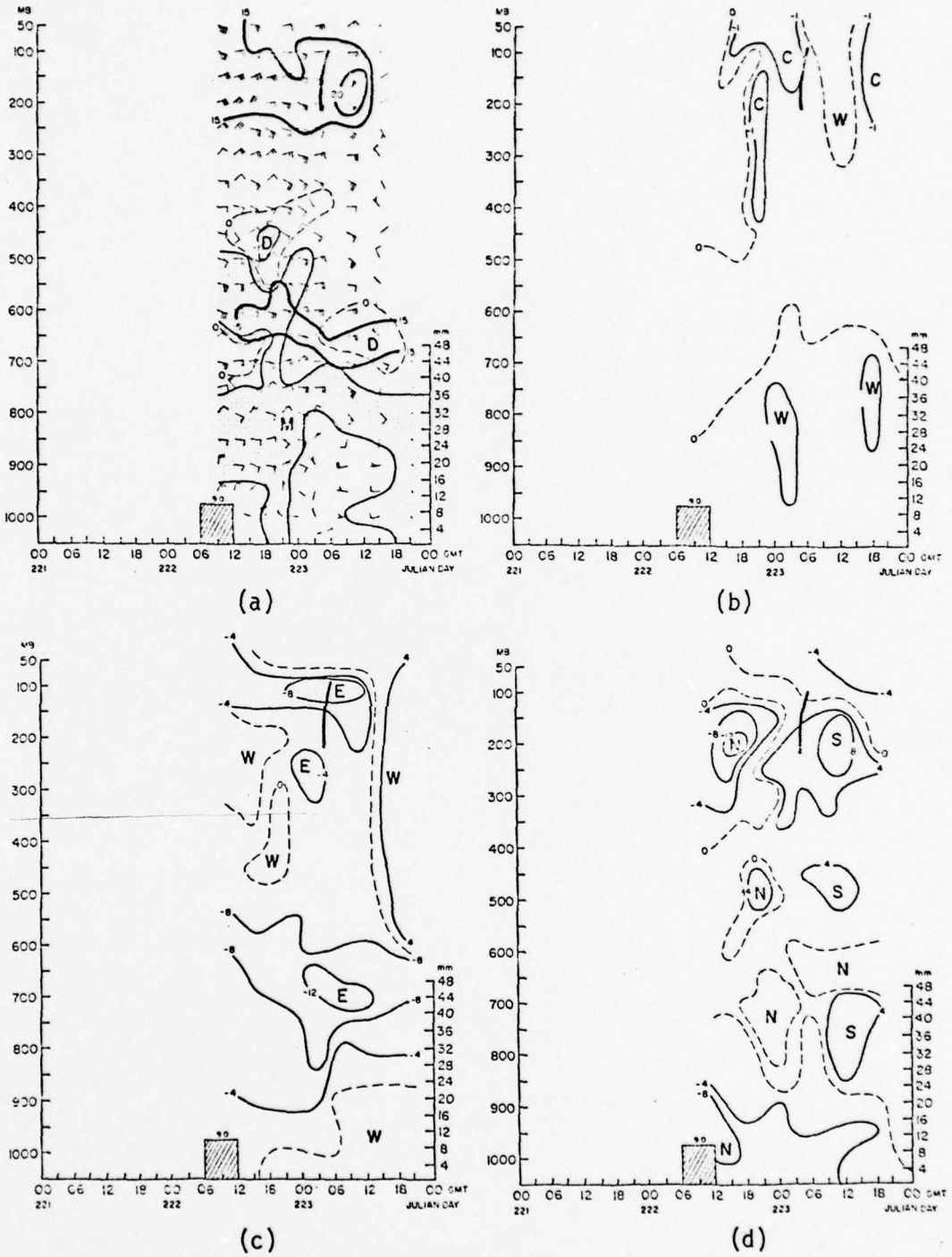


Fig. 21. Time cross-sections over the Researcher: a) moisture and wind fields, b) temperature deviation, c) u-wind deviation, v-wind deviation.

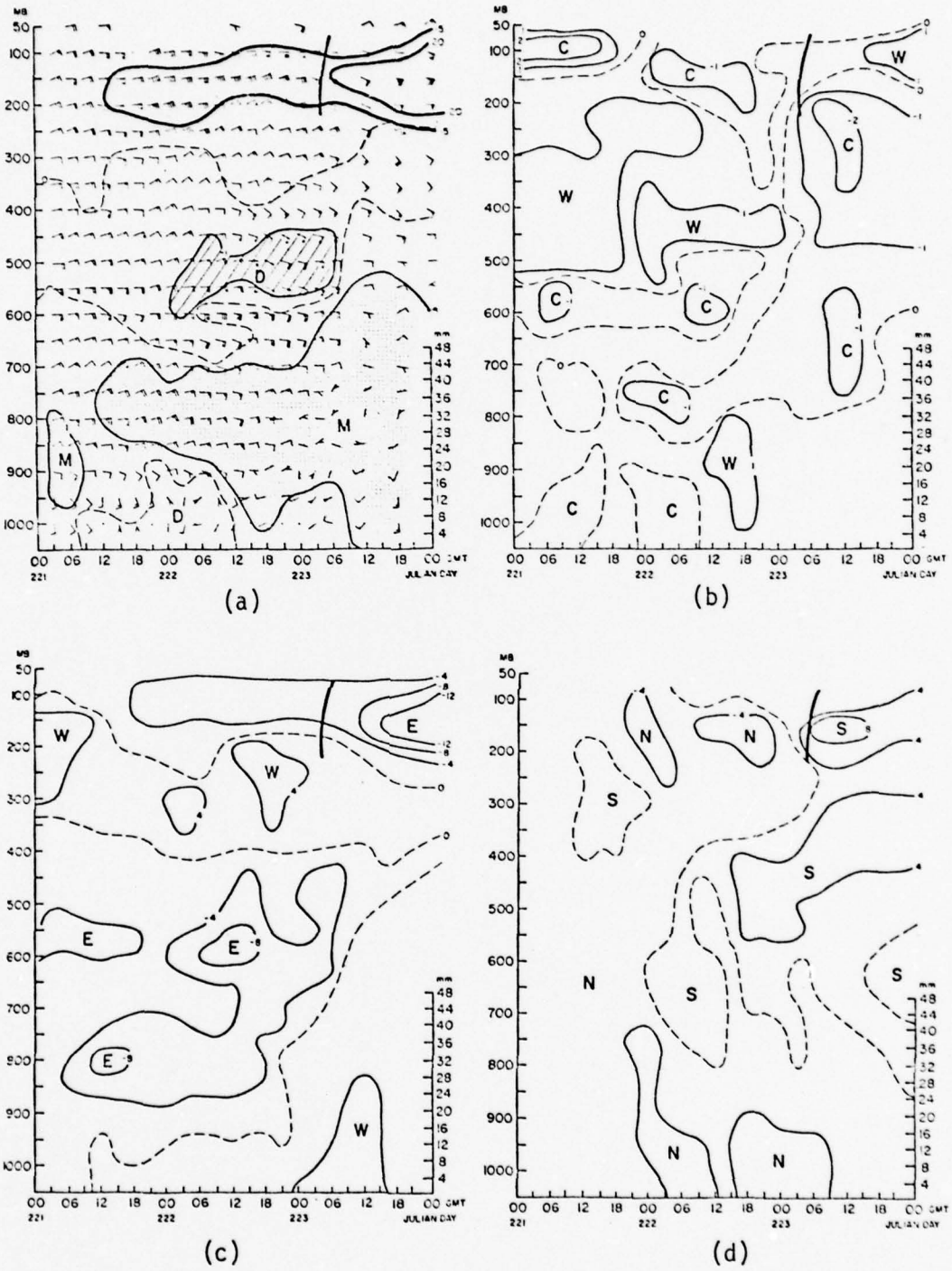


Fig. 22. Time cross-sections over the Zubov: a) moisture and wind fields, b) temperature deviation, c) u-wind deviation, d) v-wind deviation.

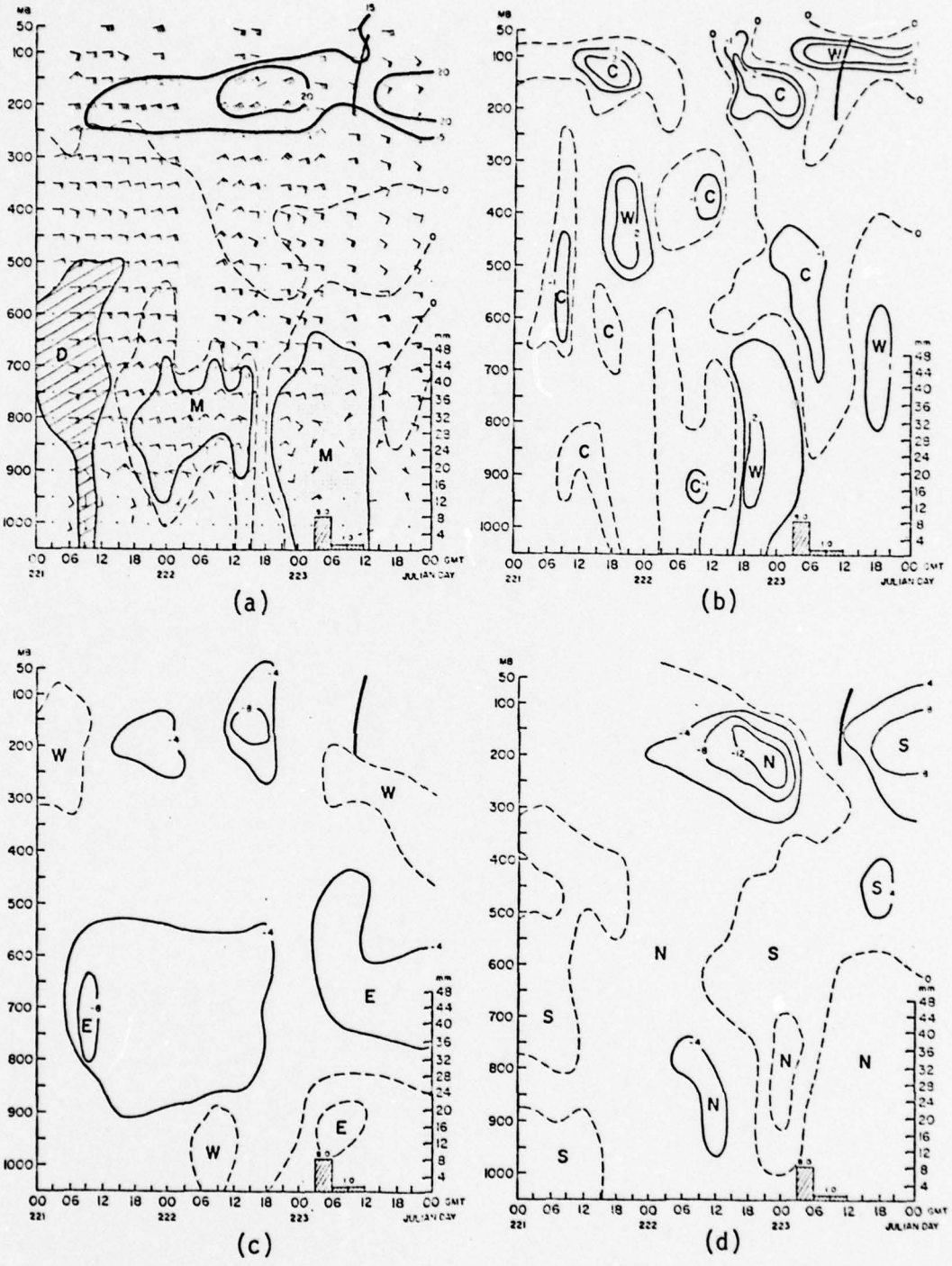


Fig. 23. Time cross-sections over the Okean: a) moisture and wind fields, b) temperature deviation, c) u-wind deviation, d) v-wind deviation.

4. An increase in moisture in the lower levels during the later part of the period (see Figures 20-23 (a)).

The existence of near zonal flow in the southern sector is still consistent with the wave structure developed by Reed et al. (1977). The composite wave they developed became nearly zonal between 4° north and the equator. This is only one degree latitude south of the most southerly ship in the A/B-scale array. The existence of zonal flow is important because it delineates the southern boundary of the wave.

The precipitation that was recorded at the Krenkel and Okean was an effect of a second system and not the wave identified in the previous sections. The fact that precipitation was not recorded early in the period at the three most southern ships supports the premise that the wave was either weak or nonexistent.

The fact that there is still support for a trough in the upper-troposphere is consistent with the earlier theory that the upper-tropospheric trough should extend further south than the mid-tropospheric system. Table 6 shows the trough passage times at each ship and the elapsed time from the passage at the first ship to the next. The timing is generally consistent with that determined earlier. The time of passage at the Okean seems a little early but there are two possible explanations for this irregularity: the time resolution factor, and the possibility that the wave may have changed structure during the latter part of the period. (The reader is referred to the previous two sections for a detailed discussion of the specific factors supporting the upper air trough.)

Table 6.

Actual values of trough passage at 150 mb and the elapsed time between the Krenkel and the next ship.

| Ship | Julian day and time of 150 mb trough passage | Elapsed time from Krenkel to next ship | |
|---|---|---|---|
| Krenkel | 222-2100 GMT | | |
| Researcher | 223-0600 GMT | 9±2 hrs | 15±2 hrs |
| Zubov | 223-0600 GMT | | |
| Okean | 223-1200 GMT | | |

The factors supporting an easterly ridge are identical to those noted earlier with the exception of an increase in moisture in the lower levels. In the previous sections drying was evident throughout the lower levels. The drying was attributed to dry Saharan air being advected over the ocean. The increase in moisture apparent in the southern sector supports an earlier premise that if Saharan air caused the drying its effect should decrease as the distance from the Sahara increases. Another factor contributing to the increase in moisture is the zonal flow dominating the area.

The zonal flow in the southern sector tends to bring moist air into the region. The moisture is a result of the increased distance from the coast and the "Tropical Wet" (Trewartha, 1968) climatic that persists along the coast at 8° north latitude.

The warming in the low levels and the weak dominance of the northerly v-component of the wind support a weak easterly ridge in the region. Like the trough it seems that the southern extent of the easterly ridge is also within the southern sector.

The cooling evident in both the northern and central sectors is again dominant in the southern region (see section 4.2 for a further explanation).

## 4.0 MERIDIONAL CROSS SECTIONS

### 4.1 General

In an effort to get a different perspective of the structure of the atmosphere during the three day period and to directly combine data from other ships into the analysis, meridional cross-sections were plotted and analyzed. The ships making up the cross-sections were located along the 23.5 meridian and included: the Korolov, Vanguard, Vize, Oceanographer, Researcher, and Zubov. Four parameters were plotted and analyzed: u-wind component, v-wind component, relative humidity and temperature deviation from the phase mean. The value of each parameter was plotted at the surface and then at 50 mb (5 kPa) intervals from the 1000 mb (100 kPa) level to the 50 mb (5 kPa) level. Cross-sections were contructed at six hour intervals starting at 0000 GMT on Julian day 221 and ending at 0000 GMT on Julian day 224. The analysis of the meridional cross-sections substantiated some of the earlier findings about the atmospheric structure and also yielded some new findings.

### 4.2 Observations

The observations of the period can be divided into two general categories: those that substantiate earlier findings and those that were obvious only from the meridional cross-sections. The results that were obvious from both the time cross-section analysis and the meridional cross-section analysis included: the increase in a mid-tropospheric wind maximum after the trough passage, the warming and drying of the mid levels (approximately 950 to 500 mb (95 to 50 kPa)),

and the increase in moisture over the area immediately before and during the trough passage. Since these results were covered in detail in the previous section, they will not be discussed in this section. The material covered in this section will deal specifically with results which were obvious only from the meridional cross-section. The results that were found include: identifying the low level confluence zone, identifying the thermal structure of the atmosphere as the wave passed over the area, and finally noting the structure of the troposphere as the wave axis approached the ships making up the meridional cross-section.

The first significant finding was identifying and locating a low level (below 95 kPa) confluence zone. The extent and location of the confluence zone became apparent from the analysis of the u- and v-component of the wind. The period actually began with no evidence of a confluence zone within the area. Southwesterly flow dominated the low levels of the northern half of the section and southeasterly flow dominated the low levels of the southern half. However, within 12 hours northwesterly winds were dominating the central ship, and southeasterly flow was dominating the southern ship. From the wind structure described, it was obvious that a strong confluence zone existed between the Korolov and Vanguard. The confluence zone traversed the area during the 3 day period and Figure 24 depicts the location of the zero change line of v-component of the wind (the center of the confluence zone) at the surface with respect to ship location and time. The confluence zone gradually shifted southward through the area and then rapidly moved northward late in the period.

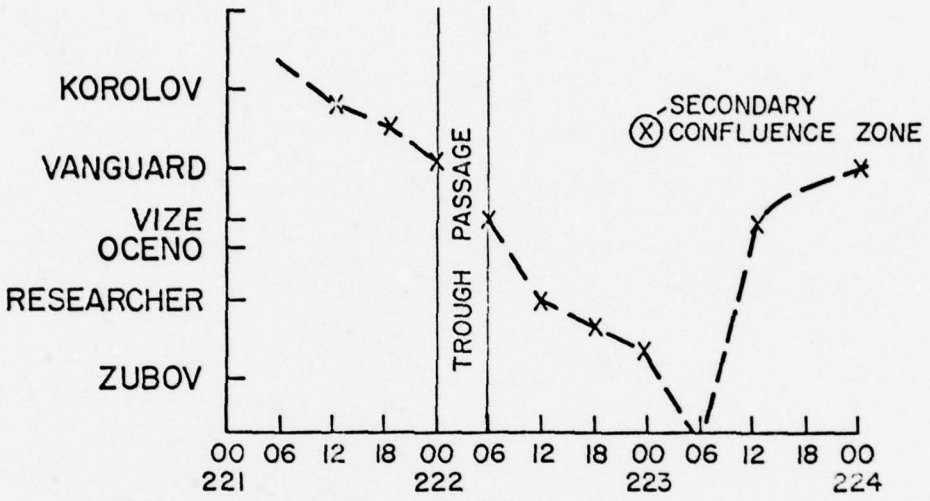


Fig. 24. Location of the intersection of the o change line of the v-component of the wind and the surface (i.e. the center of the surface confluence zone).

The shift of the confluence zone is supported, to a degree, by the location of the convection as depicted in Figures 5, 6 and 7 in an earlier section. The movement is also supported by Burpee (1975). His time section of upper level clouds showed a definite oscillation in the upper level cloud pattern. It oscillated from approximately 10° north latitude (0000 GMT, Julian day 221) to approximately 5° north latitude (0600 GMT, Julian day 223) and then gradually shifted to 9° north latitude (0000 GMT, Julian day 224). Section 5.2.1 describes the structure of the confluence zone in greater detail.

Another result which became obvious after the meridional cross-sections were analyzed was the large changes in the temperature field across the area in both the vertical and horizontal extent. Figure 25 shows two meridional cross-sections for time period 36 hours apart which demonstrate the fluctuations in the thermal field. Figure 25 (a) depicts the temperature structure of the troposphere as the axis of the trough approaches the center of the ship array. It is readily apparent that the atmosphere is colder than the phase mean temperature below 500 mb (50 kPa), warmer between 500 mb and 150 mb (50 kPa and 15 kPa), and then colder again about 150 mb (15 kPa). The extreme deviations occur over the Vanguard and Vize which leads to the premise that the wave is cold core below 500 mb (50 kPa). Although the data available does support a cold core structure, it is impossible to determine where the most intense region of the wave was because data was not available from either the Researcher or Oceanographer at 0600 GMT on Julian day 222. This result is in agreement with Carlson (1969) who noted that easterly wave over the African land mass was

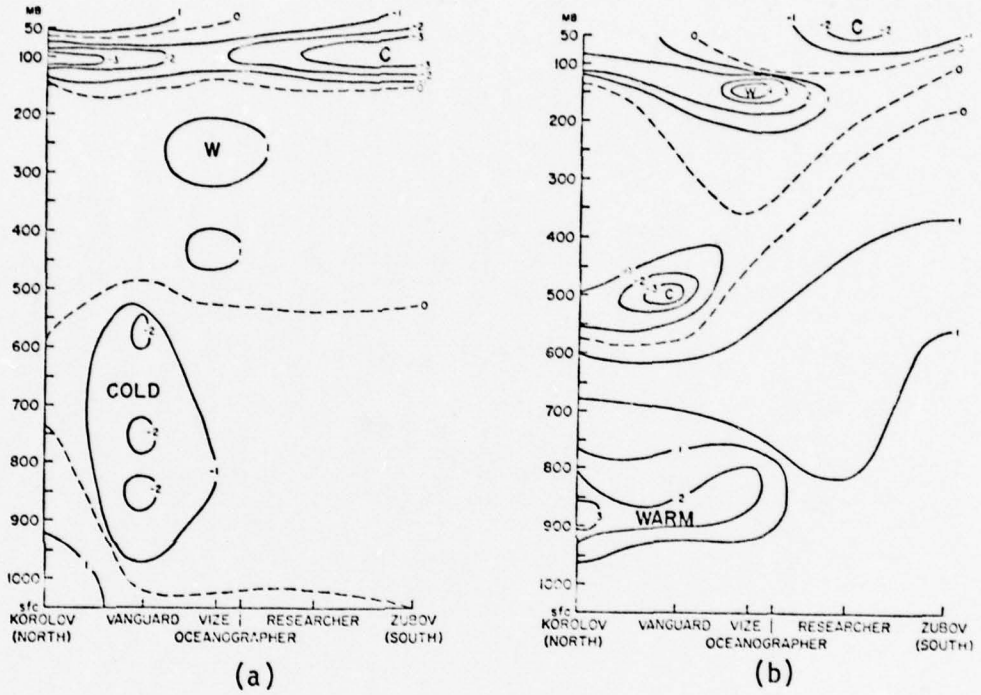


Fig. 25. Meridional cross-sections of temperature deviation: a) before trough passage, b) after trough passage.

cold core up to 500-600 mb (50-60 kPa). Figure 25 (b) depicts the temperature structure of the troposphere after the trough axis passed the center of the ship array. It is obvious that the thermal structure has reversed. Below 500 mb (50 kPa) the temperature is higher than the phase mean. The large temperature change is demonstrated by comparing the 850 mb (85 kPa) temperature at the Vanguard which changed 3°C in 36 hours. The warming that is evident in the troposphere is probably due to the warm dry air that has previously been associated with the ridge that followed the wave through the ship array.

The final result that can be derived from the meridional cross-sections is the structure of the troposphere when the trough axis was near the Vanguard, Vize, and Oceanographer. Figure 26 depicts the u- and v-wind components, the temperature deviation from the phase mean and the relative humidity at 0600 GMT on Julian day 222 (time and date estimated from the time cross-section, when the trough axis was closest to the three ships). Figure 26 (a) shows a weak westerly component to the wind with a strong easterly component above 900 mb (90 kPa). This combined with the information from Figure 26 (b) which shows that the v-component has a northerly component north of the Vize and southerly component south of the ship, shows a strong region of low level confluence centered over the Vize. Again looking at both (a) and (b) of Figure 26, it is obvious the northeasterly winds dominate the atmosphere from 950 mb (95 kPa) to 100 mb (10 kPa). This structure indicates the trough axis in the middle levels has not yet passed over the three ships. Figure 26 (c) shows the thermal

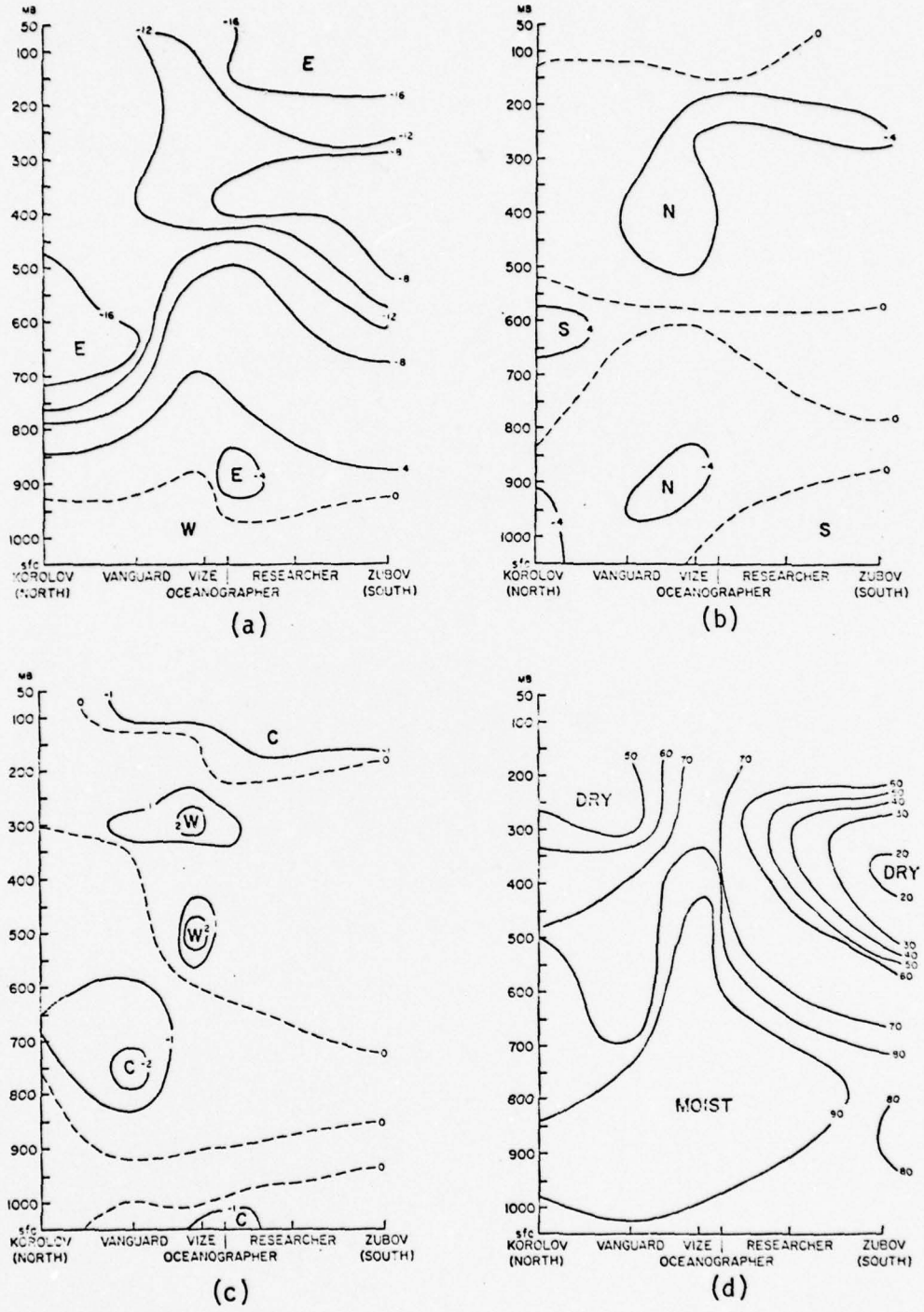


Fig. 26. Meridional cross-sections of the atmosphere immediately before the trough axis passed over the Vanguard, Vize, and Oceanographer: a) u-wind, b) v-wind, c) temperature deviation, d) relative humidity.

structure of the troposphere which shows strong evidence of the cold core structure of the wave below 600 mb (60 kPa). Figure 26 (d) depicts the relative humidity over the area and shows relative humidity of over 80% extending to 300 mb over the center of the array. The peak of the relative humidity over the Vize is even more pronounced because low relative humidity is present on either side of the peak. Since it is evident that strong convective activity is present in the area at this time (see Figure 5, time longitude section of satellite IR imagery) the moistening is probably caused by the instrument passing through the convective elements and the low relative humidities are probably due to convective scale subsidence occurring on either side of the convective elements.

## 5.0 ANALYSIS OF SELECTED LEVELS OVER THE GATE ARRAY

### 5.1 General

In order to complete the analysis of the three day period, streamline analyses were drawn for the surface, 600 mb (60 kPa) and 150 mb (15 kPa) levels over the GATE A/B and B-scale ship arrays. The hourly World Meteorological Organization (WMO) observation winds were used for the surface analysis. Because of continuity considerations analyses were drawn for each hour during the period. However, only the analysis for each synoptic hour are presented in Figures 27-38. The synoptic hour rawinsonde data were used for the 600 mb (60 kPa) and the 150 mb (15 kPa) analyses. The author did attempt to incorporate both dropsonde and aircraft data into the analysis, but the data did not correspond to either the area (dropsonde data) or the levels (aircraft data) being analyzed.

The particular levels were chosen as a result of findings described earlier in the paper. The surface was chosen in order to better analyze the low level confluence field that was noted from the analyses of the meridional cross-sections. The 600 mb (60 kPa) level was chosen because it appeared from the time-cross sections that the easterly trough was most clearly defined at that level. The 150 mb (15 kPa) surface was chosen because, from the earlier analysis, it appeared to be the level of strongest wind speed. In addition, I wanted to see if any relationship existed between the flow pattern of 600 mb (60 kPa) and the one at 150 mb (15 kPa).

In addition to the streamline analysis, a mosaic of radar echoes from the Quadra, Oceanographer, Researcher, and the Gillis were

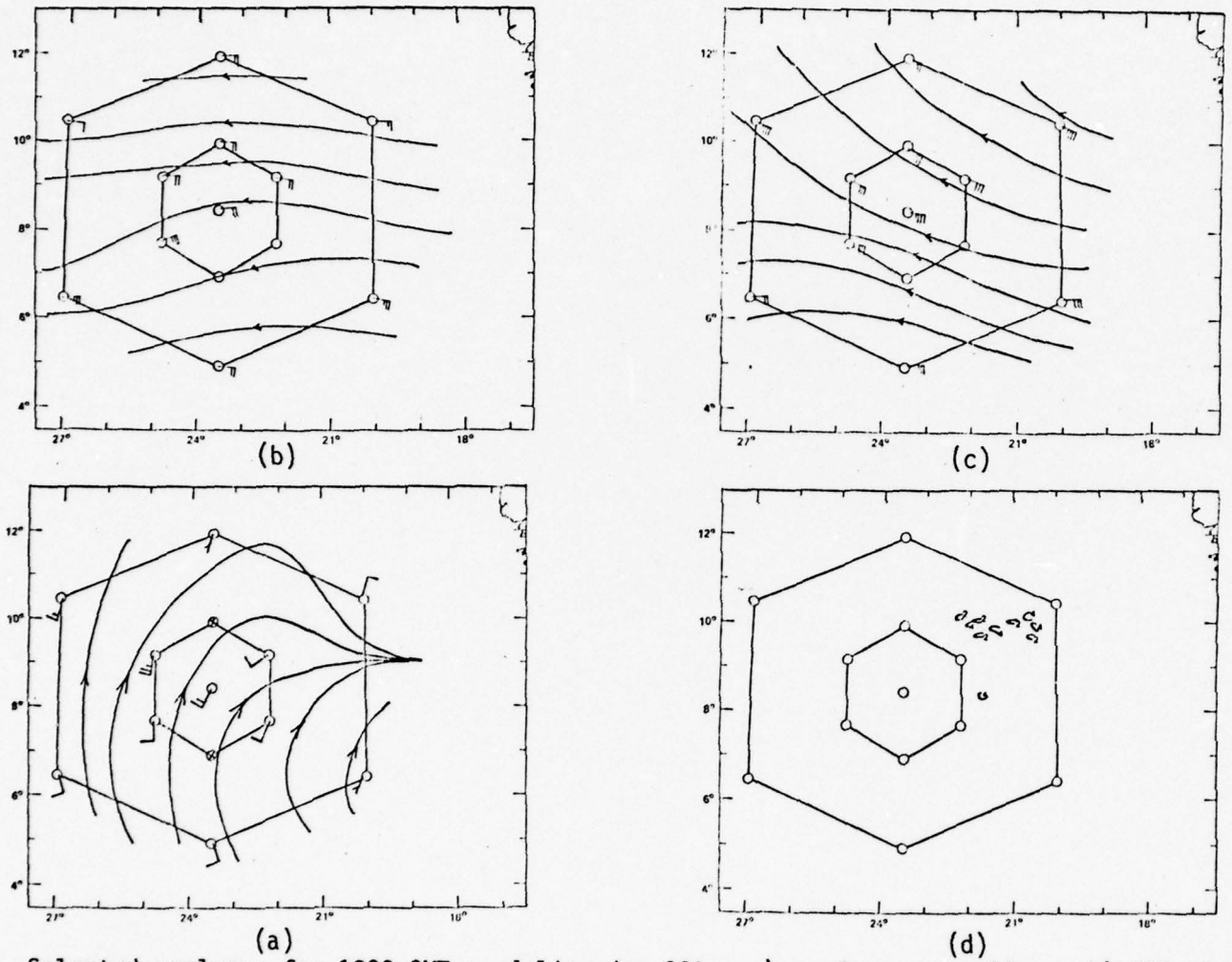


Fig. 27. Selected analyses for 1200 GMT on Julian day 221: a) surface streamlines, b) 600 mb (60 kPa) streamlines, c) 150 mb (15 kPa) streamlines, d) radar mosaic.

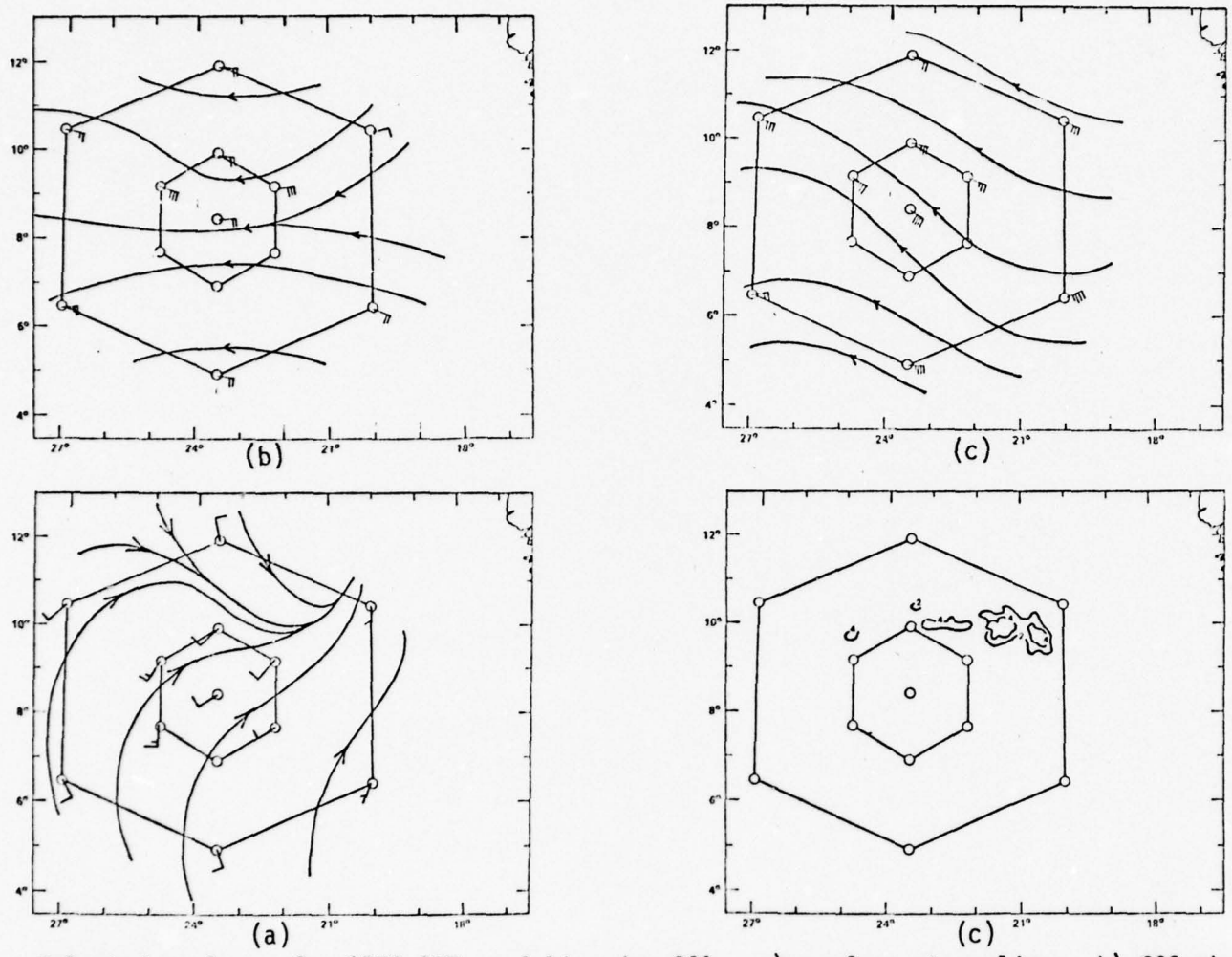


Fig. 28. Selected analyses for 1500 GMT on Julian day 221: a) surface streamlines, b) 600 mb (60 kPa) streamlines, c) 150 mb (15 kPa) streamlines, d) radar mosaic.

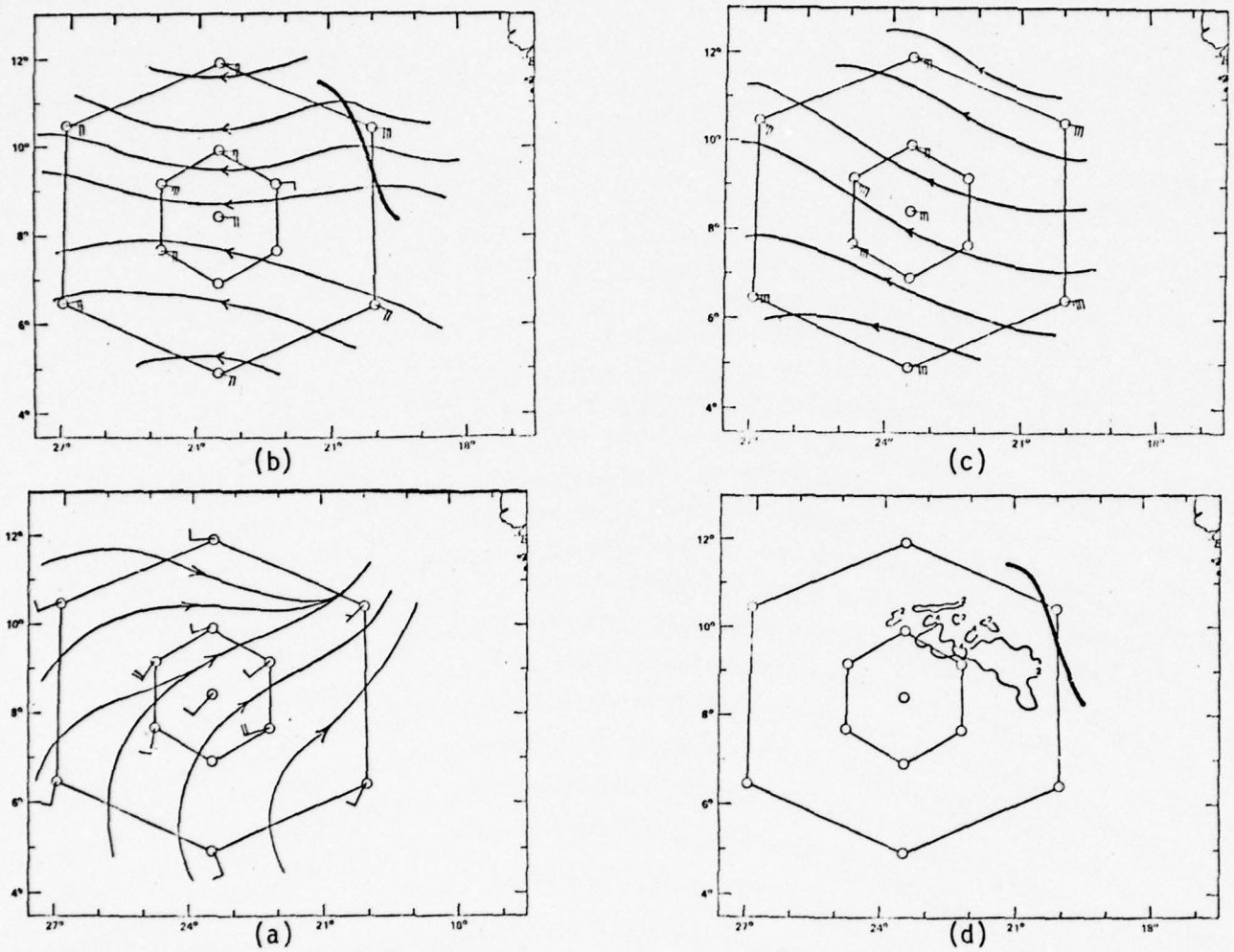


Fig. 29. Selected analyses for 1800 GMT on Julian day 221: a) surface streamlines, b) 600 mb (60 kPa) streamlines, c) 150 mb (15 kPa) streamlines, d) radar mosaic.

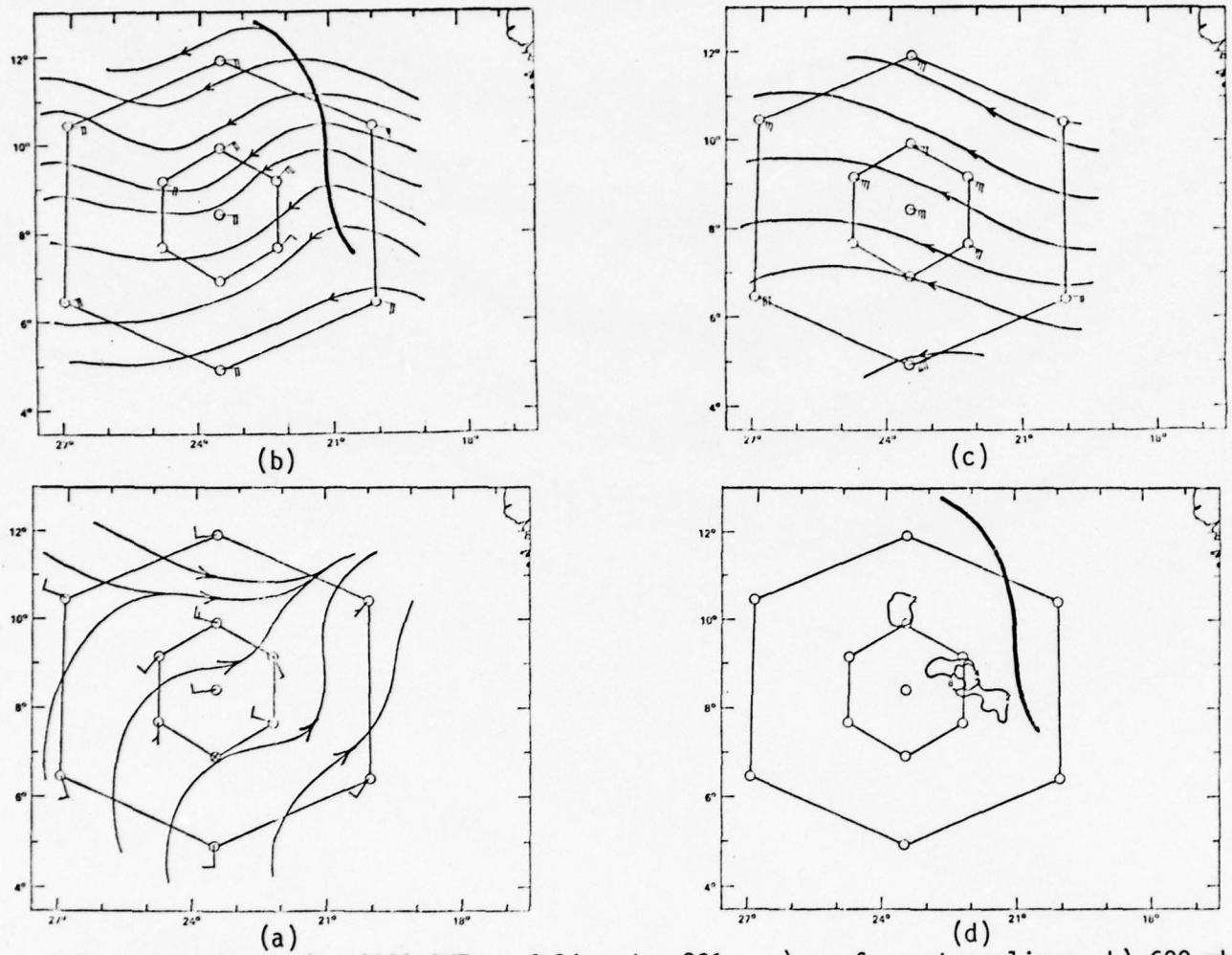


Fig. 30. Selected analyses for 2100 GMT on Julian day 221: a) surface streamlines, b) 600 mb (60 kPa) streamlines, c) 150 mb (15 kPa) streamlines, d) radar mosaic.

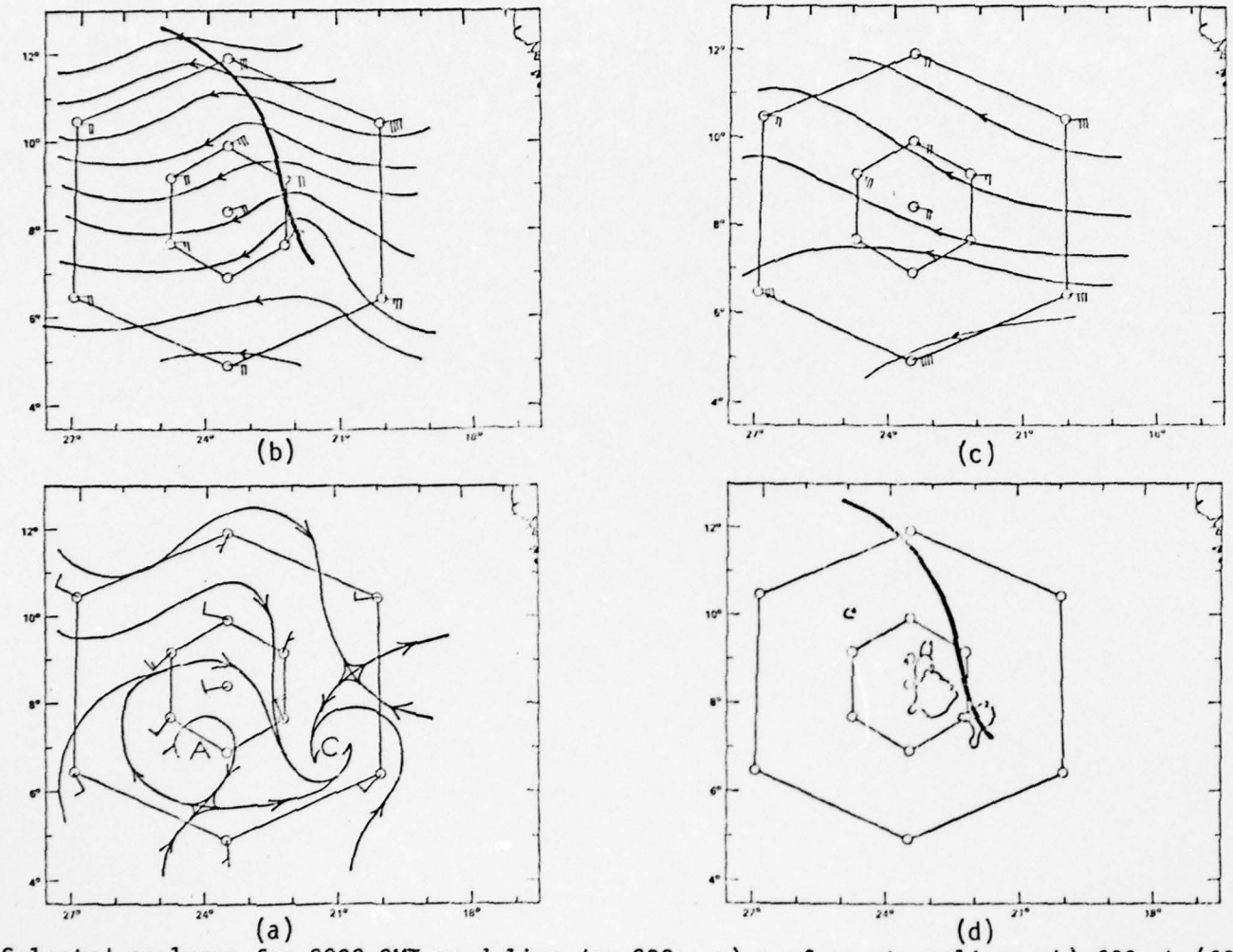


Fig. 31. Selected analyses for 0000 GMT on Julian day 222: a) surface streamlines, b) 600 mb (60 kPa) streamlines, c) 150 mb (15 kPa) streamlines, d) radar mosaic.

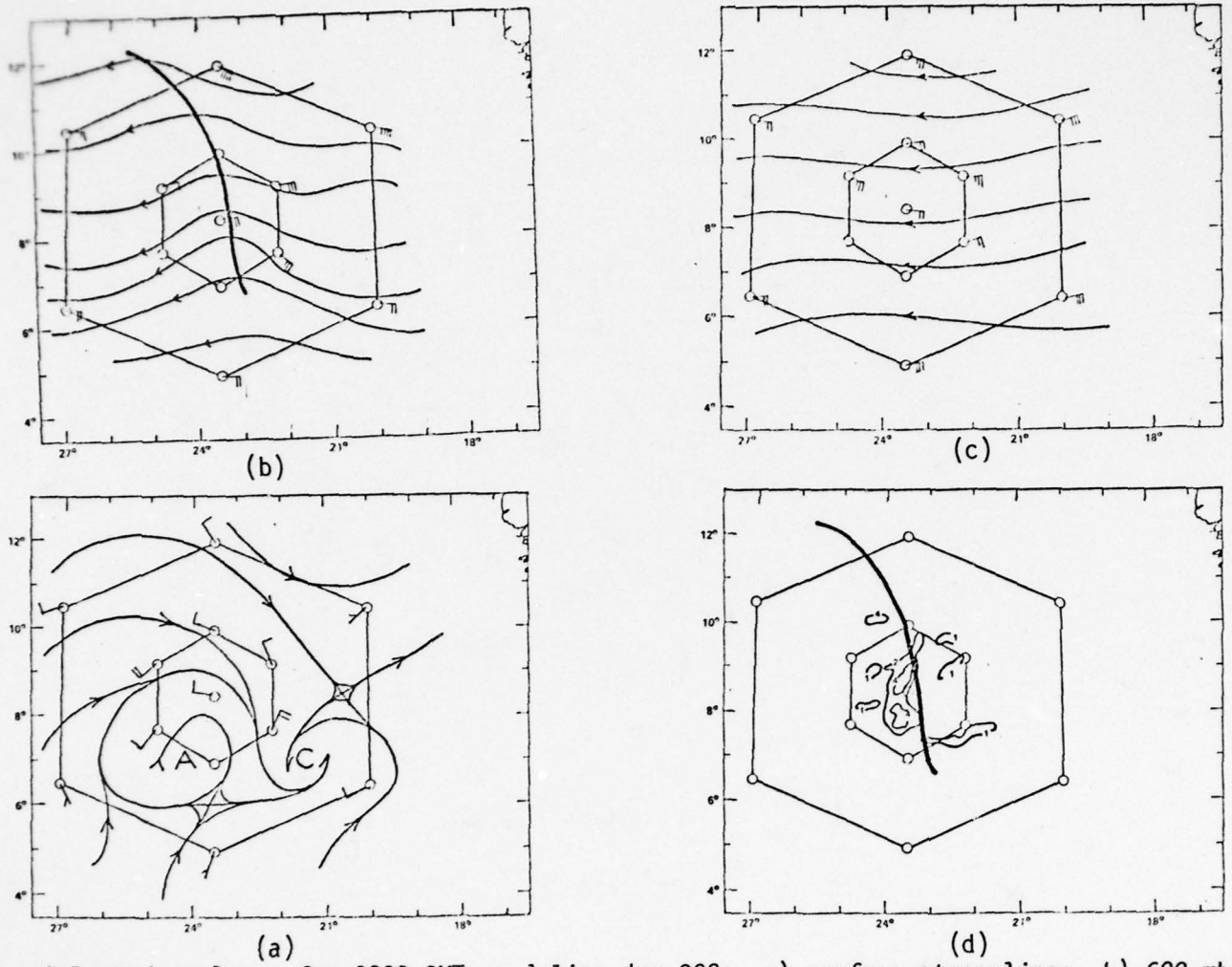


Fig. 32. Selected analyses for 0300 GMT on Julian day 222: a) surface streamlines, b) 600 mb (60 kPa) streamlines, c) 150 mb (15 kPa) streamlines, d) radar mosaics.

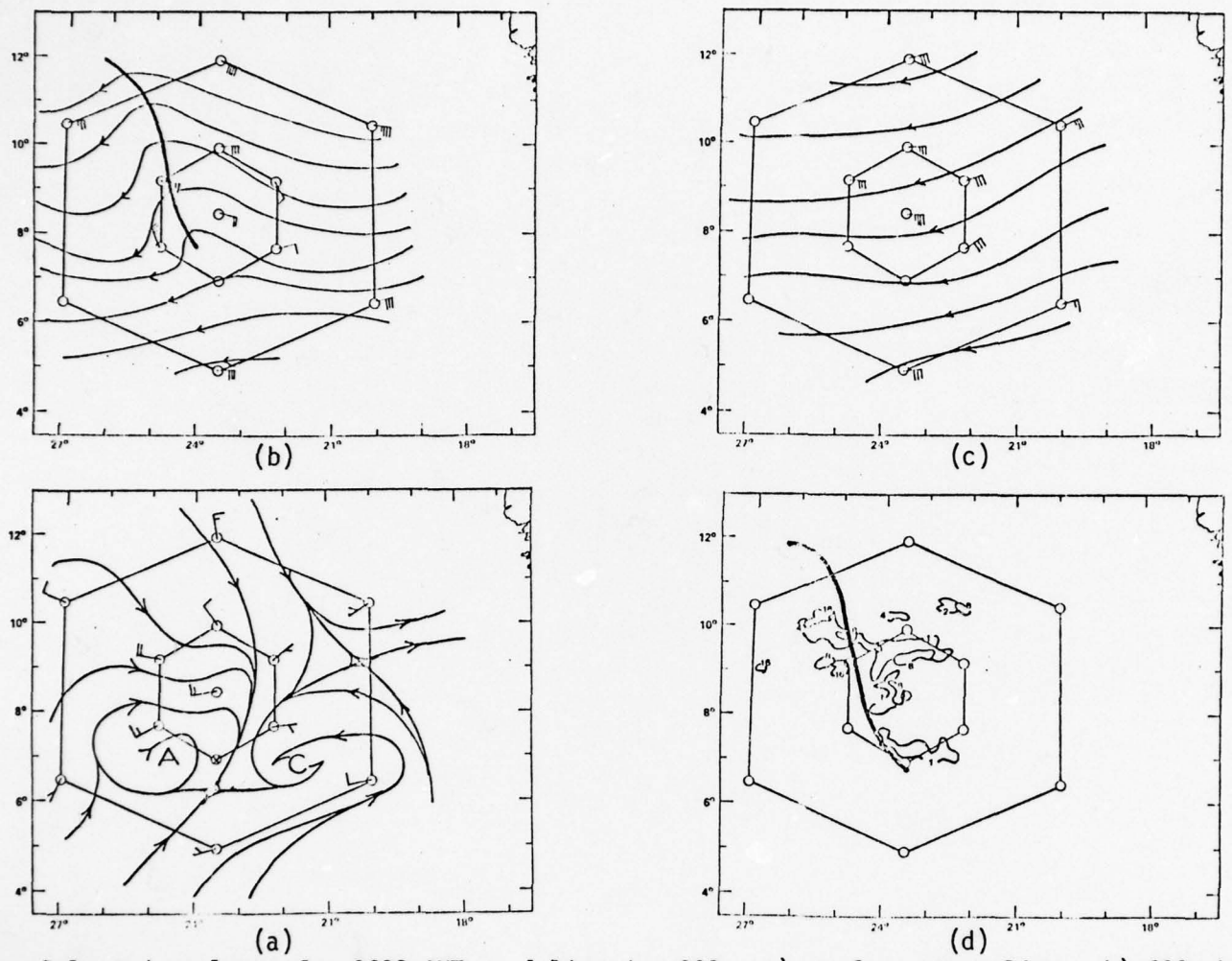


Fig. 33. Selected analyses for 0600 GMT on Julian day 222: a) surface streamlines, b) 600 mb (60 kPa) streamlines, c) 150 mb (15 kPa) streamlines, d) radar mosaic.

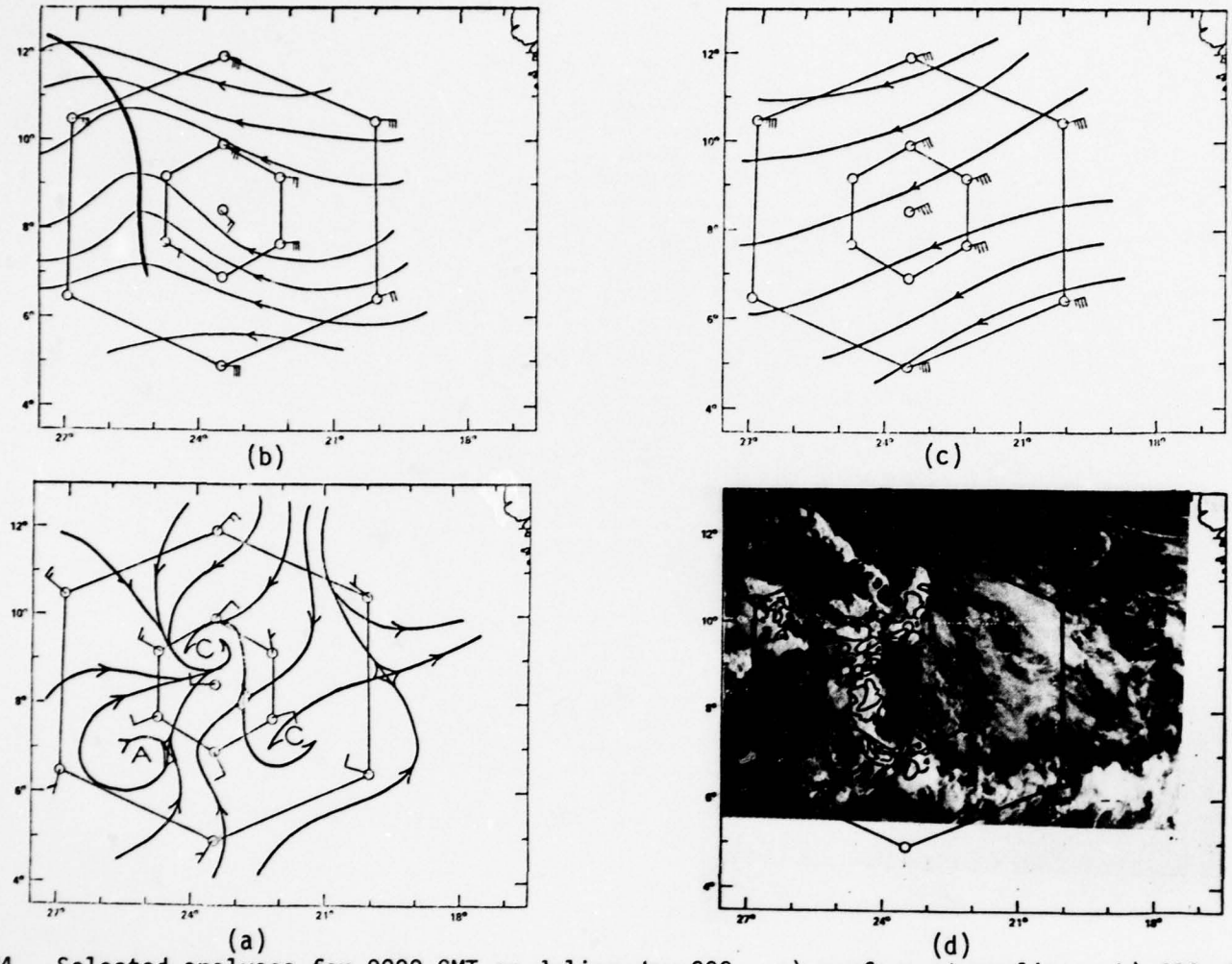


Fig. 34. Selected analyses for 0900 GMT on Julian day 222: a) surface streamlines, b) 600 mb (60 kPa) streamlines, c) 150 mb (15 kPa) streamlines, d) radar mosaic over-layed on a satellite image.

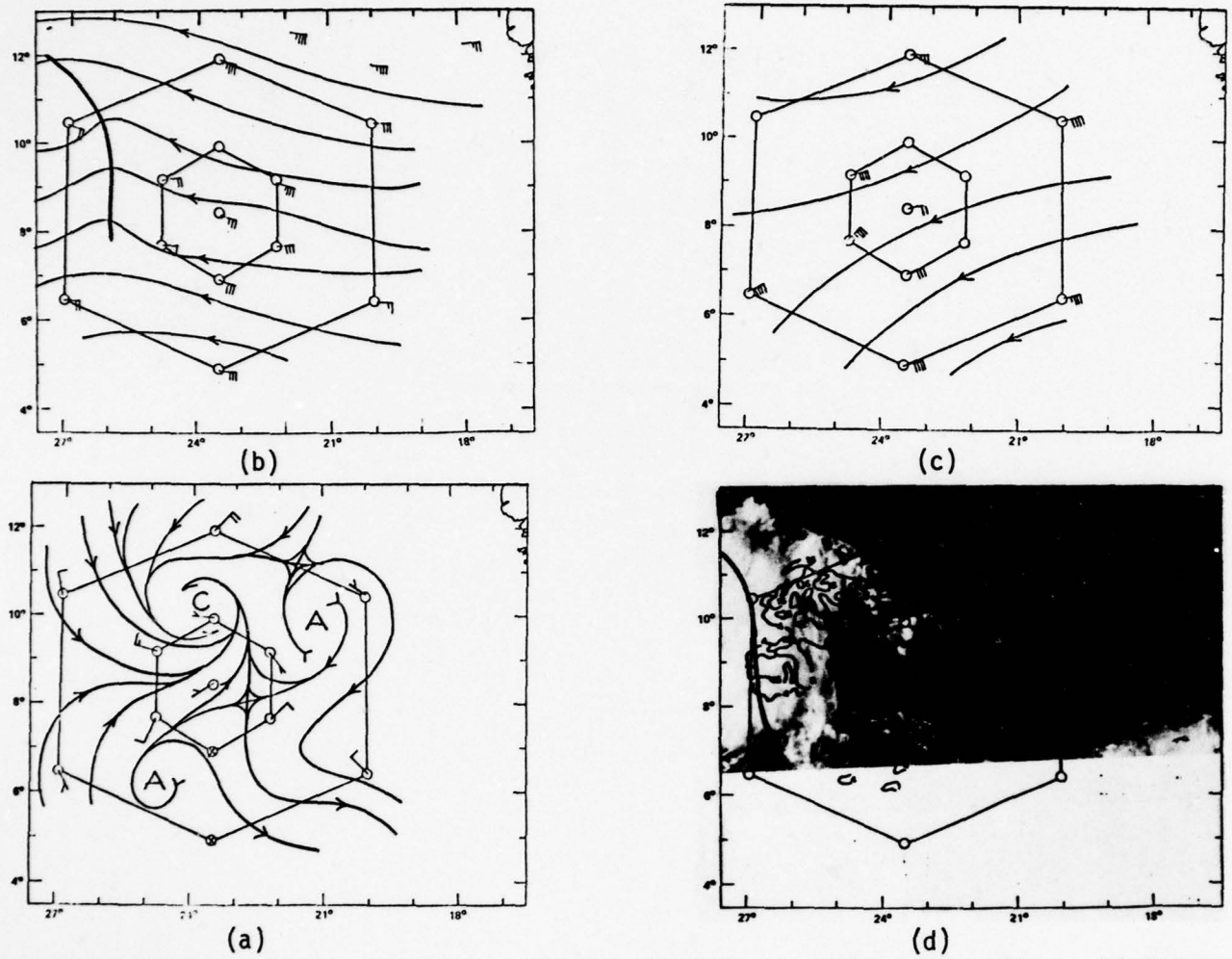


Fig. 35. Selected analyses for 1200 GMT on Julian day 222: a) surface streamlines, b) 600mb (60 kPa) streamlines, c) 150 mb (15 kPa) streamlines, d) radar mosaic over-layed on a satellite image.

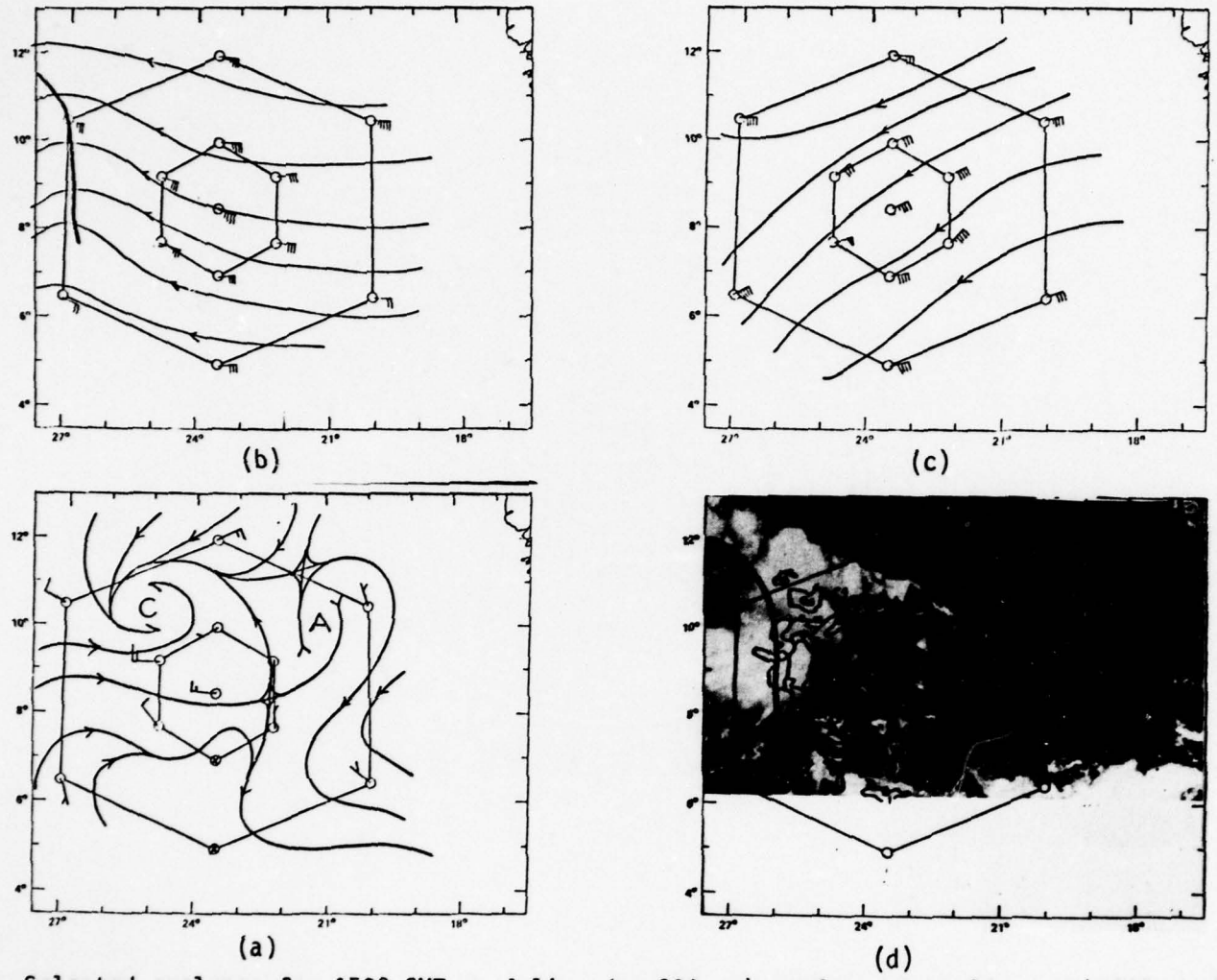


Fig. 36. Selected analyses for 1500 GMT on Julian day 222: a) surface streamlines, b) 600 mb (60 kPa) streamlines, c) 150 mb (15 kPa) streamlines, d) radar mosaic over-layed on a satellite image.

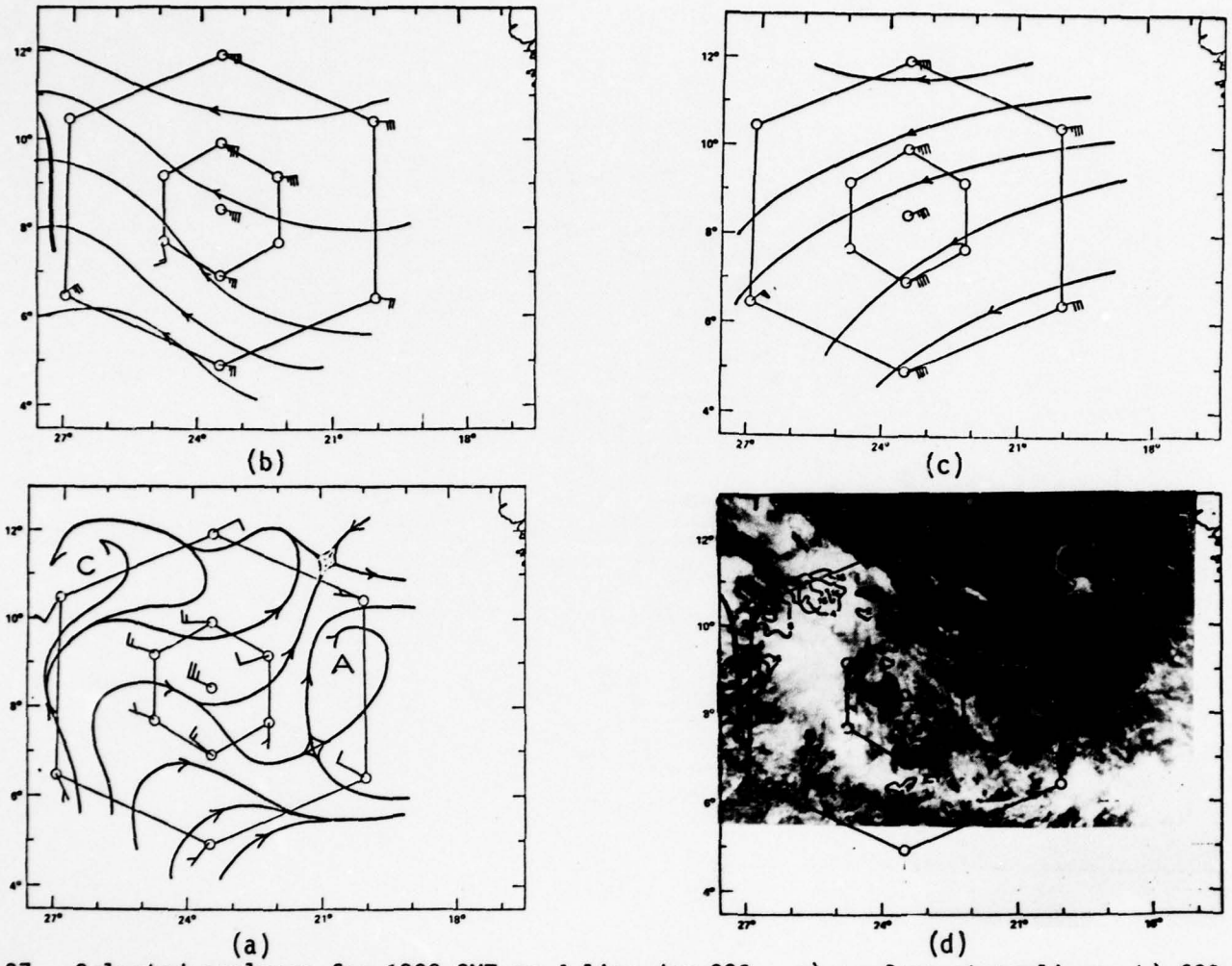


Fig. 37. Selected analyses for 1800 GMT on Julian day 222: a) surface streamlines, b) 600 mb (60 kPa) streamlines, c) 150 mb (15 kPa) streamlines, d) radar mosaic over-layed on a satellite image.

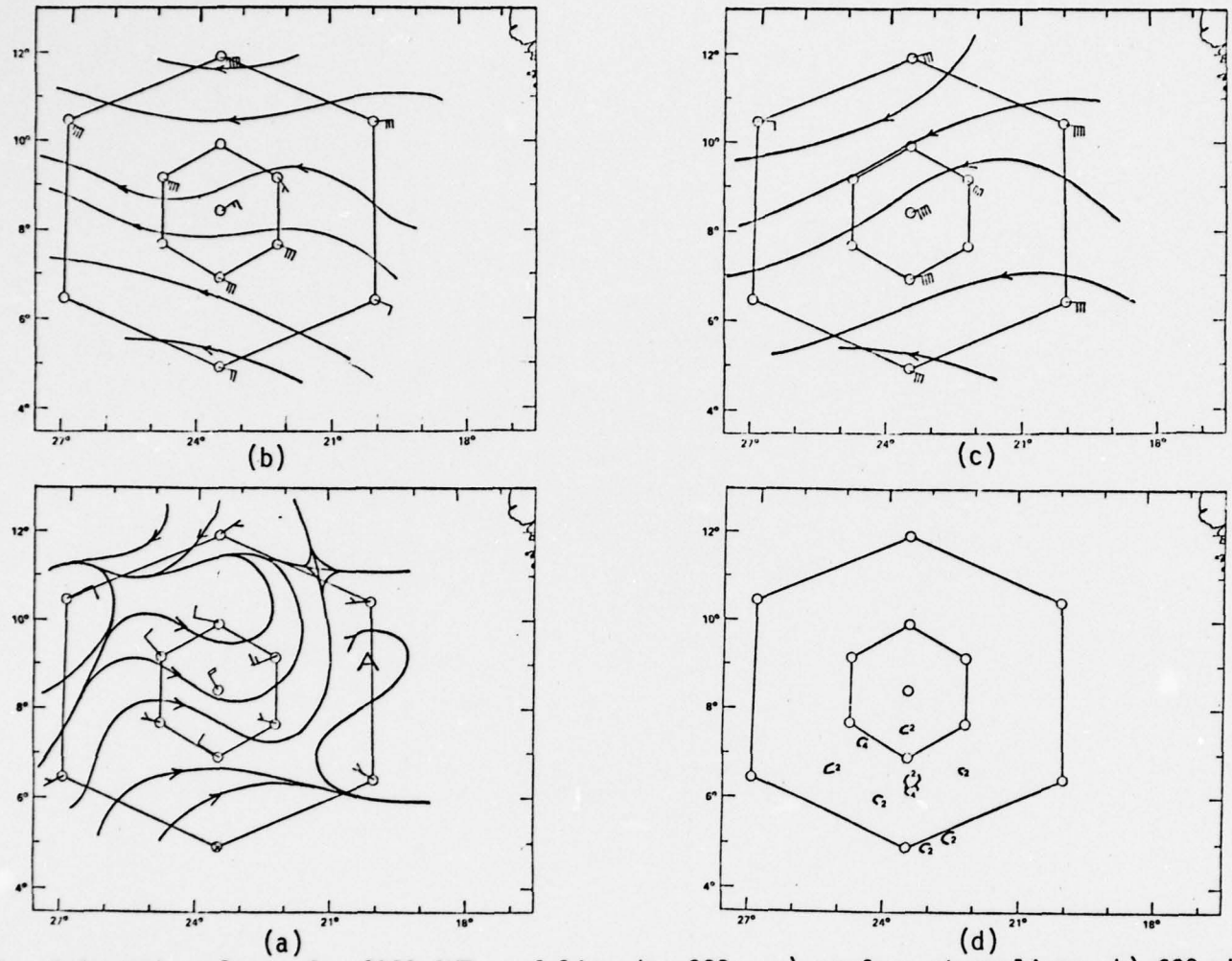


Fig. 38. Selected analyses for 2100 GMT on Julian day 222: a) surface streamlines, b) 600 mb (60 kPa) streamlines, c) 150 mb (15 kPa) streamlines, d) radar mosaic.

plotted for each synoptic hour. When available, the one-half mile resolution visual satellite image was depicted with the radar mosaic. The overlay of the two types of data enables one to separate precipitating clouds from non-precipitating ones. The radar echoes were drawn in isolines of rainfall rate in units of millimeters per hour (i.e. the 16 isoline delineates an area of 16 mm/rainfall rate). It is important to note these values are only crude estimates.

The radar mosaics were derived from different data sources. The data for the Oceanographer and Researcher were taken from the "GATE NOAA Radar Hybrid Microfilm Graphics Data", while the data for the Quadra and Gillis were taken from the "GATE International Radar Atlas" (Arkell and Hudlow, 1977).

The radar hybrid microfilm data include separate data for each ship. The data consist of digitized hybrid scans which were composited using three antenna tilt angles.[8] The isolines depicted in Figures 27-38 do not resolve the fine detail of the digitized data.

The data taken from the radar atlas is composited for different antenna angles but is not digitized.[9] The echo is delineated into different intensity levels by gradations of gray shades. The author subjectively evaluated the various gray shades in terms of decibel level and then converted that value into a rainfall rate.[10]

---

[8] A complete description of the hybrid process can be found in the "Documentation for GATE NOAA Radar Hybrid Microfilm Graphics Data".

[9] A complete description of the compositing can be found in the "GATE International Radar Atlas".

[10] Decibel level to rainfall rate conversion tables are available by ship in the "GATE International Radar Atlas".

## 5.2 Discussion

The discussion of the selected level analyses is separated by level with relationships between the horizontal level and the radar/satellite data. Figures 27 to 38 depict the surface streamline analysis (a), the 600 mb (60 kPa) level streamline analysis (b), the 150 mb (15 kPa) level streamline analysis (c), and the radar echo/satellite image (d) for each synoptic hour. The analysis begins at 1200 GMT on Julian day 221, and ends at 2100 GMT on Julian day 222. The thick line on both the 600 mb (60 kPa) and the radar echo/satellite image depiction indicates the position and shape of the 600 mb (60 kPa) easterly trough axis.

### 5.2.1 Surface Streamlines

There are two features that are obvious from the surface streamline analysis but were not evident from either the time or meridional cross-sections. The features include:

1. Identifying the structure of the surface confluence field including the position of two low-level vortex centers.
2. Obtaining evidence that the convection was aligned with the surface confluence zones and surface wind troughs.

Although a region of confluence was evident from the meridional cross-sections, its structure could not be established. The period began with evidence of single convergent asymptote existing east of the GATE array (see Figures 27-30 (a)). Within 12 hours a weak low level vortex developed within the southern half of the array (see

Figure 31 (a)). The vortex did not appear to be associated with the enhanced convection present in the region (see Figure 31 (a) and (d)). Nine hours later a second vortex developed northwest of the first and again did not appear associated with the enhanced convection within the region (see Figure 32 (a) and (d)).

The existence of low level vortices within tropical disturbances has been documented extensively (Erickson, 1977). In addition Erickson (1977) noted,

> "...that distinct areas of minimum convection coincided with forming cyclone centers...."

Since Hope (1975) identified this disturbance as the genesis cluster for tropical storm Alma, the fact that the surface vortices develop in convection free areas does support Erickson's finding.

The second significant finding was the evidence that the convection was aligned with the surface confluence zones, and the surface troughs. During the analysis, the radar echoes or the satellite images were overlayed on the surface winds and the streamlines were drawn. In each case, without violating the winds, the convection was clearly aligned with the surface flow. A similar finding was noted by Houze and Ching (1977). They noted:

> "The lower tropospheric winds appeared to control the echo motions and played a role in the horizontal alignment of echo lines."

Although the dynamics which are the underlying cause of this phenomena could be the subject of an entire research project, the finding does seem consistent with other known facts about the tropics. It has been shown and is generally accepted that the tropical atmosphere is conditionally unstable below ~800 mb (80 kPa) (Gray, 1975). It seems

reasonable that since the convection is initiated in the low levels, the low level wind flow would influence its alignment.

5.2.2 The 600 mb Level Streamlines

Analysis of the 600 mb (60 kPa) wind field supported some of the findings discussed earlier in the paper and also yielded some new findings. The observations that support earlier findings include:

1. That the shape of the trough axis changes from the northern to the central sector and is non-existent in the southern sector.
2. The strongest cyclonic shear does appear near 8° north latitude. However, there is no substantial evidence that a closed circulation center is present.

The findings that were not evident from earlier analyses include:

1. That the speed of wave was not constant during the 3-day period.
2. That the convection associated with the trough shifted from ahead of the trough axis to behind the trough axis.

The shape of the trough is in general agreement with the shape described in the earlier section on the time cross-sections. The 600 mb level analysis (Figures 27-38) does show a pronounced tilt westward in the northern sector and a very definite north-south orientation in the central sector. The wind field also shows very strong cyclonic shear at 8° north latitude, but there is no conclusive evidence that a closed vortex was ever present. South of 8° north

latitude the wind field is almost zonal and it appears the trough ends abruptly in the northern portion of the southern sector.

Features that were not evident from earlier analyses were accentuated when analyzed in the horizontal. The speed of the wave slowed during the latter portion of the period from 12 m/s to 7 m/s. The change in wave speed coincided with the change of convection from the east side of the trough axis to the west side.

The fact that convection can appear on either side of the trough axis has been documented (Riehl, 1954) and different explanations have been presented. Riehl (1954) presented a possible explanation based on the conservation of potential vorticity with the assumption that the energy cycle was insignificant. Holton (1971) developed a diagnostic model for the phenomenon. He uses the linearized primitive equations in spherical coordinates and relates perturbation geopotential to the diabatic heating pattern. In both cases it was concluded that the wind speeds are a critical factor in determining on which side of the wave the convection should appear.

Riehl (1954) concludes that when the wavespeed exceeds the mean wind speed through the wave the convection should appear on the west side of the axis, and when the mean wind exceeds the wavespeed convection should appear on the east side of the axis. The observations from these particular data generally agree with Riehl's conclusion.[11]

---

[11]On Julian day 221 between 1800 and 2400 GMT the convection was on the east side of the trough. The mean wind speed was 11 m/s and the wave speed was 12 m/s. While on Julian day 222 between 0600 and 1500 GMT the convection was predominantly on the west side of the trough axis. The mean wind speed was 13 m/s and the wave speed was 7 m/s.

However, during the latter hours of the period, there is convection on both sides of the trough axis.

Holton concluded from the results of his model that the vertical shear of the zonal mean wind (average longitudinally) is the critical factor. He concludes:

> "...With westerly shear in the lower troposphere the precipitation occurs to the east of the surface trough, but with easterly shear the precipitation zone is west of the trough...."

Observations from this data set indicate that the conditions which prevail over the GATE region may not be applicable to Holton's results. The low level flow over the GATE region during Phase II (see Figure 3) is dominated by westerly flow and the middle levels are dominated by easterly flow. These conditions result in easterly shear in the vertical. Since Holton applied his model to Western Pacific data, where the vertical structure is essentially the opposite, I do not believe his results are applicable in the GATE region.

5.2.3 The 150 mb Level Streamlines

There are two features that are obvious from the analysis of the 150 mb (15 kPa) level winds:

1. The apparent compensating response of the 150 mb (15 kPa) level wind to the 600 mb (60 kPa) level flow pattern.
2. The appearance of a diverging wind flow pattern over the convection coincident with the first indications of cirrus blow-off from the satellite imagery.

There does appear to be compensating motion at the high level responding to the wind flow at the middle levels. Figures 27 to 38 (b) and (c) show that when a westerly trough is evident at 600 mb (60 kPa) an easterly ridge is evident at 150 mb (15 kPa).

It is not clear what forces this apparent compensating flow. It may be related to the vertical transport of mass and momentum by cumulus. It may also be viewed as part of the dynamics and structure of troughs and ridges in the vertical. Attempts to explain the cause of this compensating phenomenon is beyond the scope of this paper.

The fact that the 150 mb (15 kPa) divergence wind flow pattern did not appear until the cirrus blow-off appeared suggests some kind of relationship or feedback between the convection and the upper level wind flow. The interaction of the two different scale events has been the subject of much research in recent years and is one of the objectives of the Convection Subprogramme for GATE (Betts and Rodenhuis, 1975). However, the observational analysis techniques used in this study do not lend themselves to studying the detail required to look at these interactions.

## 5.3 General Observations

Several general observations can be made about the period that became evident after comparing all three levels with the radar/satellite depictions. These include:

1. Although the convection appears aligned with the surface flow, it also appears to be closely associated with the location of the 600 mb (60 kPa) trough.

AD-A065 469 COLORADO STATE UNIV FORT COLLINS DEPT OF ATMOSPHERI--ETC F/G 4/2
A DIAGNOSTIC CASE STUDY OF THE 9-11 AUGUST PERIOD DURING GATE.(U)
1978 J J BUTCHKO NSF-ATM76-09370

UNCLASSIFIED AFIT-CI-79-114T NL

2 OF 2
AD
A 065469

END
DATE
FILMED
4-79
DDC

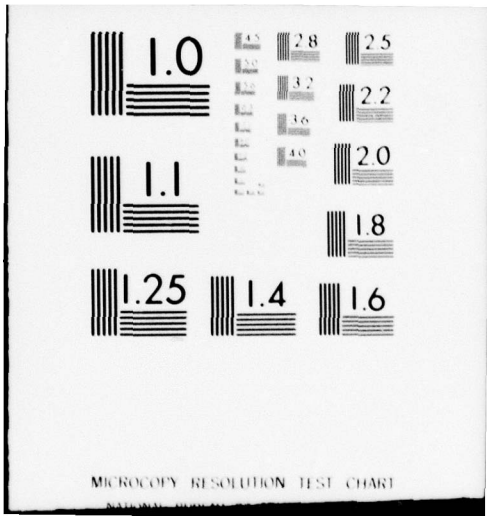
1.0
1.1
1.25
1.4
1.6
1.8
2.0
2.2
2.5
2.8
3.2
3.6
4.0
MICROCOPY RESOLUTION TEST CHART

2. It appears that as the easterly trough at 600 mb (60 kPa) entered the region the surface confluence became more enhanced and at least two low level vortices developed within the GATE array.
3. The enhanced confluence zone at the surface seemed to trigger much of the initial convection within the GATE region.
4. Although a general area of cloudiness can be traced from the African coast, it appears that the intensity and location of the convection relative to the trough axis is continually changing.
5. Although you would not expect it from viewing the satellite imagery, the wind fields associated with the area of cloudiness are organized.

## 6.0 ANALYSIS OF THE PRE-TROPICAL STORM CLOUD CLUSTER

### 6.1 General

In this section the area of convection is viewed as a pre-tropical storm cloud cluster.[12] The vorticity, divergence and vertical motion fields were determined for the entire A/B-scale array and for six sub-areas of the array (see Figure 39). This set of fields is compared to fields derived by Schubert and Reed (1974) for Phase II GATE data and to fields derived by Erickson (1977) for composited Western Pacific clusters.

### 6.2 Computation of Vorticity, Divergence, and Vertical Motion

The vorticity, divergence, and vertical motion fields were determined using average u-wind and v-wind components from the 0900 to 2100 GMT rawinsondes for Julian day 222. The fields were computed for the six triangles depicted in Figure 39. The six sets of fields were averaged by level to determine a set of fields for the entire A/B-scale ship array. The method of computation was essentially the same as that used by Schubert and Reed (1974).

The exceptions to the Schubert and Reed (1974) method are as follows:

1. Six small triangles were used rather than one large triangle.
2. The divergence was mass balanced to 150 mb (15 kPa) rather than 100 mb (10 kPa).

---

[12] Frank (1975) identified the easterly wave being studied as the genesis source of Tropical Storm Alma.

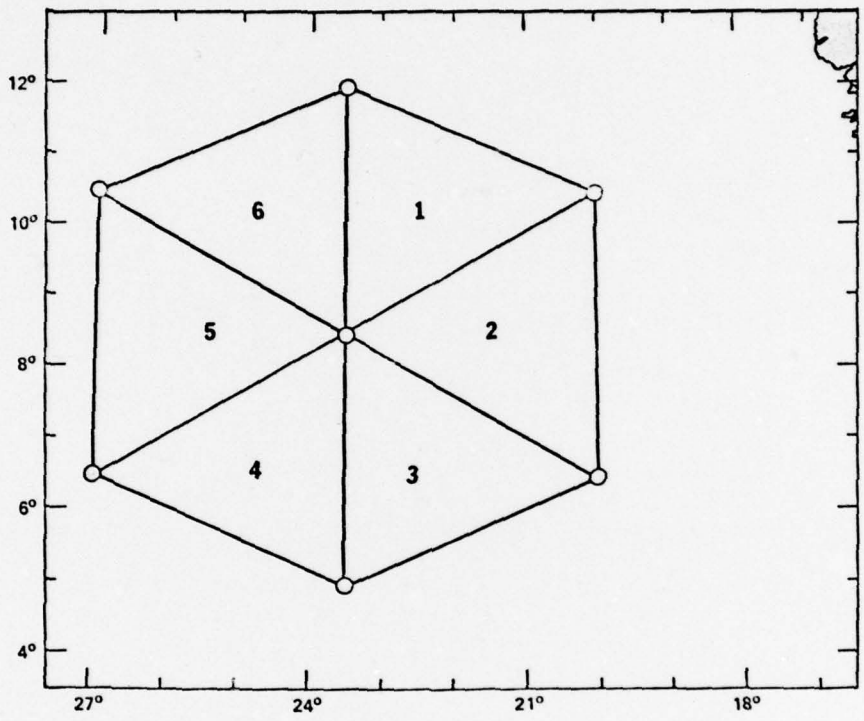


Fig. 39. Sub-areas used in the computation of the vorticity, divergence and vertical motion fields.

3. The vertical P-velocity was assumed to be zero at the surface and 125 mb (12.5 kPa) rather than 100 mb (10 kPa).

## 6.3 Comparisons of the Vorticity, Divergence, and Vertical Motion Fields

Figure 40 depicts the mean vorticity, divergence, and vertical motion profiles for the entire A/B-scale ship arrays. The profile of relative vorticity shows positive vorticity from the surface to 150 mb (15 kPa). The divergence profile shows convergence below 800 mb (80 kPa), a region of non-divergence from 800 mb (80 kPa) to 500 mb (50 kPa), and a region of divergence above 500 mb (50 kPa). The vorticity and vertical motion profiles appear relatively weak compared to the active case profile of Schubert and Reed (1974).

Schubert and Reed (1974) depict an average vertical p-velocity profile for 0600-1200 GMT on Julian day 224 which was also an active convective day. Their profile also showed upward vertical motion over the array but the peak was ∿330 mb/day. This is much stronger than the 100 mb/day value depicted in Figure 40.

Schubert and Reed (1974) depict the mean vorticity profile for the most convectively active cases during Phase II. They show positive vorticity of about the same order of magnitude as shown in Figure 40 up to 350 mb (35 kPa), but above that level the vorticity becomes negative. It should be noted here that these comparisons are misleading. The averaging technique used to determine these profiles removed most of the significant detail of the sub-area profiles.

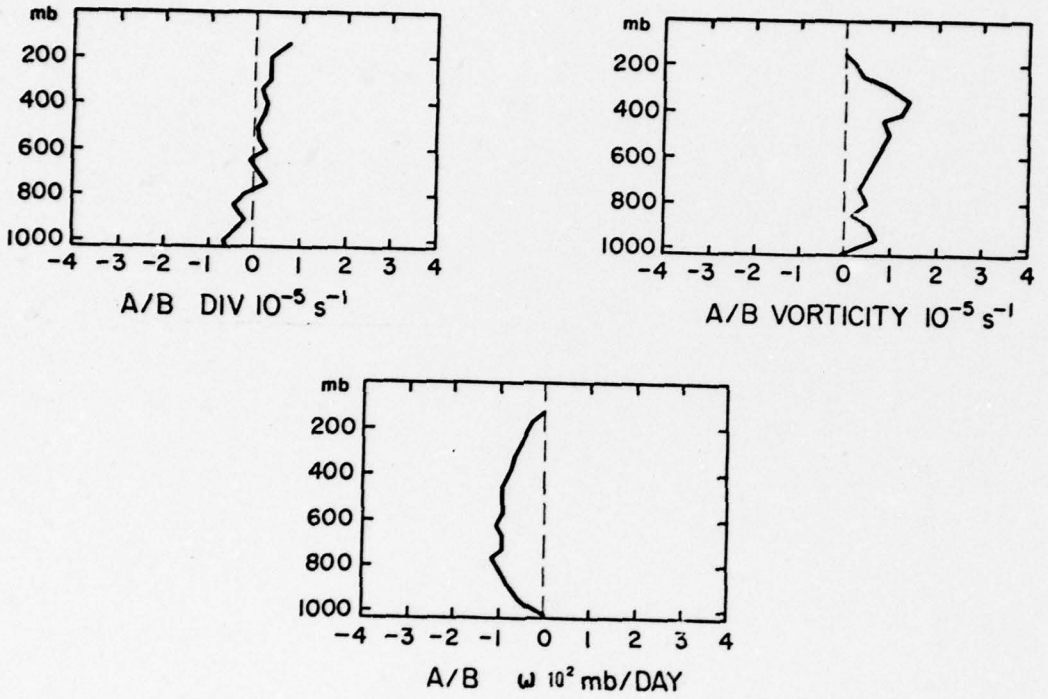


Fig. 40. Mean profiles of divergence, vorticity and vertical motion ($\omega$) for the entire A/B-scale array for 0900-2100 GMT on Julian Day 222.

Figures 41, 42, and 43 depict the vorticity, divergence, and vertical motion profiles for each of the six sub-areas. The most significant feature of all three figures is the differences which exist for each parameter across the array.

The vorticity profiles (Figure 41) can be grouped into two categories based on the structure of the profile. The profiles on the right of the array are dominated by positive relative vorticity especially in the region above 400 mb (40 kPa). The profiles on the left of the array are dominated by positive relative vorticity below 300 mb (30 kPa) with negative vorticity above that level. Figure 6 shows that the intense convection occurring during this time period was on the left side of the array.

The divergence profiles (Figure 42) also show differences across the array and can also be separated into the same areas. The right side, especially sub-areas 2 and 3, shows a region of divergence below 500 mb (50 kPa) and convergence above. These profiles are associated with a clear region (see Figure 6). The profiles for sub-areas 5 and 6 show convergence below 500 mb (50 kPa) and divergence above. These profiles are associated with areas of intense convection (see Figure 6).

The vertical motion profiles (Figure 43) show the most pronounced variability across the array. The profiles for sub-areas 2 and 3 show downward motion while the profiles for sub-areas 4, 5, and 6 show upward motion. The upward motion is associated with the convection and the subsidence is associated with the clear regions. The strong subsidence over sub-area 3 is probably due to the combined effects of the clusters on either side of that area as seen in Figure 6.

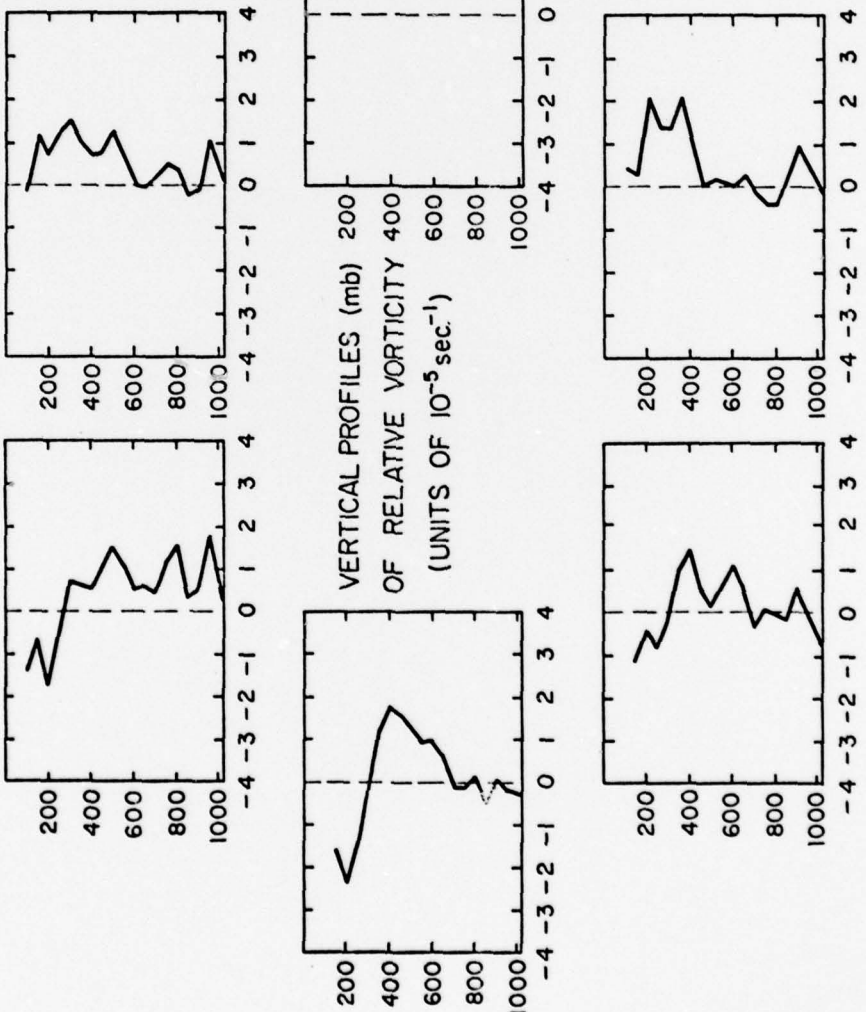


Fig. 41. Mean profiles of relative vorticity for each sub-area for 0900-2100 GMT on Julian Day 222.

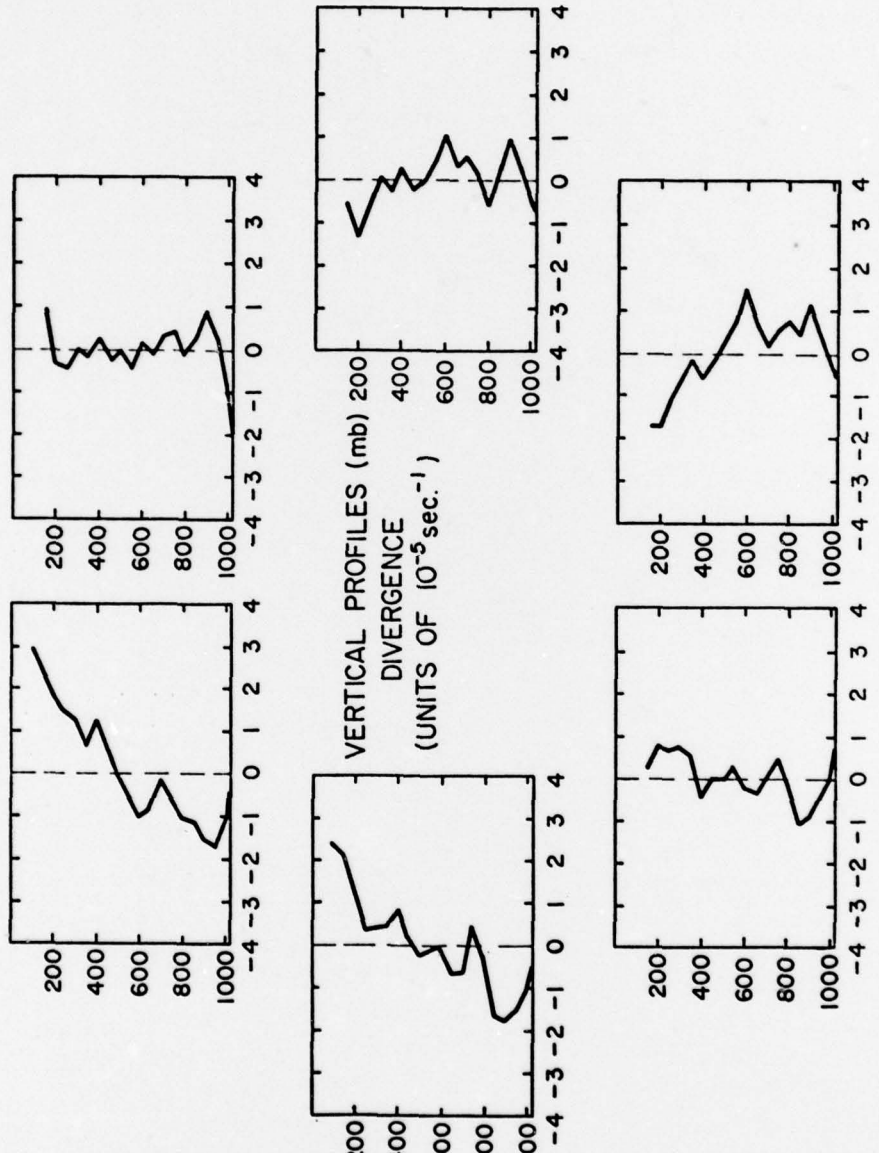


Fig. 42. Mean profiles of divergence for each sub-area for 0900-2100 GMT on Julian Day 222.

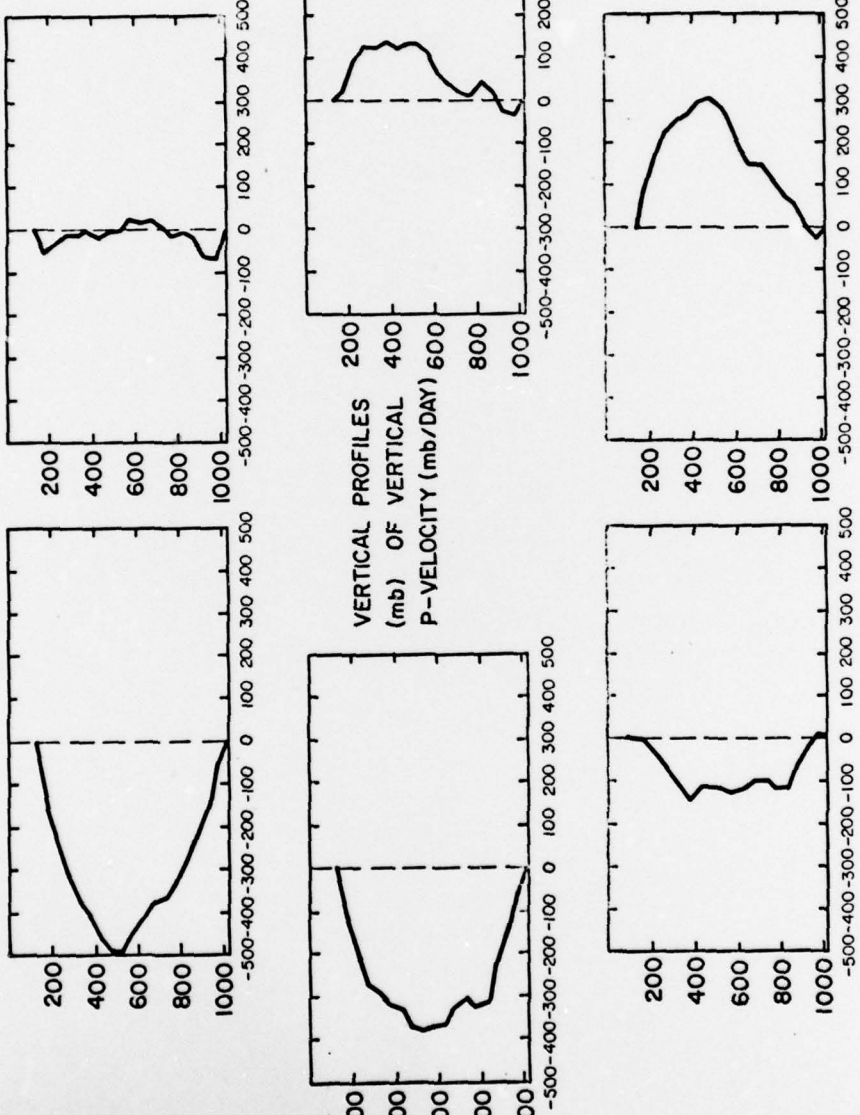


Fig. 43. Mean profiles of verticap P-velocity for each sub area for 0900-2100 GMT on Julian Day 222.

The vertical motion profiles show a distinct delineation between the convection and the clear regions. There also seems to be a good correlation between the strength of the vertical motion and the intensity of the convection. Figures 34-38 clearly show the most intense radar echoes are located within sub-area 6 which is also the region of strongest vertical motion. These profiles also provide evidence to the idea that a large portion of the upward motion associated with the cloud cluster is compensated by subsidence immediately adjacent to the cluster.

## 6.4 Comparisons of the Vorticity, Divergence, and Vertical Motion Profiles with Profiles from Western Pacific Cloud Clusters

Erickson (1977) compared the vorticity, divergence, and vertical motion fields of developing and non-developing clusters in the Western Pacific. By comparing the fields depicted in Figures 40-43 to Erickson's (1977) profiles for the 0-4° radius cluster, we may be able to make some qualitative comparisons about the profiles from cloud clusters located in the two regions.

Erickson (1977) observed the following for his developing clusters:

1. Positive relative vorticity ($\sim 2 \times 10^{-5} sec^{-1}$) from the surface to 500 mb (50 kPa).
2. Rapid change to negative relative vorticity above 500 mb (50 kPa) with a peak of $\sim -2 \times 10^{-5} sec^{-1}$ at 200 mb (20 kPa).
3. Convergence ($\sim -0.5 \times 10^{-5} sec^{-1}$) up to 500 mb (50 kPa).

4. Rapid change to divergence ($\sim -2 \times 10^{-5} sec^{-1}$) with a peak at 200 mb (20 kPa).
5. A vertical P-velocity from the surface to 100 mb (10 kPa) with a peak of $\sim$250 mb $day^{-1}$ between 300 and 400 mb (30 and 40 kPa).

It must be pointed out that direct comparisons between the two studies are not possible because different techniques were used to determine the profiles. However, some qualitative comparisons may still be possible.

The effects of averaging over the entire A/B-scale ship array become more evident when comparing the different sets of data with Erickson's (1977) results. The profiles for the entire A/B-scale appear significantly weaker and are dissimilar in general shape to Erickson's results. However, the profiles over sub-area 5 and 6 are comparable with Erickson's findings in both intensity and general shape of the curves.

These results bring up three important findings. First, there probably is not much difference between the vorticity, divergence, and vertical motion profiles in the Atlantic and Western Pacific. Second, the profiles for these parameters are highly dependent on the size of the area over which the computations are made. Third, the shape of the profile is highly dependent on the orientation of the cluster to the area where the computations are made.

# 7.0 SUMMARY OF OBSERVATIONS AND CONCLUSIONS

## 7.1 Summary

The different analysis approaches yield different observations of the phenomena that occurred over the three day period. This section simply provides a brief summary and consolidation of the observations the author believes to be important. The observations are as follows:

1. An easterly wave, which was clearly defined at 600 mb (60 kPa), moved over the GATE A/B-scale array during the period. Associated with the wave was a large area of convection which changed shape and varied in intensity during the period.
2. Warm, dry, Saharan air, which appeared associated with a strong easterly ridge, advected over the array and significantly changed the temperature and moisture fields.
3. There is evidence that the wave was cold core from the surface up to 500 mb (50 kPa).
4. The existence of both a mid-tropospheric jet and an upper-tropospheric jet caused large vertical wind shears over the area.
5. As the easterly wave entered the array, the confluence zone in the array became stronger and better defined. The enhancement of the confluence zone seemed to trigger the initial convection in the array.

6. The convection appeared aligned with the surface flow and also appeared closely associated with the 600 mb (60 kPa) trough axis.
7. The winds over the array were light relative to the mid-latitudes but were still very organized.
8. The divergence and vertical motion profiles appeared significantly different across the array.
9. Comparison with Western Pacific data is difficult because the shape and intensity of the profiles is highly dependent on the size over which the profiles are computed.

## 7.2 Conclusions

It was mentioned in section 2.0 that the cloud cluster or area of convection changed configuration during the period. Since this paper was devoted to observing the transition period, the author thought it appropriate to propose an explanation based on his observations.

It appears that the easterly wave initiated the cloud cluster transition. The wave enhanced the confluence zone and initiated small low-level vortices within the array. The vortices in turn enhanced the early convection. The establishment of the vortex further enhanced the convection by increasing the low-level convergence of warm moist air into the cluster. Because the wave and early vortex were cold core, feedback mechanisms or sub-scale processes must be included in the transition to a warm core tropical cyclone.

# REFERENCES

Arkell, R., and M. Hudlow, 1977: GATE International Meteorological Radar Atlas. NOAA, U. S. Department of Commerce.

Betts, A. K., and D. R. Rodenhuis, 1975: GATE Convection Subprogramme Field Phase Report. Department of Atmospheric Science, Colorado State University, Ft. Collins, CO.

Burpee, R. W., 1972: The Origin and Structure of Easterly Waves in the Lower Troposphere of North Africa. J. Atmos. Sci., 29, 77-90.

_____, 1974: Characteristics of North African Easterly Waves During the Summers of 1968 and 1969. J. Atmos. Sci., 31, 1556-1570.

_____, 1975: Some Features of Synoptic Scale Waves Based on a Compositing Analysis of GATE Data. Mon. Wea. Rev., 103, 921-925.

_____, and G. Dugdale, 1975: A Summary of Weather Systems Affecting Western Africa and the Eastern Atlantic During GATE. Report on the Field Phase of the GATE Scientific Programme GATE Report No. 16, 2.1-2.42.

Carlson, T. N., 1969: Synoptic Histories of Three African Disturbances that Developed into Atlantic Hurricanes. Mon. Wea. Rev., 97, 256-276.

Chang, C., 1970: Westward Propagating Cloud Patterns in the Tropical Pacific as Seen from Time-Composite Satellite Photographs. J. Atmos. Sci., 27, 133-138.

Erickson, S. L., 1977: Comparison or Developing vs. Non-Developing Tropical Disturbances. Atmospheric Science Research Paper, Department of Atmospheric Science, Colorado State University, 81 pp.

Frank, N. L., 1975: Atlantic Tropical Systems of 1974. Mon. Wea. Rev., 103, 294-300.

Frank, William, 1976: The Structure and Energetics of the Tropical Cyclone. Atmospheric Science Research Paper, Department of Atmospheric Science, Colorado State University, 180 pp.

GATE Report No. 13, The International Data Management Plan (Parts II and III). Section 10.0, Plan for National Data Management in the U.S.A. World Meteorological Organization, April 1974, pp. 134-185.

GATE NOAA Radar Hybrid Microfilm Graphics Data. CEDDA/0410, 1976, Data Type Code 36, Storage Media 10/30 reels/7m.

REFERENCES Continued

Gouind, R. K., H. L. Cole, and J. H. Smalle, 1975: GATE Dropsonde Data, Users Guide. NCAR/U531-15-1, Research Systems Facility, NCAR, Boulder, CO, December 1975.

Gray, W. M., and D. J. Shea, 1973: The Hurricane's Inner Core Region. II. Thermal Stability and Dynamic Characteristics. J. Atmos. Sci., 30, pp. 1565-1576.

Gray, W. M., 1975: Tropical Cyclone Genesis. Atmospheric Science Research Paper, Department of Atmospheric Science, Colorado State University, 121 pp.

_____, 1977: Tropical Disturbance to Cyclone Transformation. (Submitted to J. Atmos. Sci.)

Holton, J. R., 1971: A Diagnostic Model for Equatorial Wave Disturbances: The Role of Vertical Shear of the Mean Zonal Wind. J. Atmos. Sci., 28, 55-64.

Hope, J. R., 1975: Atlantic Hurricane Season of 1974. Mon. Wea. Rev., 103, 285-289.

Houze, R. A., and C. P. Chang, 1977: Radar Characteristics of Tropical Convection Observed During GATE: Mean Properties and Trends over the Summer Season. Mon. Wea. Rev., 105, 964-980.

Palmen, E., 1948: On the Formation and Structure of Tropical Hurricanes. Geophysica, 26-38.

_____, and C. W. Newton, 1969: Atmospheric Circulation Systems. Academic Press, N. Y., 603 pp.

Reed, R. J., and E. E. Recker, 1971: Structure and Properties of Synoptic-Scale Wave Disturbances in the Equatorial Western Pacific. J. Atmos. Sci., 28, 1117-1133.

Reed, R. J., D. C. Norquist, and E. E. Recker, 1977: The Structure and Properties of African Wave Disturbances as Observed During Phase III of GATE. Mon. Wea. Rev., 105, 317-333.

Riehl, H., 1954: Tropical Meteorology. McGraw-Hill Book Company, Inc., N. Y., 392 pp.

Sadler, J. C., 1975: The Monsoon Circulation and Cloudiness over the GATE Area. Mon. Wea. Rev., 103, 369-387.

REFERENCES Continued

Schubert, W. H., and R. J. Reed, 1974: Vertical Motion and Vorticity in the A/B-Scale Area: Phase II. GATE Report No. 14, Preliminary Scientific Results (Volume I), World Meteorological Organization, January 1975, pp. 137-144.

Sequin, W. R., and D. Sabol, 1976: GATE Convection Subprogram Date Center: Shipboard Precipitation Data. NOAA Tech. Report, ED 18, U. S. Department of Commerce, 73 pp.

Shea, D. J., and W. M. Gray, 1973: The Hurricane's Inner Core Region. I. Symmetric and Asymmetric Structure. J. Atmos. Sci., 30, pp. 1544-1564.

Yanai, M., 1961: A Detailed Analysis of Typhoon Formation., Journ. Met. Soc. Japan, 39, 187-213.

_____, 1964: Formation of Tropical Cyclones. Reviews of Geophysics, 2, 367-414.

# APPENDIX A

## The Criteria and Method Used to Select the Case Study Periods

The criteria for choosing the case study period were selected to support the initial objective of the project (i.e. to study the synoptic scale meteorological features of a convective cloud area). The type of criteria used can be classified into 3 categories: the primary criteria, the secondary criteria, and the additional factors that lend to choosing Julian days 221, 222, and 223.

The primary criteria included the following:

1. At least 3 of the 14 ships of the A/B and B-scale arrays reported 12 mm (~.5 inches) of rain or greater in a single day.
2. At least 4 of the 6 ships in the B-scale array took a rawinsonde observation at each synoptic hour during the day.
3. Aircraft data was taken and is available on the day in question.
4. Satellite imagery indicated that the convection area was of sufficient size and duration for a synoptic analysis.

The precipitation criteria was used first because, I thought, it would give a good indication of the extent and intensity of the convection for a particular day. The criteria was applied using the tabulated precipitation data in NOAA Technical Report EDS 18, Sequin and Sabol (1976). The 3 ships with 12 mm (~.5 inches) of rain criteria

were selected arbitrarily after scanning the tables but applying the criteria reduced the possible days for study from 63 to 26.

The rawinsonde criteria was used because of the necessity of good upper air data needed for a synoptic scale analysis. The criteria was applied using the data depicted in the GATE Convective Subprogramme Field Phase Report, Betts and Rodenhuis (1975). Applying the criteria reduced the possible days for study from 26 to 17.

The aircraft data criteria were considered important because of the additional data which was made available from these flights. The criteria was applied using the data compiled in the GATE Convective Subprogramme Field Phase Report, Betts and Rodenhuis (1975). Using this criteria reduces the possible days from 17 to 12.

The satellite criteria was a subjective evaluation using the SMS data on microfilm. The two most important aspects considered were area covered by the convection and duration of the event. Using this criteria reduced the possible days from 12 to 8.

The primary criteria was very effective and reduced the possible days for study from 63 to 8. The 8 cases were studied further and the secondary criteria were established to reduce the possibilities further.

The secondary criteria established included the following:

1. That there be little or no work so far done on the day selected.
2. That hybrid radar data be available for the day.
3. That dropsonde data be available for the day.
4. That most of the convective activity occurred within the GATE A/B-scale array.

The first criteria, which concerned work done already, eliminated all the possible days in phase III. Phase III included the "GATE Priority Period" (5-12 Sept) and other days that were being processed either at CSU or NCAR. Applying this criteria reduced the possible days for study from 8 to 3. The 3 days remaining included Julian days 194, 195 and 222. It was decided to group Julian days 194 and 195 into one period which left 2 possible choices.

The hybrid radar data[1] was considered important in order to objectively evaluate the intensity and extent of the convection. Data for two U.S. ships, the Oceanographer and Researcher, are on microfilm and the criteria was applied using that data. Since both periods had data available this criteria did not aid in elimination process.

The Dropsonde criteria were considered important because of the additional information which was available. The criteria was applied using the GATE Diopsonde Data, Users Guide, Gouind, et al. (1975). Julian day 222 did have dropsonde data available while Julian days 194 and 195 did not.

The final criteria which involved the horizontal extent of the convection was considered important because of the location of Rawinsonde network. It was considered favorable if most of the convection was within the A/B-scale array so a complete analysis could be made. The criteria also supported Julian day 222.

---

[1]The hybrid Radar data was prepared by CEDDA. The data set contains PPI graphic images which were generated from the hybrid digital data using NOAA's FR-80 graphics system. The microfilm set includes the hybrid scan from the 2 NOAA C-band radars for the third phase of GATE.

Although the secondary criteria reduced the possible days to one, there were additional factors which led to the selection of Julian day 222. The additional factors include the following:

1. The convection became organized during the daylight hours. This was important because high resolution visual satellite data could be used in the analysis.
2. The convective cloud mass later developed into tropical storm Alma.
3. The satellite data indicated the convective cloud mass was organized and moved off the West African coast and through the GATE array. The organization and movement seemed to support the existance of an easterly wave. If conventional data support this idea, we could compare it with the composite wave developed by Reed, Norquist and Recker (1977).

## APPENDIX B

### The Method Used to Determine the Tilt of the Trough Axis

The tilt of the trough axis was determined using trial and error, simple geometry, and the estimated wave speed. The procedure is outlined as follows:

1. Estimate an angle that describes the tilt of the axis.
2. Knowing the angle and the lenght of the adjacent side, the lenght of the opposite side is determined by multiplying the tangent of the angle by the lenght of the adjacent side.
3. By adding or subtracting the lenght just determined from the horizontal difference between the ships, you determine the distance the wave must travel.
4. Divide the distance just determined by the wave speed to determine the time of travel between the two ships.
5. Repeat the procedure using different angles until the time period calculated approximates the actual value.